"Carol Davila" University of Medicine and Pharmaceutics
Bucharest, Romania
2009

# New Psychophysical Methods for Investigation of Amblyopic Patients

- doctoral thesis -

Supervisor:
Prof. Dr. Constanța Ganea

Author:
Adrian Iftime

*In memoriam*

Prof. Dr. Ruxandra Sireteanu
(1945 - 2008)

*Max Planck Institute for Brain Research (Psychophysics)*
*Goethe University (Biopsychology)*
*Frankfurt am Main, Germany*

Titlul tezei de doctorat: “Metode psihofizice noi de investigare a pacienţilor cu ambliopie”

Îndrumător doctorat:

- Prof. Dr. Constanţa Ganea (UMF “Carol Davila” - Bucuresti, Romania)

Data predării tezei de doctorat: .....

Pe parcursul elaborării tezei de faţă autorul a beneficiat de finanţare parţială din proiectul *Deutscheforshungsgemeineschaft DFG SI 344/17-1,2,3* (Ruxandra Sireteanu, Germania) şi din proiectul *CNCSIS TD-48/2008* (Adrian Iftime, Romania).

Romanian title: “Metode psihofizice noi de investigare a pacienţilor cu ambliopie”

English title: “New Psychophysical Methods for Investigation of Amblyopic Patients”

Supervisor:

- Prof. Dr. Constanţa Ganea (UMF “Carol Davila” - Bucharest, Romania)

Thesis Submission Date: .....

This work was partially funded by research grants *Deutscheforshungsgemeineschaft DFG SI 344/17-1,2,3* (to Ruxandra Sireteanu, Germany) and *CNCSIS TD-48/2008* (to Adrian Iftime, Romania).

## Abstract

Amblyopia is a developmental disease of visual system; it may appear as a result of an early exposure in life to an abnormal visual experience (strabismus, anisometropia, visual deprivation etc.).

Usually only one eye is affected, patients complaining of reduced visual acuity, reduced contrast sensitivity and loss of stereopsis. Additionally, some patients report anomalous perceptual experiences (spatial distortions and temporal instability of the percept). These strange experiences were described only in qualitative terms. This PhD thesis suggests new psychophysical methods devised to describe them in quantitative, measurable terms.

We have analyzed three broad categories of data: a) spatial mis-localizations, b) reported spatial distortions and c) reported temporal instabilities of particular geometrical stimuli. For each of these categories, we proposed new methods for measurements, and we obtained the following novel results:

**a) investigation of spatial mis-localizations (CEXGRAPHER and DISIM methods)**

- we showed that a deep acuity loss and a history of strabismus are related to increased spatial displacements and higher spatial uncertainty

- we found that subjects that have significantly higher spatial uncertainties tend to experience temporal instability of percept

**b) investigation of reported spatial distortions (ENTPACK and ENTGRID methods)**

- we found that an exposure to static high frequency gratings ($\geq$ 1.6 cycles/degree) is a better way to elicit the appearance of distorted perceptions in amblyopic subjects. The spatially distorted percept does not always occur at lower spatial frequencies.

- we observed that the spatial distortions are not evenly distributed in the visual field, but very often confined to a central ellipsoidal area; we proposed a 3D model of the visual field in order to explain this phenomenon

**c) investigation of reported temporal instabilities (ENTPACK-TEMP and TEDI methods)**

- we were able to observe that the static stimuli with higher spatial frequencies tend to yield temporal instabilities more frequently than other stimuli.

- the temporal instabilities present themselves as cyclical phenomena, with frequencies < 2 Hz, for almost all the cases that we investigated

- In our data sets, we could observe and classify two kinds of temporal instabilities:

- *cyclical variations;* vast majority of the subjects reports them; these could be described as vibrating edges, oscillations like back-and-forth movements or increasing / decreasing of apparent size of features in the visual fields (blobs, foggy areas, etc). These can be measured by our proposed methods.

- *drifting motions;* these are hard to describe; the patients have the impression that the image is continuously, endlessly moving in one direction.

# Contents


**I Introduction to amblyopic visual problems 10**

**1 Amblyopia 11**

1.1 The Problem . . . 11
1.2 Definition of Amblyopia . . . 11
1.3 Aetiology . . . 12
1.4 Basic pathology . . . 14

**2 Visual Deficits in Amblyopia 15**

2.1 Visual acuity . . . 15
2.2 Contrast Sensitivity . . . 18
2.3 Visual Field . . . 20
2.4 Particular perceptual problems . . . 22

**II Analysis of spatial mislocalizations 26**

**3 Introduction to “Circle Experiment” 27**

**4 “CEXGRAPHER” METHOD 30**

4.1 Purpose . . . 30
4.2 Materials and Method . . . 30
4.3 Results . . . 36
4.4 Discussion and Conclusions . . . 44

**5 “DISIM” METHOD 46**

5.1 Introduction . . . 46
5.2 Materials and Method . . . 46
5.3 Results . . . 51
5.4 Discussion and Conclusions . . . 55

**III Analysis of subjective spatial distorted images and temporal instabilities 57**

**6 Recording distortions (brief introduction) 58**

**7 ENTPACK - Analysis of static distortions 63**
7.1 Introduction . . . 63
7.2 Materials and Method . . . 64
7.3 Results . . . 67
7.4 Discussion and Conclusions . . . 68

**8 ENTGRID - Localization of distortions 69**
8.1 Introduction . . . 69
8.2 Materials and Method . . . 69
8.3 Results . . . 71
8.4 Discussion and Conclusions . . . 72

**9 ENTPACK-TEMP Method 78**
9.1 Introduction: Analysis of recorded temporal instabilities . . . 78
9.2 Purpose of using the ENTPACK-TEMP method . . . 78
9.3 Materials and Method . . . 79
9.4 Results . . . 80
9.5 Discussion and Conclusions . . . 84

**10 TEDI Experiment 85**
10.1 Purpose . . . 85
10.2 Materials and Method . . . 85
10.3 Results . . . 90
10.4 Discussion and Conclusions . . . 91

**IV Conclusions 92**

**11 Summary of the original contributions 93**

**12 Publications related to this thesis 98**

**Bibliography 100**

# Dedication

*This thesis is dedicated to my family and my uncle Eugen Ionel, the engineer who taught me how amazing the wonders of Nature are. He gave me a living example on how to find delight and heart-warming experiences in everything that surrounds us.*

*I am grateful to my Teachers who chiseled my thinking and helped me to see the world in different, original ways: Ing. Serban Derlogea and Prof. Dan Eremia.*

# Acknowledgments

This work wouldn't have been possible without the guidance, help and support from a lot of people.

*Prof. Ruxandra Sireteanu* (Max Planck Institute for Brain Research & JW Goethe University - Frankfurt/Main) was my principal supervisor. I am very grateful for being accepted as a PhD student under the guidance of such a world renowned specialist. Through long and thoughtful discussions she shaped and clarified my ideas on the subject. She constantly amazed me with an extraordinary care for even the minute details of our work. Unfortunately a tragic accident stopped prematurely her broad activities.

*Prof. Constanta Ganea* ("Carol Davila" University of Medicine, Bucharest) is my other supervisor. She kindly and generously allowed me to use the scientific computing infrastructure of her lab. Without her constant, gentle advices and support this thesis wouldn't have been completed, especially in the dark days after the tragic loss of Prof. R. Sireteanu.

I thank *Prof. Wolf Singer* (Director, Max Planck Institute for Brain Research) for moral and logistic support. Without his hospitality this work would not have been possible.

Most of the experimental data on human subjects was collected in the Psychophysics Labs of Max Planck Institute for Brain Research and Goethe University - Frankfurt, by PhD co-workers: *Dr. Claudia Baeumer* and *Psych. Aylin Thiel*. I thank them for their enthusiasm and remarkable managerial efforts. Working together with them and solving countless of encountered problems was a truly Bildungsroman for me.

A lot of laboratory-related problems were solved and orthoptics examinations were carefully performed by the following hard-working orthoptists: *Doris Baldauf, Iris Bachert, Licia Cirina* and *Peggy Feige*. I thank them for teaching me subtler details of their craft.

I have received useful solutions, numerous advices from *Dr. Ing. Bhaskar Choubey* (Oxford); his serious but light-hearted approach to difficult subjects inspired me to continue the work despite adversities.

Many thanks for my colleagues *Dr. Alina Jurcoane* (Frankfurt) and *Dr. Anca Popescu* (Bucharest) who inspired me with their intelligence and a positive, problem-solving attitude.

I thank our *subjects* for their patience for the long hours spent in our labs. We are confident that their efforts were not in vain and they helped the advancement of the knowledge in this field. Due to ethic regulations, they shall remain anonymous here.

I have received brilliant hints from three engineers: *Raul Muresan, Vlad Moca* and *Ovidiu Jurjut*; I am very fortunate to have such very good friends who also cheerfully discuss any kind or difficult topics.

I thank to *Dr. Eva Katona* (Bucharest) who gave me valuable counsels regarding administrative and health-related tasks and to *Dr. Sonia Herman* for a generous donation of laboratory equipment.

Finally, I want to express my gratitude to all my friends who helped me in various ways and patiently waited for this work to be completed.

The work described in this thesis was completed in three different locations:

1. *Max Planck Institute for Brain Research, (Psychophysics Lab)*, Frankfurt am Main, Germany

2. *Goethe University, (Physiologische Psychologie / Biopsychologie)*, Frankfurt am Main, Germany

3. *Carol Davila University of Medicine* (*Biophysics Department*), Bucharest, Romania.

The patients and control subjects were investigated in locations *1* and *2*, and most data analysis and modeling was performed in location *3*.

Parts of this work were funded by research grants *Deutscheforshungsgemeineschaft DFG SI 344/17-1,2,3* to Ruxandra Sireteanu and by *CNCSIS TD-48/2008* to Adrian Iftime. The author received a bursary from *European Biophysical Societies' Association* to support presentation of work described in Chapter 7 at EBSA 2007 Conference.

# Part I

# Introduction to amblyopic visual problems

# Chapter 1

# Amblyopia

## 1.1 The Problem

Amblyopia is one of the most frequent visual disabling condition of youngsters, with 2-4% prevalence in general population (DUKE-ELDER/WYBAR, 1973). Within the general public it is known (incorrectly) as "lazy eye", due to inability to see clearly with the affected eye, despite any attempts to correct the vision with spectacles.

The disease is known and described from ancient times: in ancient Greek, amblyopia means literally "blunt eye". In spite of its long history, the usual ophthalmological investigation procedures are still incomplete or inadequate for the particular problems of this disease (GREENWALD/PARKS, 2000).

The present work aims to improve the existing exploratory methods and to introduce new ones (especially in analyzing temporal aspects of amblyopic vision). We attempt to introduce methods that are able to quantify these problems in an objective way.

We hope that these new methods can be used to further increase medical knowledge about this disease, and to better monitor its evolution in time.

## 1.2 Definition of Amblyopia

Traditionally, amblyopia is defined as a decrease in visual acuity in one or both eyes, in spite of apparent normal optical media, normal retina and normal optic nerve. We shall see that there is a broad range of visual deficits in addition to loss of visual acuity (see Chapter 2).

We know that it appears in childhood during the growth of nervous visual system (first 10 years of life), in the kids with initial ocular problems which are not promptly cured (VAEGAN, 1979). If the disease appears, it is very likely that it will persist for the entire life, even if the initial ocular problem is cured or disappears afterwards. Because

of this persistence in spite of normalized optical structures, it is believed that amblyopia is a disease of the visual nervous system.

Usually, the amblyopia is diagnosed by exclusion: if a patient have visual deficits that cannot be explained by ocular and retinal problems, or by a clear nervous lesion (tumor, stroke etc), and also had some severe ocular problems in childhood, then gets diagnosed with amblyopia. Therefore this term covers a large number of possible causes. We outline them in the section below.

## 1.3 Aetiology

The known pathological conditions that leads to amblyopia are:

i) impossibility to obtain two clear, equivalent images on the two retinas;

ii) impossibility to simultaneously focus both eyes on the same object.

These two conditions have a single outcome: the exposure of visual system to two images that cannot be fused together in a single, meaningful percept. As a result, the brain makes a dramatic choice: it uses only the input from one eye (called dominant eye) and suppresses the visual input of the other.

From a clinical viewpoint, these two mechanisms can arise single or in combination, and usually they are described in the following categories:

### *a) Strabismus (Squinting)*

It is the permanent or temporary inability to fixate the same object with both eyes. So, on each retina, a completely different image is formed, and they cannot be fused in a single image. There are several strabismus types, listed in Fig. 1.1 (a). Only 35-50% of the strabismic kids develop amblyopia (LEVI/CARKEET, 1993). Probably there are also some other factors involved, like the genetics, the age of onset of strabismus (the earlier the worse) or type of strabismus.

Convergent strabismus (esotropia) is more amblyogenic than the divergent one (exotropia).

### *b) Optical problems*

The failure of ocular refractive media leads to blurred images on the retina.

Anisometropia is defined as a strong difference in optical characteristics of both eyes, for instance: one eye is optically sound and produces a clear image on the retina, but the other has a problem that cannot be naturally compensated and will produce a blurred image - Fig. 1.1, (b).

A difference of 1...3 Diopters, if left untreated, can lead to amblyopia; also this can develop if both eyes cannot produce clear images (JAMPOLSKY et al., 1955).

Hypermetropia is more amblyogenic than myopia. In the latter, even if severe, the patient can still obtain a clear image if he / she brings the object very close to the eye. Thus the patient still has a chance to obtain - at least temporarily - two clear, equivalent retinal images.

In the case of severe bilateral optical aberrations, hypermetropias greater than +6 diopters tend to end up in an amblyopia. Astigmatism, if severe and left untreated, can cause a rare form of the disease, called *meridional amblyopia*. This is often under diagnosed because it has small negative effects on standard visual acuity, as measured in clinical settings (GREENWALD/PARKS, 2000).

## c) Occlusion

The term refers to interruption of light propagation in its way to retina e.g. by palpebral ptosis (congenital dropping of upper eye lid (see Fig. 1.1.c), congenital cataract (see Fig. 1.1.d ), abnormal vitreous body vascularization, corneal scars acquired as infant, etc).

Lens opacities bigger than 3 mm in diameter are extremely dangerous if left untreated in childhood; they produce a diffuse illumination and unclear images on the retina, continuously. Even accidentally acquired cataracts, at an age 6 to 8 years can lead to a severe amblyopia if not treated as soon as possible (PARKS, 1982).

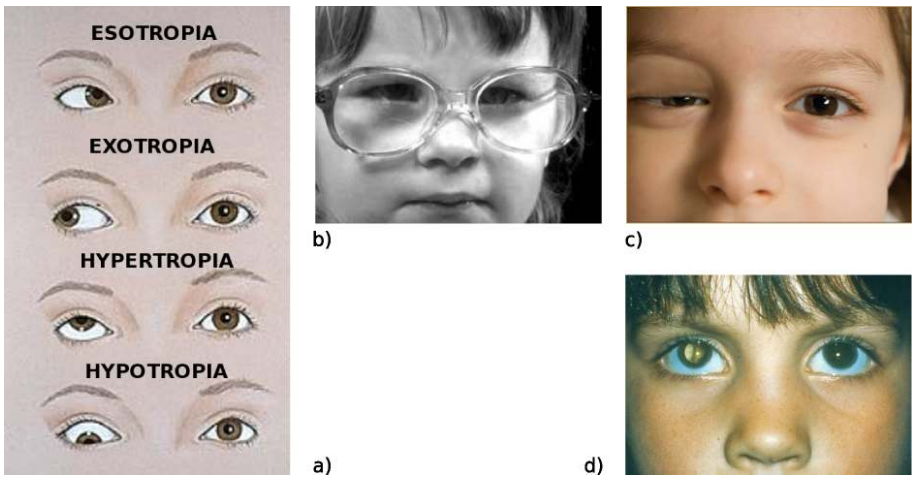


Figure 1.1: Clinical conditions that can lead to amblyopia. a) different types of *Strabismus* b) *Anisometropia* c) *Blefaroptosis* d) *Cataract* (in all examples, the right eye is the affected one)

## 1.4 Basic pathology

The above classification is a formal one; usually the physician is confronted with combinations (e.g.: strabismus + anisometropia), or with severe cases aggravated by unsuccessful treatments (e.g. convergent strabismus converted in divergent strabismus after eye surgery).

As a consequence of these unfortunate conditions, the infant cannot fuse the two retinal images into a coherent single percept; he / she is thus exposed to a confusing visual experience: *diplopia* (double vision) or even worse, a confusing fog that won't go away, covering the world. If left in this state, without medical intervention, the visual system chooses only one eye as a primary input, and actively **suppresses** the other eye.

Usually, the suppression is definitive (lasts for the entire life) and affects a single eye (the non-dominant eye). There are situations where the suppression is alternating (the patient uses one eye or the other, alternatively) without being necessarily conscious about this phenomenon.

The suppressed eye (now amblyopic) can be used if the patient voluntarily does not use the sound eye, for instance if he / she voluntarily covers the good eye and explore the world using the amblyopic eye. The quality of resulting visual perception is diminished, sometimes quite dramatically; this particular percept is described in a greater detail in the next chapter.

If, by an unfortunate accident, the patient loses the good eye, he / she is forced to use the remaining amblyopic eye. Therefore, it is very important to be able to understand these patients fully; their perceptual problems are special, and they need to be approached with special means.

# Chapter 2

# Visual Deficits in Amblyopia

The amblyopic percept is difficult and hard to describe; the best information we have so far are from the patients with unilateral amblyopia. They can use the good eye and bad eye alternately, and have two distinct perceptual experiences (the normal one and the amblyopic one). The patients describe qualitative differences which cannot be explained or corrected with optical correction aids (spectacles, prisms, etc).

These problems are difficult to be accounted for, even by specialists or researchers; an accurate description of these problems is hard to make only with standard acuity tests (GREENWALD/PARKS, 2000). In the following pages we will briefly describe the problems occurring in:

1) visual acuity

2) contrast sensitivity

3) visual field

4) particular perceptual problems.

## 2.1 Visual acuity

### Definition of visual acuity

Visual acuity is a measure of clearness of vision; it is dependent on two factors: a) the proper optical focusing within the eye and b) the ability of the nervous structures to analyze, transfer and interpret the optical information. Usually is measured with the help of printed black symbols on a white chart shown to the subject at a standardized distance. There are different variations of the charts, the most common used for testing adults being:

- the Snellen chart (letters)

- Landolt C-rings (broken rings with different orientations)

- Tumbling E charts (symbols like letter E, with different orientations)

An average normal sighted person is defined as having a normal vision (100% or 1.00). This translates in being able to see and distinguish details separated by 1 arc minute. The charts have symbols with calibrated sizes so they will be properly seen by a normal sighted person when seated at 6 meters apart (or the equivalent 20 feet, in U.S.).

The measured visual acuity is expressed as a ratio, e.g.: 6/6 meaning that the tested person is able to see the symbols from 6 meters, like an average person (so he / she has a normal vision). A ratio like 3/6 meaning that the tested person is only able to see the symbols if comes closer, at 3 meters, instead the 6 meters; this person has a lower acuity, only 50% of the normal vision. Depending on the country, the same visual acuity can be expressed as a metric ratio (e.g. 3/6), an imperial ratio (e.g. 10/20), by its decimal equivalent (e.g. 0.50). These are widely used by clinicians, and we used them in the present study (expressed as decimal numbers).

In the following pages we will deal with the problems that affect some subtler aspects of the visual acuity in amblyopia: simple acuity loss, crowding, grating acuity, vernier acuity.

## Vision acuity and amblyopia

The amblyopia patients have a visual acuity deficit as measured in clinical settings (with acuity charts - optotypes). We shall remember that clinical diagnostic of amblyopia is held: a) if the acuity is less than normal (i.e. 20/20), which cannot be explained by ocular deficits and b) if the patient had visual problems in childhood.

Their acuity loss is exacerbated by spatial distortions (see section 2.4 on page 22), and sometimes clinicians find it difficult to distinguish clearly between these two forms of amblyopia.

### 2.1.1 “Crowding” - the contour interactions problems

It is already well known (FLOM/WEYMOUTH/KAHNEMAN, 1961) that amblyopic patients find it difficult to recognize shapes (e.g. letters) if they are presented more than one, closely spaced together (in rows or columns, like in normal texts).

For instance, an amblyopic patient with an apparent normal visual acuity (20/20) for single letters, may well have a sharp fall in acuity (20/100) if several letters are presented together. This phenomenon is known as “*crowding*” or “*contour separation / interaction deficit*”.

This appears in amblyopia if the distance between the edges of the shapes (in foveal

image) is less that 1-3 min / arc. It is believed that this problem of amblyopic vision is caused not by anatomical problems, but physiological ones - the spatial summation and lateral inhibition (that normally occur during the processing of visual images).

### 2.1.2 Grating acuity

Gratings are specially crafted images (usually black and white or various grey shades) that are used in visual psychophysics (see Fig. 2.1).

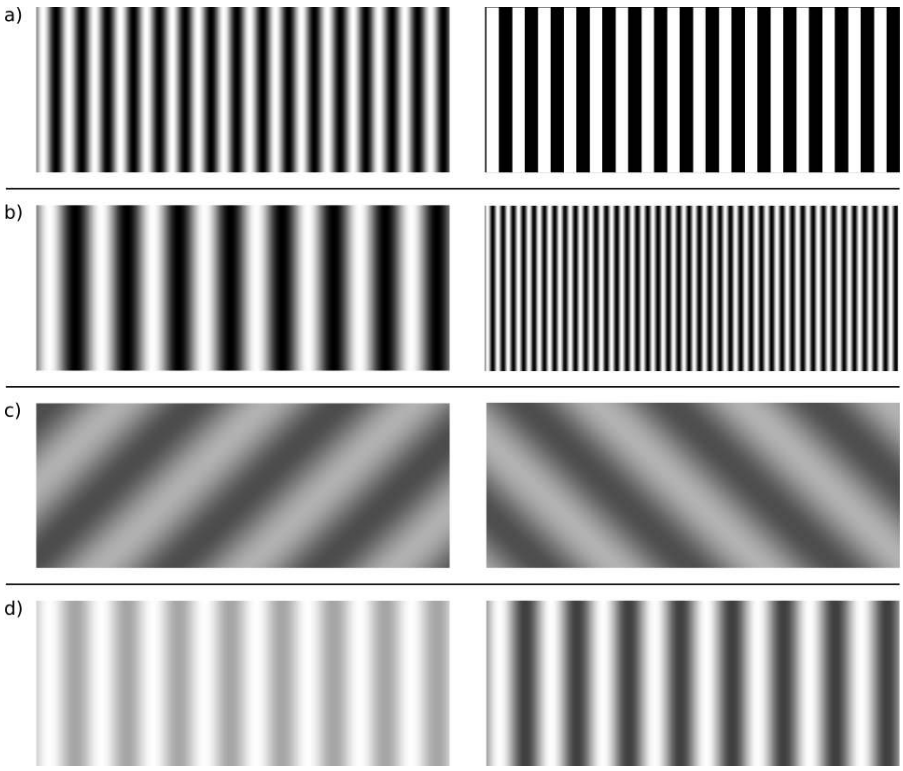


Figure 2.1: Different grating types. a) sine-wave vs. square-wave b) low frequency vs. high frequency c) different orientations d) low contrast (35%) vs. higher contrast (75%)

The gratings simplify the investigation of visual acuity, addressing one subtle problem of the optotypes: the classical acuity cards (Snellen, Landolt C-rings etc) test two functions at once: a) contour detection and b) form recognition. Accurate form recognition depends on higher cerebral functions, learning and experience (for instance, one cannot test illiterate individuals or infants with letter-based cards). The use of grating-based stimuli eliminates the recognition step. They also present the benefit of testing contrast sensitivity (see below).

The most used gratings are those based on cyclical mathematical functions. The amplitude of a function can be used to modify the luminosity in a image, along one chosen axis. The elements of the obtained stimuli are:

a) function (sinusoidal - smooth transitions between maximum and minimum, and square-wave - black and white stripes, with clear edges) (Fig. 2.1.a)

b) frequency (usually expressed in cycles / degree of visual angle) (Fig. 2.1.b)

c) orientation (usually expressed in degrees from vertical meridian) (Fig. 2.1.c)

d) contrast (the absolute difference between the maximum and minimum luminosity or black coverage) (Fig. 2.1.d)

A normal person has a peak grating acuity of approx. 30-40 cycles per degree at optimal contrast.

Some amblyopic patients, *especially those with strabismus in history*, have differences between the visual acuity measured with classical optotypes (Snellen) and with gratings (MAYER/FULTON/RODIER, 1984).

Also, there are subtler perceptual problems from them: even if they can detect the grating, some describe the uniform patterns of the image as being deformed, non-regular (HESS/CAMPBELL/GREENHALGH, 1978). These peculiar problems are described in depth ( 2.4 on page 22)

### 2.1.3 Vernier acuity (continuity detection)

The ability to detect if two lines are collinear is called vernier acuity.

The vernier acuity is reduced in strabismic amblyopia (even more reduced than grating acuity). This difference is generally not present in anisometropia amblyopic patients (LEVI/KLEIN, 1982). This is another argument which strongly suggests that neurological deficits are the root of the problems in amblyopic vision, and that there are differences in these deficits, according to the aetiology.

## 2.2 Contrast Sensitivity

Human visual system can perceive a large range of spatial frequencies. But for a given spatial frequency, the stimulus is perceived only if there is a certain difference between the maximum and the minimum luminous intensity, across the length of the stimulus. The difference between the extremes is called the contrast of the stimulus (see Fig. 2.1.d for examples of contrast 35% vs. 75%). The contrast is created by the difference in luminance (the amount of reflected light) of two adjacent surfaces. It can be defined in different ways; the Michelson formula is used in clinical work (we also used it in this work):

$$Contrast = \frac{L_{max} - L_{min}}{L_{max} + L_{min}}$$ ($L_{max}$, $L_{min}$: maximum and minimum luminance)

Humans are able to see a stimulus clearly only if it has a certain contrast to surrounding areas. It has been found that this contrast threshold is not absolute for all stimuli. It varies with geometrical properties of the stimulus, especially with its spatial frequency (i.e. how dense the geometry is).

Figure 2.2: Different contrasts for the same stimulus. The left image has 100% contrast, the subsequent images have half of the previous (50%, 25%, 12.5% and 6.2%). The lower the contrast, the more difficult it is for us to perceive it.

If the last seen contrast is plotted against the spatial frequency of the stimulus, a typical curve is obtained. This is known as "contrast sensitivity measurement". The majority of healthy adults have a sensitivity peak at stimuli with frequencies around 3 to 6 cycles / degree (i.e. these stimuli are well perceived, even if they have a very low contrast to surrounding areas). The sensitivity gradually decreases at different frequencies (ARDEN, 1978). In current ophthalmological investigations, contrast sensitivity is measured with VCTS charts from VisTech Consultants, Dayton, OH. These are standardized stimuli (sinusoidal gratings) of different contrasts.

Investigation of contrast sensitivity in amblyopic patients shown that they have some perception deficits (if compared with healthy individuals). Their problems were initially classified in two broad categories (HESS/HOWELL, 1977):

- *amblyopia type I*: contrast sensitivity is reduced only for higher spatial frequencies (i.e. the patients do not perceive high frequency gratings with low contrast as well as healthy subjects).

- *amblyopia type II*: contrast sensitivity is reduced for both lower and higher spatial frequencies (i.e. the patients do not perceive very well all low contrast gratings as well as healthy subjects).

These problems are present only in the amblyopic eye, not in the sound one. There seems to be no relationship between aetiology and type I or II, or any other association with clinical features or history (GREENWALD/PARKS, 2000).

- *amblyopia type III*: bilateral contrast sensitivity loss (contrast sensitivity was subnormal in both eyes). This is a novel finding, published very recently (SIRETEANU/BAEUMER/IFTIME, 2008)

## 2.3 Visual Field

The visual field is the portion of physical space which is visible during steady fixation of gaze in one direction. The monocular visual field consists of:

- central vision, which includes the central fixation point (i.e. where the patient is looking at) and the inner 30 degrees of vision (roughly symmetrical)
- the peripheral visual field, which extends 100 degrees laterally, 60 degrees medially, 60 degrees upward, and 75 degrees downward. (WALKER/HALL/HURST, 1990)

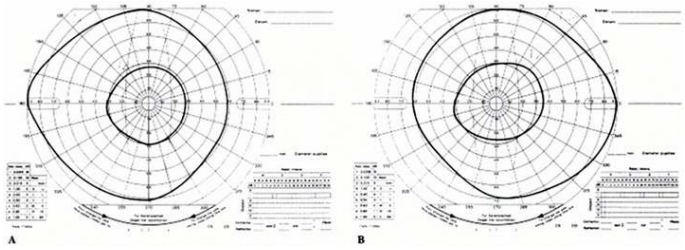

(a) The spread of normal visual field. Inner black line: central visual field. Outer black line: periphery of the visual field (outside this line there is no vision).

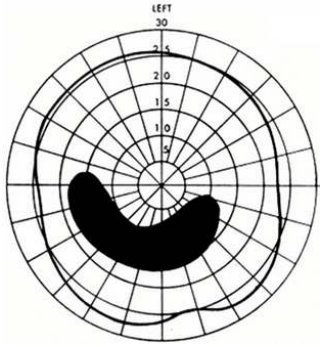


(b) Pathological visual field: an inner arcuate scotoma (loss of vision confined in the black region)

Figure 2.3: Maps of normal and pathological visual fields (WALKER/HALL/HURST, 1990:)

Usually, the extent of the visual field is depicted in a graphical form as a polar coordinate map, with the centre corresponding to the fixation point, and with circles and radii drawn to ease the localization. A normal extent of the visual field is shown in Fig. 2.3a. If there is a visual problem which affects only portions of the entire field, its position is marked (e.g. Fig. 2.3b).

In the sections below we will briefly present the amblyopia influences on visual field.

### 2.3.1 Deficit spread in the visual space

In the previous sections of this chapter, the following problem was not addressed: are the amblyopic deficits affecting the whole visual field of the eye, or are they confined to some specific parts?

Research addressing this question started in the '80s, as investigation techniques were more and more refined. Answering this problem is difficult because the deficits are subtle and hard to catch without a special experimental setup. In addition, some patients cannot maintain a fixed eye position enough time - as required by standard procedures for visual field investigation.

These mapping techniques are used for analyzing the visual field (sector by sector or point by point) while the subject is required to fixate an immobile target with his eye. In this way, it is possible to say that in a particular sector of the visual field, the visual acuity is different than in others. It is possible to investigate several other features in addition to acuity, like the ability to precisely locate a target, vernier acuity, etc.

It was found that the amblyopia mainly affects the central zone of the visual field. For the same visual acuity, the anisometropic amblyopia patients have a bigger area of visual loss than those with strabismus in aetiology (HESS/POINTER, 1985).

### 2.3.2 Spatial uncertainty

It has been found that the amblyopia patients cannot always tell precisely the position of a target in the visual field (i.e. they know that there is an object, but cannot tell its exact location).

This particular phenomenon was called "*spatial uncertainty*", and appears more frequently in strabismic amblyopia patients (BEDELL/FLOM, 1983).

The functional differences between sectors of visual field can be investigated using several techniques:

1. Collinear alignment tasks
2. Distortions maps

***Collinear alignment tasks***: the patients are required to arrange several scattered distributed stimuli in a vertical line (between two fixed targets). It has been found that if they are using the amblyopic eye, they will arrange targets on a curve, not on a line. This shows that the functional performance of the amblyopic eye is different in the centre of the visual field (as compared with the sound eye) (FRONIUS/SIRETEANU, 1989).

***Distortion maps***: these are more sophisticated procedures which yield bi- dimensional charts of the localization deficits (Fig. 2.4). In these procedures, the subject looks monocularly to fixed points symmetrically distributed in space, with sound eye or amblyopic eye. The subject perceives the localization of the points in shifted positions when he looks with the amblyopic eye. The shifting pattern is neither isotropic nor specific. It was possible to demonstrate that the strabismic amblyopia patients have spatial localization deficits that are more severe than those with other aetiologies.

Also, these maps show that each subject tends to have a quite specific distortion pattern (LAGREZE/SIRETEANU, 1991). In this work, we propose improvement to this method; see Chapter 3 on page 27.

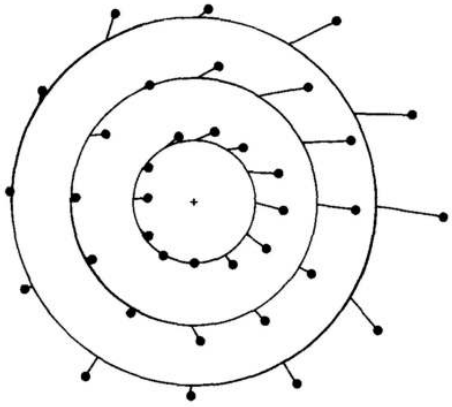

Figure 2.4: A distortion map example. Correspondence pattern of subject S.M. Solid symbols indicate loci in the amblyopic eye corresponding to the 36 positions in the dominant eye (connected by lines). Figure from Lagreze and Sireteanu, 1991.

These two techniques (alignment tasks and distortion maps) are very interesting because can easily provide a striking comparison between the sound eye - amblyopic eye (in amblyopia patients), and between sound eye (amblyopic patients) - normal eye (control subjects). This double comparison brings in a bridge in the understanding of amblyopic percept.

Lagrèze & Sireteanu (1991) have shown that there are no significant differences (for localization tasks) between the healthy control subjects and amblyopia patients - if they are using their sound eye [idem]. So it seems safe to assume that *all the functions are normal in the sound eye of the amblyopic patients*.

This leads to the conclusion that we can reliable use their description of perceptual differences between good eye and bad eye.

In the present thesis, we will describe our improvements to this mapping method and also some new comparison methods, in Chapter 4, starting on page 30.

## 2.4 Particular perceptual problems

*An important note for the clinician ophthalmologist or optometrist*: in our studies we have found that some patients are sometimes shy or unsure about describing their strange perceptual experience. If they are only routinely investigated, and not specifically asked, they tend to skip over the description of these particular problems, leaving

the investigator clueless. We are giving below a short review of these problems: a) spatial distortions, b) temporal instability of percept.

### 2.4.1 Spatial distortions

In addition to all clinical problems described above, some of amblyopia patients can report accurately some strange alterations of their visual percept (when using the amblyopic eye): changes in the shapes of the objects and changes of their contrast.

For instance, subjects investigated in a study (PUGH, 1958) described the following deformations in the stimuli presented (letters): the edge was perceived as jagged, rubbed, unclear in some portions; the circular forms were flattened and sometimes with a diminished contrast (i.e. black shapes tended to appear greyish). These distortions were not symmetrical or evenly distributed.

Using the gratings as stimuli, the subjects describe sometimes big deformations in symmetry and their regularity (HESS/CAMPBELL/GREENHALGH, 1978).

Since the 80s it has become clear that the spatial distortions perceived by the patients are the key element in the amblyopic vision, especially in those with strabismus in aetiology (BEDELL/FLOM, 1981).

Recent studies have shown that the amblyopic patients have spatial distortions especially at higher spatial frequencies of the stimuli. The most frequent distortions were: blurring of some visual field areas; missing portions from the image (apparent scotoma).

In the stimuli with lower spatial frequencies the stripes in the gratings are perceived as being unevenly distributed, and they seem to be bent (they are not perceived as vertical), or have different oddities, unexplainable by mere optical problems (SIRETEANU/

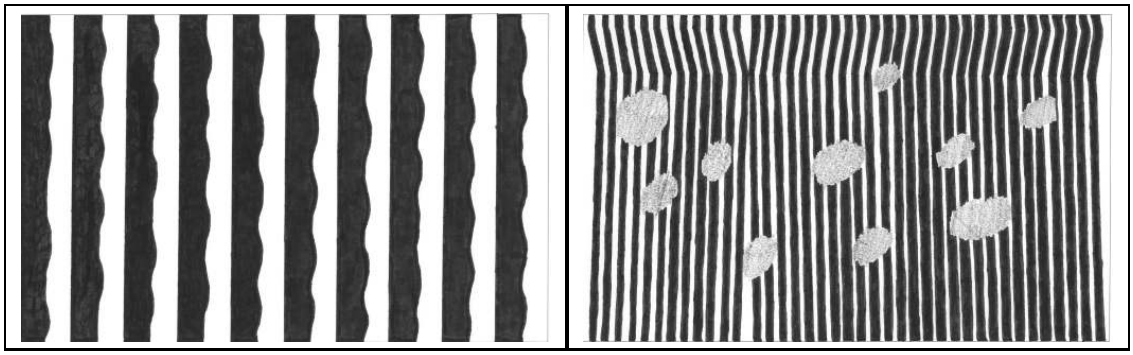

Figure 2.5: Examples of spatial distortions, as recorded by Psych. C. Baeumer, Max Planck Institute for Brain Research. *Left*: patient S.B; *Right*: patient B.B. The images are their descriptions of amblyopic percept, while observing black-and-white regular stripes printed on paper.

LAGREZE/CONSTANTINESCU, 1993). For the clarity of the text, we present here two such recorded descriptions, see for example Fig. 2.5, from BAEUMER, 2005).

Another attempt to search these distortions compared them with the available psychophysical data (LAGREZE/SIRETEANU, 1991; or for a first attempt to recreate digital versions see SIRETEANU/LAGREZE/CONSTANTINESCU, 1993).

The objective visual mapping procedures (described above) seem to show bigger distortions than those subjectively reported by the patients. This is perhaps due to the fact that different cortical functions are used in each experiment (recognition, memory, hand-eye coordination, etc.).

The attempt to quantify the subjectively reported distortions also led to this approach: it had been proposed that the distortions should be classified in broad (yet consistent) categories. Using standardized gratings it had been found that about one out of three patients does not have spatial distortions problems, but the other 2/3 have (BARRETT et al., 2003). The researchers classified the problems in five big classes (which can appear alone or in combinations):

- a) straight lines appear wavy;
- b) edges of the lines appear jagged;
- c) erroneous orientations;
- d) fragmented percept: lines appear broken (with discontinuities)
- e) missing fragments from the visual fields (scotoma; important: they are functional, i.e. not produced by retinal or neurological lesions);

Very interestingly, these phenomena are not constant over a broad range of stimuli; they show up for particular stimuli and disappear for others (i.e. at a spatial frequency, a subject can report distortions from a class, and at other spatial frequency, a different class of distortions).

### 2.4.2 Anomalous colour perception

In a recent study (SIRETEANU/BAEUMER/IFTIME, 2008) it has been reported that some amblyopic subjects have colour anomalies in perception of black and white high spatial frequency patterns. The authors reported two types of colours phenomena occurring on the edges of black-white lines:

- in the first one, all kinds of colours in the rainbow spectrum were perceived.
- in the second, only one or two colours (green, red, yellow, or blue) were reported.

The authors also observed that anomalous colour perception was accompanied by a temporal instability of perception.

### 2.4.3 Temporal instability of percept

In addition to what was described above, some patients report that their perceptions are not stable in time (over a short period of time) (BARRETT et al., 2003).

These peculiar things was briefly mentioned in several amblyopia studies, see HESS/CAMPBELL/GREENHALGH (1978); SIRETEANU (2000).

Some amblyopia patients describe the images seen through the amblyopic eye as moving ("as through hot air") - even if they are conscious that the images itself are static (SIRETEANU, 2000).

Very recently, using sophisticated digital and psychophysical techniques, it became possible to reproduce qualitatively these perceptions as short animated movies (BAEUMER, 2005). A part of the present thesis is dedicated to a quantitative approach to these phenomena ( see III, starting on page 57).

It is important to stress that these problems described are not related to the real motion perception (i.e. how patients see moving objects). Motion perception studies yielded these results:

-patients have a deficit in flicker perception (see footnote: flicker: rapid alternation of dark and light stimuli); it depends on spatial properties of the stimulus (e.g. its size / area occupied in the visual field), but also on the severity of amblyopia (BRADLEY/FREEMANN, 1985).

- a performance decrease in a temporal integration tasks; it has been also observed a correlation of the deficit with the severity of amblyopia (ALTMANN/SINGER, 1986).

To dispel some possible confusion, we are giving now some concise explanations for the relevant terms:

- "temporal instability" - the patients report that they observe a false movement of a static stimulus; i.e. their perception is unstable over a given time span. We do focus on these features, starting with chapter 9.

- "motion perception" - how the patients are seeing a stimulus that moves (dynamic stimulus). We are not investigating / describing these phenomena in this work.

# Part II

# Analysis of spatial mislocalizations

# Chapter 3

# Introduction to “Circle Experiment”

It has been observed that the amblyopic patients found it difficult to precisely locate objects in the visual field (see 2.3.2 on page 21). In order to finely investigate these phenomena, we used data collected by an exploratory “mapping” technique, named “Circle Experiment”. This is a graphical way of depicting the position of these deficits in the visual field of the patient. The method was developed by LAGREZE/SIRETEANU (1991). We used an improvement of the method (using a finer grain of the tested points and an improved testing protocol). The full protocol of this method was published by BAEUMER (2005).

In order to spare the reader’s time, we present here a very short description of the “Circle Experiment” mapping method.

The task of the subject was to remember the position of a target in the visual field; the target was removed, and the subject was asked to pinpoint its location, with the following protocol:

The subjects were asked to fixate monocularly a small cross (25 arcmin arm length and 4 arcmin arm width) at the centre of the screen, after which a circle centred on the fixation cross was presented for 5 seconds.

The radius of the circle could be 1°, 2°, 3°, 4°, 5° or 6° in the visual field. The subjects were asked to memorize the radius of the circle, after which they heard a number ranging from 1 to 12, similar to the hours on an analogue watch.

The task of the subjects was to move a small target (a disc with a diameter of 30 arcmin), under the control of the amblyopic or the dominant eye, from the fixation point to the imagined position on the memorized circumference of the circle. The test point could be moved only after the memorization period of 5 seconds was completed. The final position of the test point was recorded. The subjects were asked to keep fixation on the central cross throughout this procedure.

To ensure that the stimuli were visible only to one eye at a time, the subjects

wore red-green goggles. The stimuli on the screen were presented in colours perfectly matched to the colours of the goggles. The fixation cross and the circles to be memorized were shown only to the fixating eye, while the test dot could be shown to each eye in turn. The acoustically presented numbers, which indicated the angular position of the target, had been pre-recorded on tape. The numbers were heard through speakers placed symmetrically on the right and left of the screen. A control experiment ensured that all numbers could be understood perfectly by all subjects.

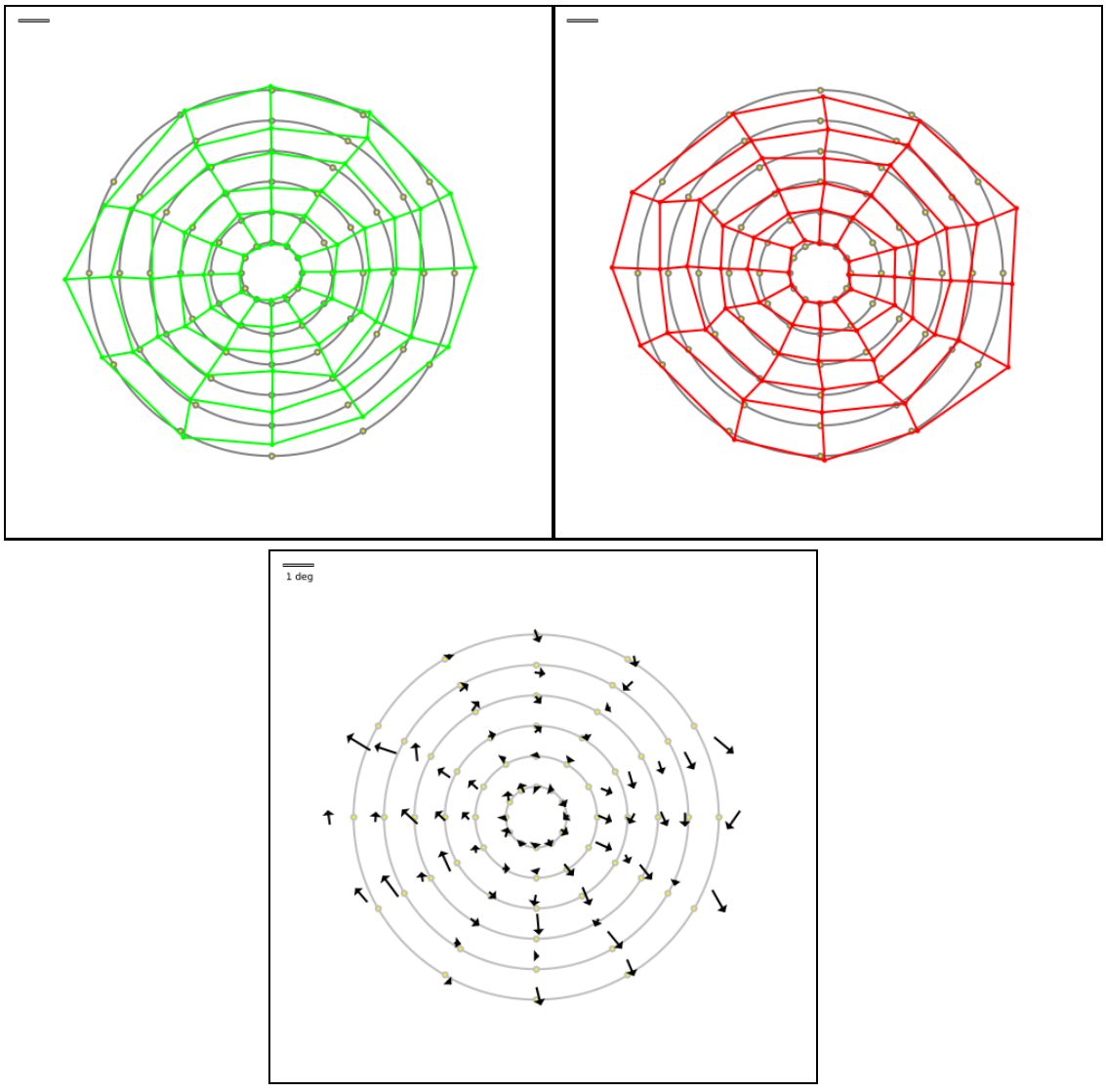


Figure 3.1: "Circle Experiment" mapping data sample from subject C.L. *Top-left*: dominant (sound) eye map. *Top-right*: non-dominant (amblyopic) eye map. *Yellow dots*: presented target positions; *Coloured dots (red/green)*: recorded positions. *Centre*: vectorial subtraction between left and right.

Data collection lasted approximately 1.5 hours per subject, with breaks whenever necessary. To avoid the effects of fatigue, the experiment was performed in the se-

quence ABBA in one experimental session and BAAB in the next. The observer's head was placed on a chin rest with a head-band, to ensure a fixed eye-to-monitor distance of 57 cm, all the time.

The radii of the circles, the different positions, and the colours corresponding to the two eyes were intermixed randomly. There were 72 target positions recorded in the visual field of each eye. Each target position was recorded five times for each eye. The total number of data-points collected per subject was 72 x 2 x 5 = 720.

Thus two maps are obtained for each eye. The normal sighted subjects have statistically similar mappings between the eyes; this is not the case with the majority of amblyopia patients.

The difference between the two eye maps can be synthetically expressed by a vectorial subtraction between the maps. In the Fig.3.1 we are giving an example of such maps, showing a torsion phenomenon in the horizontal portions of the visual field.

We present in this work two new improvements of this mapping technique:

- *"CEXGRAPHER" Method*: introduces new ways of analyzing mapping data obtained by "Circle Experiment". This is presented in detail in Chapter 4 on the following page.
- *"DISIM" Method*: uses the mapping data to automatically create spatial distortions in real-world images. This is presented in detail in Chapter 5 on page 46.

# Chapter 4

# “CEXGRAPHER” METHOD

## 4.1 Purpose

The original “Circle Experiment” setup provides valuable mis-localization information: it allowed researchers to see the localization errors in a graphical way, as a displacement map (see Fig. 2.4 on page 22). Due to technical limitations this method a) could only provide a low-resolution distortion map and b) it could not give information about how difficult was for patients to locate the targets when using the amblyopic eye. We pursued a method to address these issues.

In order to explore in depth the information provided by improved mapping techniques, we propose a different data analysis procedure, named “*CEXGRAPHER*”. The acronym comes from “*C*ircle *Ex*periment *Graph*ic Mak*er*). In the following pages we are using the term “spatial uncertainty” as the amount of difficulty in locating a target, and we suggest here that this entity can be measured.

## 4.2 Materials and Method

### Subjects

We used volunteer subjects (adults with amblyopia and healthy individuals). They were recruited through leaflets distributed in the Goethe University (Frankfurt aM) and surroundings.

Exclusion criteria for all subjects were:

- neurological or psychiatric disorders
- colour deficiency
- use of medication.

All subjects underwent full refraction and orthoptic assessment before testing. The orthoptic measurements were performed by professional orthoptists. Corrected visual acuity (visus cc) for near was measured (C-Test; Oculus, Dutenhofen, Germany) at a 40-cm distance. Angle of squint was assessed with the simultaneous and alternate cover and prism tests for far and near fixation. Fixation was determined with the aid of a visuscope. Stereopsis was assessed with the TNO-test. For the evaluation of retinal correspondence, the subjects were tested with the Maddox cross in connection with dark and light red filters and with Bagolini striated glasses for far and near vision. Eye dominance for near was assessed with a cover test.

To be included in the study, the amblyopic subjects must:

- have little or no stereopsis (cut-off disparity was 250 minutes, measured with the TNO test) and
- have an acuity of not more than a 0.5 decimal acuity in the most affected eye, measured with the Landolt C test for single optotypes (1.0 corresponds to 6/6 visual acuity).

*Anisometropia criteria*: subjects were required to have a minimum difference in refraction of 1.5 D spherical equivalent between the two eyes.

Before psychophysical testing, the subjects' contrast sensitivity was tested for far (3 m) and near (40 cm). Testing was done monocularly using the Vistech Contrast Sensitivity Test (VCTS 600 charts).

Testing of the subjects was performed in accordance with the tenets of the Declaration of Helsinki. Written informed consent was obtained from all subjects after the nature and purpose of the study had been fully explained. The study was approved by the Ethics Committee of Goethe University (Frankfurt aM).

The orthoptic data of this group of subjects is given in Table 4.1.Ten naïve normally sighted observers aged between 21 and 40 years (5 women and 5 men) were included as control subjects.

## Data analysis

After completion of the standard "Circle Experiment" data gathering procedure, the raw data sets for *each eye* of the each participant consisted of:

- 72 positions of the presented targets (6 circles and 12 azimuths) - the targets are presented as yellow dots in Fig. 3.1)

| Subject | Gender, age | Eye | Refraction | Visus c.c. (near) | Fixation | Strabismus (sim. cover test) | Stereopsis | Corresp. | History |
|---|---|---|---|---|---|---|---|---|---|
| ***Strabismic amblyopes*** | | | | | | | | | |
| **M.K.** | male, 29 yr | RE*<br>LE | + 5.50 -4.00 / 145°<br>+ 5.00 -4.75 / 5° | 0.10<br>1.00 | temporal<br>foveolar | far +1½° + VD½°<br>near +1½° + VD¾° | negative, excl. RE | h arc | Strabismus from early childhood, occlusion at 5 yr |
| **D.S.** | male, 51 yr | RE*<br>LE | + 5.25 -2.50 / 100°<br>+ 4.50 -2.25 / 95° | 0.25<br>1.00 | fov. margin<br>foveolar | far ± 0°<br>near +4° - VD | negative, excl. RE | nh arc | Glasses at 6 yr |
| **L.P.** | female, 33 yr | RE<br>LE* | + 0.50 sph<br>+ 0.75 sph | 1.00<br>0.25 | foveolar<br>temporal | far -12½°+ VD 1°<br>near ~± 0° | negative, excl. LE | nrc | Occlusion at 4 yr, glasses until 15 yr, Turner syndrome |
| **A.F.** | female, 22 yr | RE<br>LE* | - 1.25 -2.00 / 85°<br>- 1.25 -1.75 / 105° | 1.00<br>0.32 | foveolar<br>temp. margin | far +3° - VD 1°<br>near +4½°- VD 1° | negative, excl. LE | h arc | Strabismus from early childhood, glasses and occlusion at 5 yr for one year |
| **G.P.** | female, 27 yr | RE*<br>LE | + 1.25 sph<br>+ 1.25 sph | 0.50<br>1.00 | 1° nasal<br>foveolar | far +1°<br>near +1° | negative, excl. RE | nrc | Occlusion at 6 yr, glasses at 7 yr |
| ***Strabismic and anisometropic amblyopes*** | | | | | | | | | |
| **B.B.** | female, 29 yr | RE*<br>LE | - 0.75 sph<br>- 1.50 -2.00 / 175° | 0.08<br>0.90 | temp. margin<br>foveolar | far + ½° + VD 3°<br>near - 2½° + VD 2° | negative, excl. RE | nh arc | Strabismus from early childhood, glasses at 3 yr, occlusion 3-6 yr, surgery at 20 months |
| **M.H.** | female, 31 yr | RE<br>LE* | +5.00 -0.75 / 142°<br>+1.50 -0.50 / 0° | 1.00<br>0.08 | foveolar<br>nasal | far +1½° ± VD<br>near +4° | negative, excl. LE | h arc | Family history, strabismus from early childhood, glasses at 3 yr, occlusion 4–5 yr, surgery at 5 yr |
| **C.L.** | male, 28 yr | RE<br>LE* | - 3.50 -1.50 / 20°<br>+ 1.00 -1.25 / 0° | 1.00<br>0.50 | foveolar<br>nasal - fovea | far +15° +VD 1°<br>near +15° +VD 2° | negative, excl. LE | nh arc | Strabismus from early childhood, occlusion in kindergarten for 3 yr, surgery at 4 yr |

Table 4.1: Orthoptic data of the 1st group of tested subjects. *LEGEND*: *RE* - right eye; *LE* - left eye; *visus c.c.* - corrected decimal visual acuity; *VD* - vertical deviation; *plano* - no correction required; *nrc* - normal retinal correspondence; *nh arc* - nonharmonious anomalous retinal correspondence; *h arc* - harmonious anomalous retinal correspondence; * - amblyopic eye.

| Subject | Gender, age | Eye | Refraction | Visus c.c. (near) | Fixation | Strabismus (sim. cover test) | Stereopsis | Corresp. | History |
|---|---|---|---|---|---|---|---|---|---|
| ***Bilateral ametropic and strabismic amblyopes*** | | | | | | | | | |
| **R.S.** | male, 58 yr | RE<br>LE* | + 6.00 -1.25 / 171°<br>+ 6.75 -1.50 / 5° | 0.60<br>0.10 | foveolar<br>1.5°-2° nasal | far +2½°+ VD<br>near +3° + VD | negative, excl. LE | h arc | Occlusion at 1 yr, glasses and visual therapy from age 1 yr |
| **S.B.** | female, 25 yr | RE*<br>LE | -10.0 sph<br>- 9.0 sph | 0.30<br>0.60 | temporal<br>foveolar | far +12° + VD<br>near +12° + VD 7° | negative, excl. RE | nh arc | Family history, strabismus from early childhood, glasses at 5 yr |
| ***Anisometropic amblyopes*** | | | | | | | | | |
| **H.L.** | male, 27 yr | RE<br>LE* | plano<br>+ 6.25 sph | 1.40<br>0.25 | foveolar<br>foveolar | 0° | negative, sim. vision | nrc | Occlusion at 11 yr, glasses at 18 yr |
| **T.S.** | male, 30 yr | RE<br>LE* | + 1.25 sph<br>+ 2.75 -3.75 / 135° | 1.00<br>0.40 | foveolar<br>nasal margin | 0° | negative, excl. LE | nrc | Occlusion and glasses at 6 yr |
| **J.B.** | male, 26 yr | RE<br>LE* | - 2.25 sph<br>- 0.75 -2.00 / 15° | 1.00<br>0.50 | foveolar<br>temporal | 0° | positive, 250" | nrc | Occlusion and glasses at 6 yr |
| **M.B.** | male, 34 yr | RE<br>LE* | - 0.50 -0.50 / 45°<br>- 3.00 -3.25 / 2° | 1.00<br>0.50 | foveolar<br>foveolar | 0° | positive, 250" | nrc | Glasses at 17 yr |
| ***Strabismics with alternating fixation*** | | | | | | | | | |
| **R.F.** | female, 25 yr | RE<br>LE | plano<br>- 4.00 -1.0 / 15° | 1.00<br>1.00 | foveolar<br>foveolar | far - 8° + VD<br>near - 3° | negative | nrc | Strabismus from early childhood, glasses and pleoptic therapy at 2 yr |
| **M.O.** | female, 23 yr | RE<br>LE | - 0.50 -1.0 / 163°<br>- 1.00 -1.0 / 27° | 1.00<br>1.00 | foveolar<br>foveolar | far 0.0 +VD1.5°<br>near -1.5°+ VD 5° | negative | nrc | Family history, glasses at 14 yr |
| **J.Z.** | male, 27 yr | RE<br>LE | - 7.75 sph<br>- 8.50 sph | 1.25<br>1.25 | foveolar<br>foveolar | far + 4° - VD<br>near + 4° - VD | negative | arc | Glasses and occlusion at 5 yr |

*(continued from previous page)*

- 72 positions recorded from the subject (i.e. positions where he / she pereceived the target). Each position is an average from 5 measurements for each target, so the raw data sets consists of 72 x 5=360 recorded positions).

We performed a novel analysis of this kind of data, in addition to already known and used vectorial maps. This analysis yielded two useful indices:

1. $SD_{Area}Ratio$ (standard deviations area ratio)
2. $AVL$ (average vector length)

### $SD_{Area}Ratio$ index

This index is a synthetic expression of how worse the amblyopic eye is (versus the sound eye) in the localization tasks. Values around 1.0 suggests that the both eyes perform similarly. The greater the value above 1.0, the worse the difference between the eyes is. It is expressed as:

$SD_{ratio} = \frac{SD_{n-dom}}{SD_{dom}}$ , where $SD$ means standard deviation area, as explained below.

For each target presented on the screen, several positions were recorded from the subject (using polar coordinates, i.e. radius and angle, from the fixation point). The recorded positions were not exactly located over the target, but subjects made errors while targeting. We used the standard deviation ($sd$) as a measure of variability (dispersion) of the data set. A low standard deviation is found in data sets where collected points are very close to the mean; a high standard deviation indicates that the data points are spread out (from the mean).

We calculated the standard deviations for radial values ($sd_r$) and for angular values ($sd_a$), for the given target. Thus we could know the degree of dispersion of the data in both polar coordinates.

We can express the spreading of the data points as an area, defined by the sector ring with a radial section identical with $sd_r$ and the arc identical with $sd_a$. We call the area of this sector, Standard Deviation Area ($SD_{area}$) of the given target; it is expressed in $deg^2$. An example of the calculated areas is given in Fig. 4.1, for both non-amblyopic and amblyopic eye. These are shown as green or red[1] ring sectors, centred on their average value. Already from the visual representation, a difference between the two eyes becomes apparent: the total area of the red sectors is bigger than the total area

[1]Note: *green* colour is used to show information related to dominant eye and *red* colour is used for the information related to amblyopic eye. We have followed the same convention for all images that depict differences between the eyes.

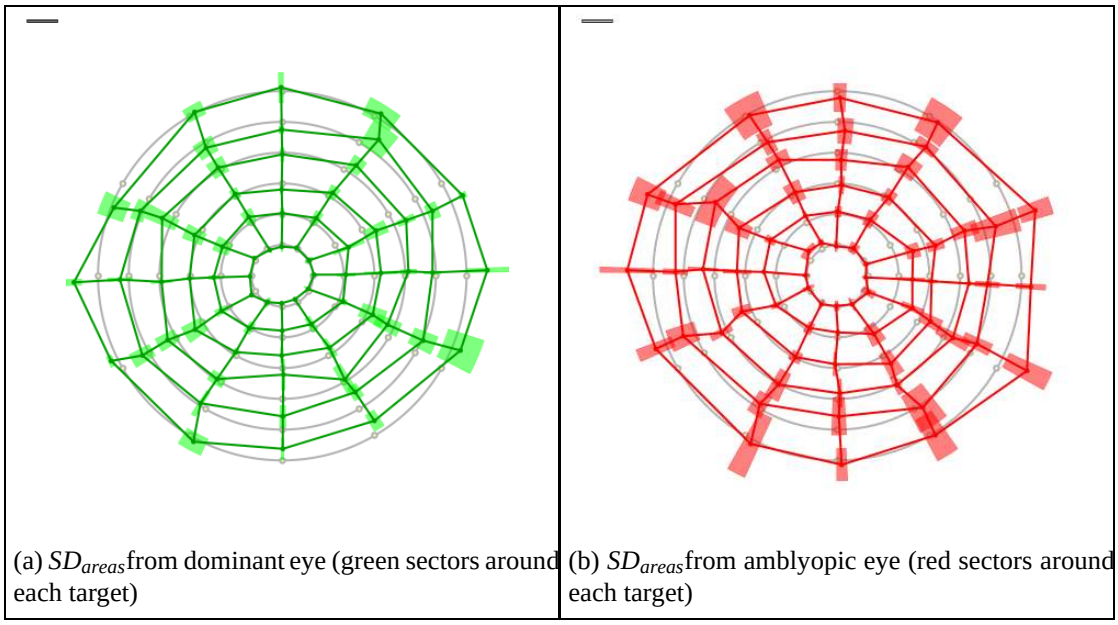

(a) $SD_{areas}$ from dominant eye (green sectors around each target)

(b) $SD_{areas}$ from amblyopic eye (red sectors around each target)

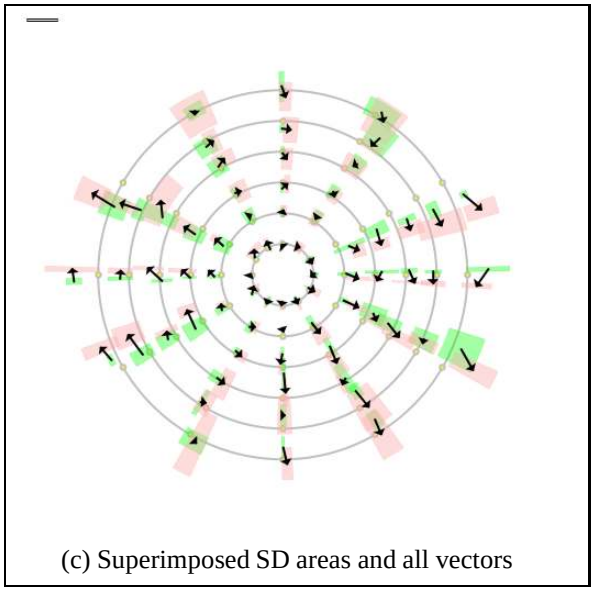

(c) Superimposed SD areas and all vectors

Figure 4.1: Example of $SD_{areas}$ (*a*) and (*b*) and the improved vectorial map (*c*). Data set from subject C.L.

of green sectors. This means that in the mapping task, the amblyopic eye (red) had difficulties in targeting (a bigger spread of localizations).

We define as $SD_{dom}$ the average area made up the individual 72 $SD_{areas}$ corresponding to dominant (sound) eye (coloured with green in the figure). Also, we define $SD_{n-dom}$ the average area made up the individual 72 $SD_{areas}$ corresponding to amblyopic eye (red in the figure).

Thus, we can define:

$SD_{ratio} = \frac{SD_{n-dom}}{SD_{dom}}$ , to give a measure of spatial uncertainty.

*AVL* **index**

As a measure of the total displacements that took place in a map, we calculate the average value of all the displacement vectors in the map (they are expressed in visual degrees). In the following sections we call this index *Average Vector Length (AVL)*

Statistical evaluation of the results was performed with a repeated measures multivariate analysis of variance (MANOVA) model that included:

- as independent variables: the eye and position of the test points,
- as dependent variables: the amount of spatial distortion (length of the vectors connecting the mean settings through the two eyes) and the amount of spatial uncertainty (*SD* areas of the settings of the two eyes).

The level was set at 0.05 for omnibus tests, Wilk's was used as a test statistic. Separate error terms and Bonferroni adjustments were used for planned comparisons and contrasts.

## 4.3 Results

### 4.3.1 Individual Data

The results from all subjects and the 10 normally sighted control subjects (*SD* areas, $SD_{ratio}$, *AVL*) are listed in Table 4.2.

As reported in previous studies, (LAGREZE/SIRETEANU, 1991), (SIRETEANU/LAGREZE/CONSTANTINESCU, 1993), the mean settings of the normally sighted observers were very accurate. The linear sizes of the $SD_{areas}$ increased with increasing distance from the fixation point. Whenever consistent deviations from the original positions occurred, they correlated highly between the two eyes of the same subject (for an example, see

| Subject | Average Vector Length (deg) | Average $SD_{n\text{-}dom}$ ($deg^2$) | Average $SD_{dom}$ ($deg^2$) | $SD_{n\text{-}dom}$ / $SD_{dom}$ |
|---|---|---|---|---|
| ***Strabismic amblyopes*** | | | | |
| **M.K.** | 0.54 | 0.61 | 0.38 | 1.61 |
| **D.S.** | 0.35 | 0.41 | 0.25 | 1.64 |
| **L.P.** | 0.25 | 0.45 | 0.29 | 1.54 |
| ***Strabismic and anisometropic amblyopes*** | | | | |
| **B.B.** | 0.53 | 0.47 | 0.22 | 2.10 |
| **M.H.** | 0.30 | 0.47 | 0.34 | 1.35 |
| **C.L.** | 0.32 | 0.31 | 0.18 | 1.75 |
| ***Bilateral ametropic and strabismic amblyopes*** | | | | |
| **R.S.** | 0.36 | 0.61 | 0.48 | 1.25 |
| **S.B.** | 0.64 | 0.85 | 0.77 | 1.10 |
| ***Anisometropic amblyopes*** | | | | |
| **H.L.** | 0.49 | 0.22 | 0.22 | 0.99 |
| **T.S.** | 0.30 | 0.32 | 0.28 | 1.15 |
| **J.B.** | 0.27 | 0.31 | 0.35 | 0.89 |
| **M.B.** | 0.21 | 0.17 | 0.20 | 0.86 |
| ***Strabismus with alternating fixation*** | | | | |
| **R.F.** | 0.59 | 0.95 | 0.69 | 1.38 |
| **M.O.** | 0.34 | 0.35 | 0.34 | 1.01 |
| **J.Z.** | 0.38 | 0.28 | 0.29 | 0.95 |
| ***Controls*** | | | | |
| **D.G.** | 0.35 | 0.86 | 0.63 | 1.35 |
| **M.N.** | 0.26 | 0.37 | 0.34 | 1.10 |
| **S.H.** | 0.31 | 0.59 | 0.65 | 0.87 |
| **A.Fr.** | 0.22 | 0.22 | 0.21 | 1.04 |
| **E.B.** | 0.26 | 0.31 | 0.31 | 1.01 |
| **E.G.** | 0.28 | 0.21 | 0.19 | 1.10 |
| **M.Y.** | 0.27 | 0.32 | 0.47 | 0.66 |
| **P.G.** | 0.33 | 0.52 | 0.41 | 1.25 |
| **R.P.** | 0.24 | 0.31 | 0.33 | 0.94 |
| **T.W.** | 0.23 | 0.29 | 0.23 | 1.30 |

Table 4.2: *Average Vector Lengths* (*AVL*) and *Standard Deviation Areas (SD)* for all examined subjects

Figs. 4.2 and 4.3 ). Overall, the ratios of the average *SD* areas did not differ significantly from 1.0 (see Table 4.2). The vectorial subtraction maps of the amblyopic subjects showed idiosyncratic patterns of expansion, contraction or torsion of portions of the visual field, confirming previous cited studies (Fig. 4.2 and 4.3).

In subjects with strabismic and strabismic–anisometropic amblyopia (Fig. 4.2), both the vector lengths and the $SD_{areas}$ areas were larger and more irregular than in control subjects. In the four subjects with anisometropia without strabismus (Fig. 4.3), vectorial displacements and $SD_{areas}$ areas were comparable to those of normally sighted subjects. Particularly pronounced distortions were shown by the two subjects with a bilateral ametropic amblyopia (R.S. and S.B.). Both subjects showed large mapping errors and enormous $SD_{areas}$ , affecting both eyes. One of the three subjects with alternating fixation and good vision in both eyes (R.F.) showed larger displacements and $SD_{areas}$ than the normal control subjects, comparable to those of some subjects with strabismic amblyopia. This subject was previously strabismic–anisometropic amblyopic, treated by pleoptic therapy at an early age. *These results suggest that an early treatment may be beneficial for visual acuity, but less efficient in eliminating the spatial misperceptions which accompany an early strabismic amblyopia.*

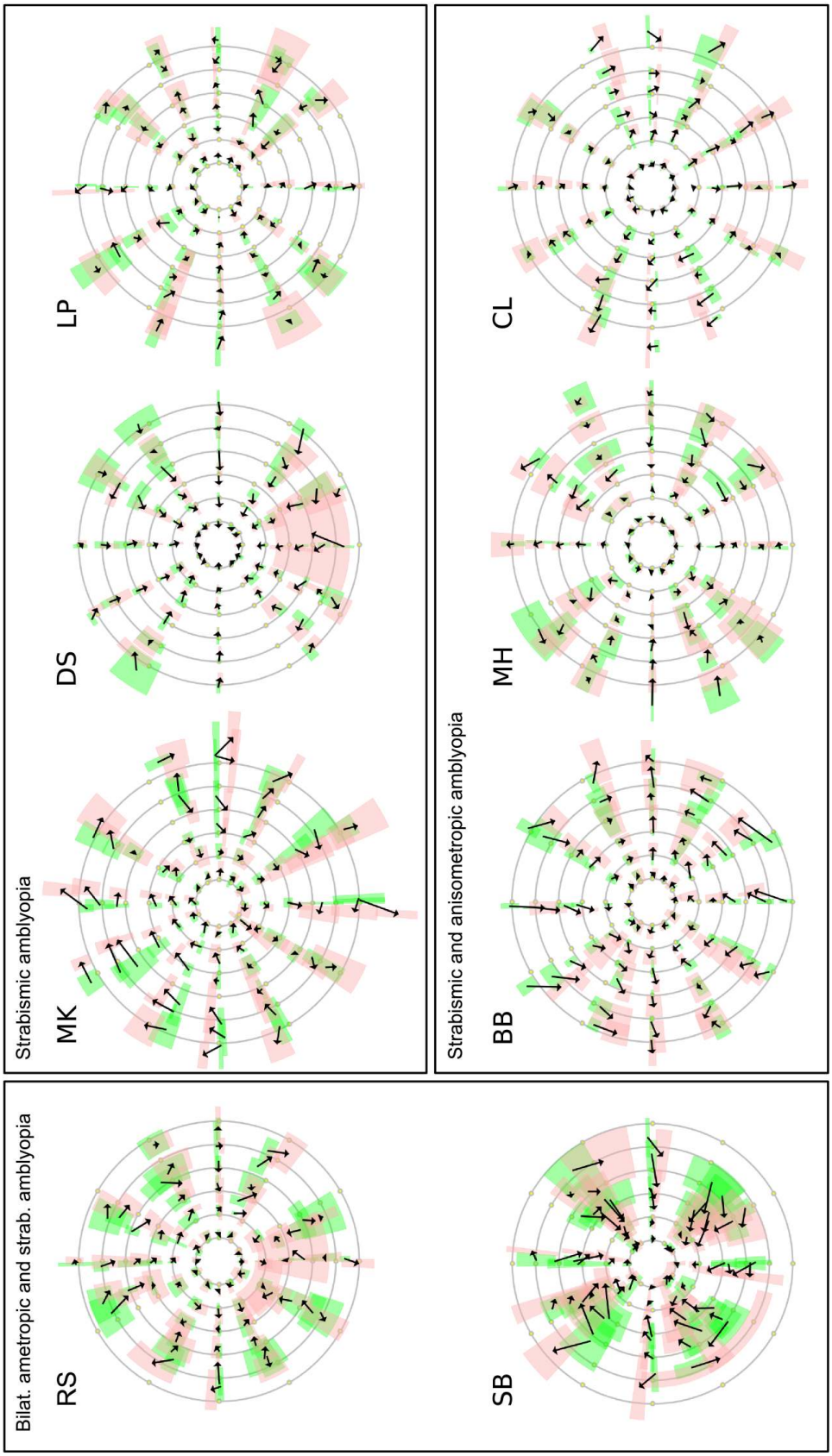


Figure 4.2: Individual spatial displacement maps of the experimental subjects. The average displacements are indicated by *arrows* (bases of the arrows: average settings through the dominant eyes; tips of the arrows: average settings through the nondominant eyes). *Green areas*: $SD_{areas}$ of the dominant eyes; *Red areas*: $SD_{areas}$ of the nondominant eyes. Each point is based on five measurements.

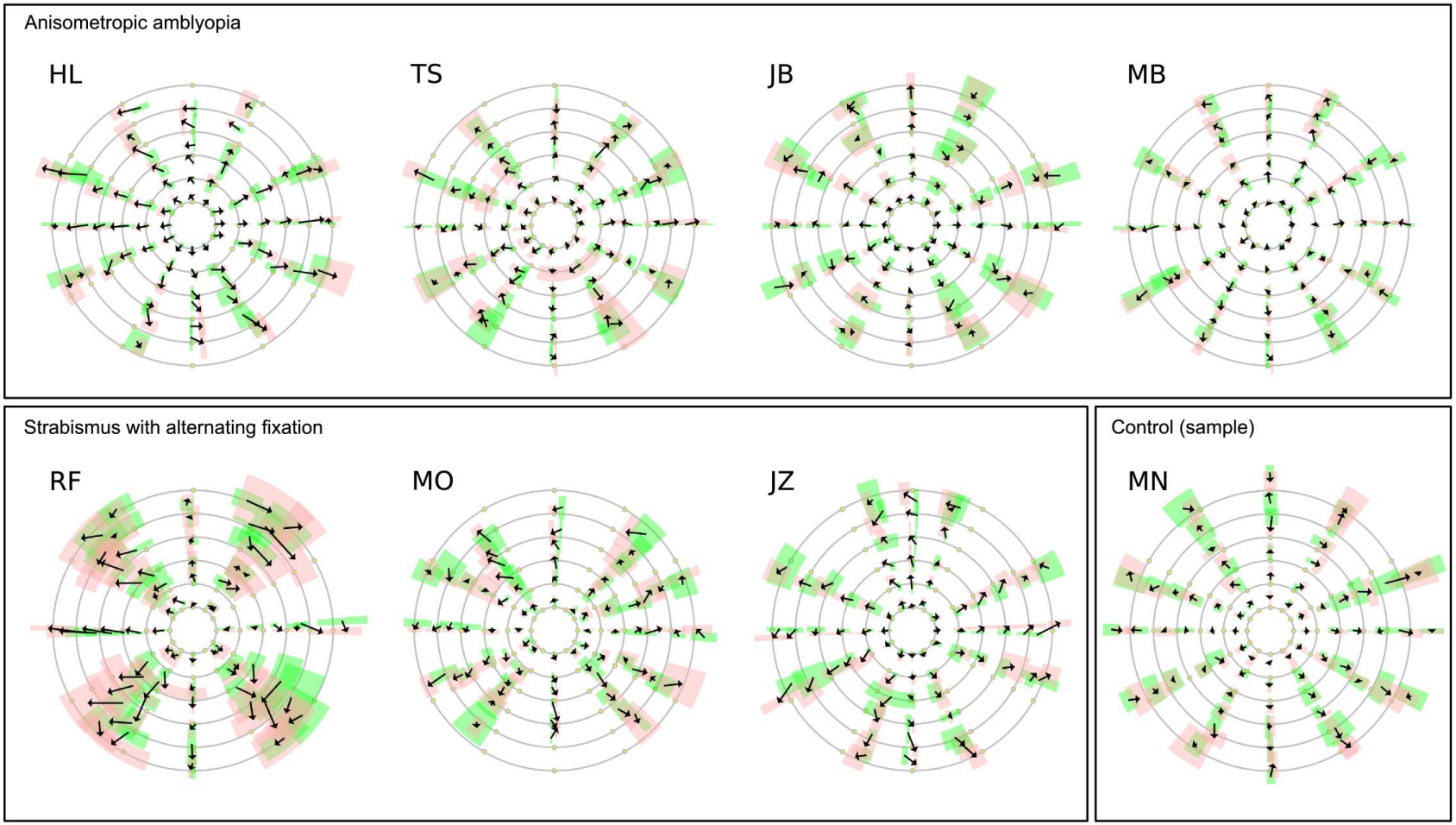


Figure 4.3: Individual spatial displacement maps of the experimental subjects. The average displacements are indicated by *arrows* (bases of the arrows: average settings through the dominant eyes; tips of the arrows: average settings through the nondominant eyes). *Green areas*: $SD_{areas}$ of the dominant eyes; *Red areas*: $SD_{areas}$ of the nondominant eyes. Each point is based on five measurements.

### 4.3.2 Group Data

Figure 4.4 on the next page shows the dependence of the individual *AVL*s and the ratios of the mean SD areas ($SD_{ratio}$) on the visual acuity of the nondominant eye of each subject. Subjects with different aetiologies are indicated by different symbols. Subjects who had reported a stable perception are indicated by open symbols and subjects experiencing temporal instabilities by filled symbols. Figure 4.4 suggests that, despite the inevitable variability of the individual data, subjects with more profound acuity losses and a strabismic aetiology showed higher spatial displacements and higher ratios of $SD_{areas}$. Subjects reporting temporal instabilities also tended to cluster in the higher range for the ratios of the $SD_{areas}$ , but they did not seem to differ in the distribution of the average vector lengths.

To verify the statistical significance of these observations, the data of all subjects were grouped according to different criteria: visual acuity loss (left clusters in Fig. on page 43), aetiology (middle clusters), and temporal stability (right clusters). The left panels in Figure 4.5 indicate the *AVL*s of the different groups and the right panels the ratios of the SD areas of the same groups ($SD_{ratios}$).

### 4.3.3 Relationship between Spatial Displacements and Visual Acuity Loss.

The 15 experimental subjects were grouped according to their visual acuity loss in:

- group A: subjects with deep acuity losses (corrected visus of 0.08 – 0.32) in the nondominant eye; (n=8) and
- group B: subjects with moderate or no acuity loss ( 0.40 –1.25; n=7);

The group data and results are presented in Fig. 4.5 on page 43.

Subjects with a deep amblyopia (group A) showed significantly larger spatial displacements (mean *AVL*, 0.43°) than the normally sighted observers (0.27°; t(16) 3.5, p=0.01), but the difference was not significant in subjects with a moderate or no acuity loss (0.34°; t(15) 1.7, p=0.10).

$SD_{ratio}$ for the subjects with deep amblyopia was *1.45*, which was significantly higher than for normally sighted observers (*1.07*; t(16) 2.9, p=0.01).

$SD_{ratios}$ of subjects with a moderate acuity loss was *1.14*, which did not differ significantly from those of normally sighted control subjects. Mean $SD_{ratio}$ of subjects with deep amblyopia was higher than that for subjects with moderate or no amblyopia, but this difference did not reach statistical significance (t(13) 1.7, p=0.10).

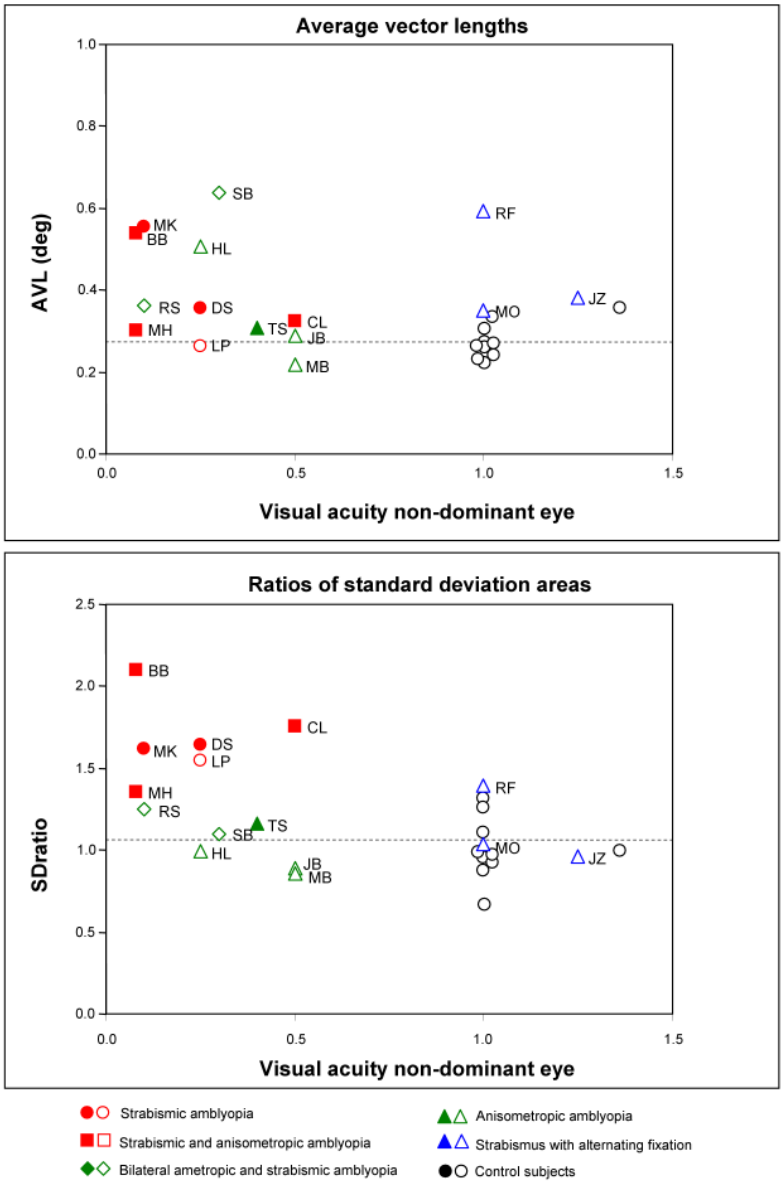


Figure 4.4: Average vector lengths (a) and ratios of $SD_{areas}$ (b) for individual subjects, as a function of visual acuity. The different aetiology groups are indicated by different symbols. *Filled symbols*: subjects experiencing temporal instabilities; *open symbols*: subjects with stable perception. Not all categories are represented.

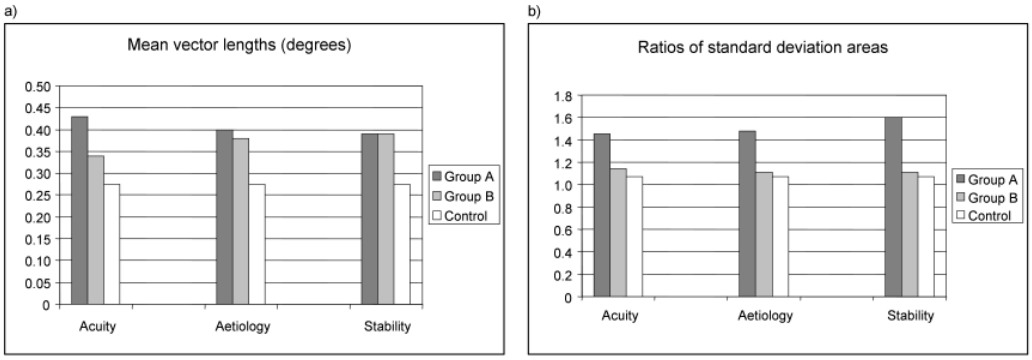


Figure 4.5: (a) Mean vector lengths and (b) ratios of $SD_{areas}$ for all subjects, grouped according to the depth of amblyopia (left clusters), their aetiology (middle clusters), and the presence of temporal stability (right clusters). Subjects in *group A* have either deeper amblyopia (left clusters), an aetiology of strabismus (middle clusters), or an unstable perception (right clusters). *Group B*: subjects with mild amblyopia (left clusters), with a refractive aetiology (middle clusters), or with stable perception (right clusters). Each cluster contains the data of all 15 experimental and 10 control subjects.

### 4.3.4 Relationship between the Magnitude of Spatial Displacements and aetiology.

To quantify the spatial displacements of subjects with different aetiologies, we compared the results of subjects with a history of strabismus (strabismic amblyopia, strabismic–anisometropic amblyopia, and strabismus with alternating fixation; n=9) with those with a refractive aetiology (bilaterally ametropic and anisometropic amblyopia; n=6; Fig. 4.5, middle clusters).

*AVL*s were significantly larger in subjects with a history of strabismus (0.40°) than in normally sighted observers (0.27°; t(17) 3.1, p=0.01). The difference was not statistically significant in subjects with a refractive error aetiology (0.38°; t(14) 2.0, p=0.06).

There was no significant difference between the *AVL*s of the subjects with a history of strabismus and those of subjects with a refractive error aetiology (Fig. 4.5.a). $SD_{ratios}$ of the subjects with a history of strabismus were significantly higher (1.48) than those of the subjects with a refractive aetiology (1.04; t(13) 2.8, P 0.01) and of the normally sighted observers (1.07; t(17) 3.1, p=0.01).

$SD_{ratios}$ on the amblyopic subjects with a refractive aetiology did not differ significantly from those of the control subjects (see Fig. 4.5.b).

*Thus, it seems that both a deep acuity loss and a history of strabismus are related to increased spatial displacements and higher spatial uncertainty.*

### 4.3.5 Relationship between Spatial Displacements and Temporal Instability.

We wondered whether the temporal instability experienced by amblyopic subjects may be related to an increased disorder of the spatial map experienced by these subjects. Inspection of Figures 4.2, 4.3 and 4.4 suggests that a simple correlation is unlikely.

Indeed, the subjects showing the most pronounced displacements (R.S., S.B., and R.F.) did not report any temporal instability (Fig. 4.4). Also, the mean spatial displacements of the subjects experiencing temporal instability (Fig. 4.4.a, filled symbols) were not higher than those of the subjects with a stable perception (Fig. 4.4.a, open symbols).

For a quantitative comparison, we grouped together the subjects who reported experiencing temporal instability in the previous experiment (n=6) and those with a stable perception (six amblyopic subjects and three strabismic subjects with alternating fixation; n=9). The results are shown in the right clusters in Figure 4.5. The mean vector lengths of the subjects experiencing temporal instability and those with a stable perception were identical (mean *AVL* was 0.39° in both groups). Both were significantly higher than the mean *AVL* of the normally sighted subjects (0.27°; t(17) 2.4, p=0.05 for subjects with a stable perception and t(14) 3.0, p=0.01 for subjects experiencing temporal instability; Fig. 4.5a).

*Subjects experiencing temporal instability showed significantly higher spatial uncertainties* (the averaged $SD_{ratio}$ was 1.60) than subjects with a stable perception (1.11; t(13) 3.4, p=0.01) and normally sighted subjects (1.07; t(14) 4.0, p=0.001).

Subjects with a stable perception did not differ significantly from normal control subjects (see Fig. 4.5b).

These results demonstrate that, while all groups of experimental subjects showed abnormally large spatial displacements, *only subjects experiencing temporal instability also had an increased positional uncertainty in the amblyopic eyes*. One possible interpretation of these results is that a system that perceives visual stimuli as unstable may be more likely to mislocalize these stimuli. Thus, temporal instability may be causally related to the increased spatial imprecision in amblyopic vision.

## 4.4 Discussion and Conclusions

The "CEXGRAPHER" method refines the data analysis from the two-dimensional mapping procedure of the amblyopic displacements. As reported in previous studies, (BEDELL/FLOM 1981; BEDELL/FLOM 1983; FRONIUS/SIRETEANU 1989; LAGREZE/

SIRETEANU 1991; SIRETEANU/LAGREZE/CONSTANTINESCU 1993) we found that amblyopic subjects showed idiosyncratic expansions, shrinkages, or torsions of portions of the visual field. In addition, the precision of the settings through the amblyopic eyes was dramatically impaired. These impairments affected mainly subjects with a history of strabismus and a deep amblyopia, rather than those with a refractive aetiology and mild acuity loss.

Point-by-point mapping of the visual space is more disturbed in strabismic subjects with a deep amblyopia than in amblyopic subjects with a refractive aetiology and a mild acuity loss. Subjects experiencing temporal instabilities show significantly more pronounced spatial uncertainty in the amblyopic eye than do subjects with stable perception. We suggest that the weakness of the brain mechanisms responsible for binocular fusion may be responsible for these effects. Looking with a habitually disused eye may require more effort and evoke more (but less organized) cortical activity than viewing with a habitually seeing eye. The uncontrolled activity through the amblyopic eye may be responsible for the nonveridical perception of contours, colours, and movement.

# Chapter 5

# “DISIM” METHOD

## 5.1 Introduction

Spatial distortions in amblyopic vision can be captured by:

- subjective reports (i.e. what the patients tell, sketch or draw), like the ones presented in Fig. 2.5 on page 23;
- objective mapping (like point-by-point mapping of the central part of the visual field described in the previous chapter).

The results yielded by these two methods cannot be easily compared, because of their different nature (subjective data vs. numerical, objective data). We wanted to see if there is a connection between the two kinds of results. First obvious way to explore this issue was to create a method that can computationally distort an arbitrary image based on the vectorial field data.

We named this method “*DISIM*” as an acronym from “*Di*stortion *Sim*ulation”. With this method we tried to explore the comparison problem, and also to use it as a visualization tool (to distort any arbitrary real-world image).

## 5.2 Materials and Method

### Datasets

For this method, we needed the two data sets (vectorial maps and drawings) from the same subjects:

1. *subjective reports* : we were provided with the sketches of the amblyopic percepts for the geometrical patterns in Fig 5.1. The pictures with the subjective

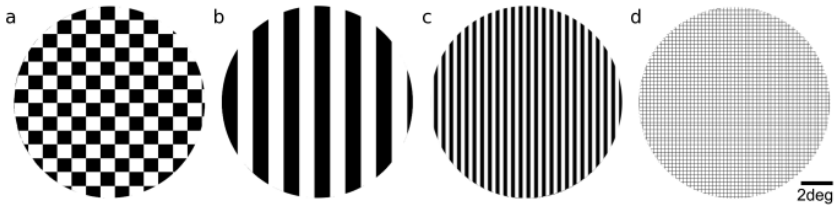


Figure 5.1: Sample stimuli (masked) used for the "DISIM" method

distortions were recorded by our colleague psych. Claudia Baeumer (BAEUMER, 2005).

2. *objective mapping*: We used the psychophysical mapping data collected in the study described in the previous chapter, for this group of subjects.

We used in this study the data from 12 amblyopic subjects (5 strabismic, 4 anisometropic and 3 strabismic-anisometropic) . This was a subgroup of the patients listed in Table 4.1 on page 32; we excluded the subjects that did not have the sketches / drawings completed or completely validated.

## Distortion algorithm

We wanted to see if there is a connection between vectorial maps (mislocalizations) and the subjective descriptions. First obvious way to explore this issue was to create a method that can computationally distort an arbitrary image based on the vectorial field data. Such explorations were attempted in the past (SIRETEANU/LAGREZE/ CONSTANTINESCU, 1993), but were limited by the digital technology available at the time.

The perfect distortion algorithm should be able to take as input: a) *the vectorial* data and b) *an arbitrary image* (digitized), and produce as result *a distorted image*, with color data from the original image displaced according to vectorial data.

However, there are several problems waiting to be solved:

- *uneven information density*. In the vectorial field collected through "Circle Experiment" method, there is an uneven distribution of information regarding mislocalizations (there are more points per square degree in the central zone than in more peripheral regions). This means that the distortion algorithm is bound to be more inaccurate in the peripheral regions;

- *central (fixation) point problem*. There is no vectorial data collected in the fixation zone (because the subject has to fixate continuously the fixation cross). So, the algorithm should not produce any artificial distortions in this area.

- *boundary problem*. The collected vectorial data is confined to a circular area with a radius of 6° in the visual field. Beyond this limit, we have no information, so we preferred to mask the outside regions. In addition, there might be sharp artefacts resulting from imposing an artificial cut-out limit at 6°, so we preferred a progressive, linear reduction in the vectorial displacement beyond this limit. Therefore, the masking should also cover this region, and we set it at 5 degrees. For this reason, all the images produced by this method are circularly masked either at 6 degrees (stimuli) or at 5 degrees (distorted images).

We interpret these problems as a particular 2D anisotropic mapping problem. We could solve these problems by breaking them into smaller steps:

1. Each vectorial chart (from the amblyopic and the sound eye) is decomposed in 60 quadrilaterals (12 for each two adjacent circles)

2. Each individual quadrilateral has in corners four displacement vectors from the original data set. Since we have no information on the displacements inside this area, we assumed a planar interpolation based on four nearest neighbours to find the displacement. The displacement can be simply interpreted locally, in this area, as a perspective transform of a quadrilateral. That is, the colour information from source quadrilateral is mapped into the warped space of the second quadrilateral. The logic of transformation is given in Fig. 5.2 (adapted from SUN MICROSYSTEMS, 1999).

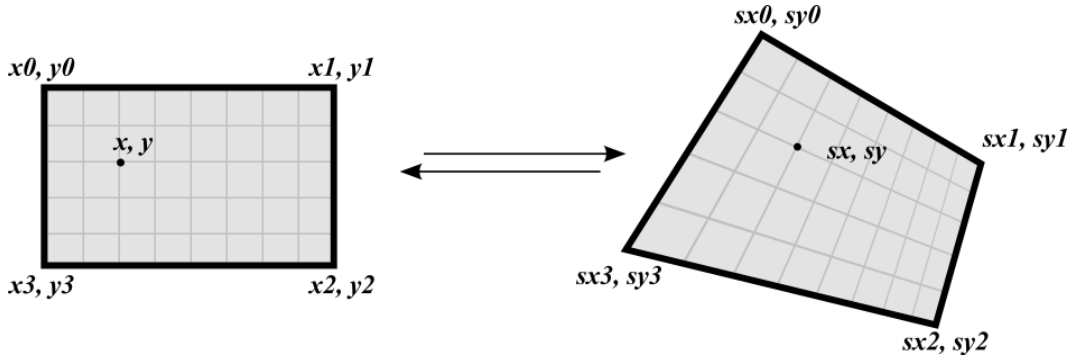


$$xfrac = \frac{x-x0}{x1-x0}, \qquad yfrac = \frac{y-y0}{y1-y0}$$

$$s = sx0 + (sx1 - sx0) \cdot xfrac$$

$$t = sy0 + (sy1 - sy0) \cdot xfrac$$

$$u = sx2 + (sx3 - sx2) \cdot xfrac$$

$$v = sy2 + (sy3 - sy2) \cdot xfrac$$

*Transformation relation is:*

$$sx = s + (u - s) \cdot yfrac$$

$$sy = t + (v - t) \cdot yfrac$$

Figure 5.2: Perspective transform. The points from one quadrilateral can be uniquely mapped into the space of the other.

It should be noted that this perspective mapping technique, albeit simple, cannot work if there are some conditions that can lead to division-by-zero errors (for instance, two corners are in the same position, flipping of two diagonal corners, or if one quadrilateral becomes concave); these conditions should be checked beforehand.

After applying step 2, the displacement information in the vectorial field is stored as a series of discrete perspective transforms.

3. In order to interpolate all the boundary regions between these mapping regions, a final step is required. A control grid interpolation (SUN MICROSYSTEMS, 1999) is applied.

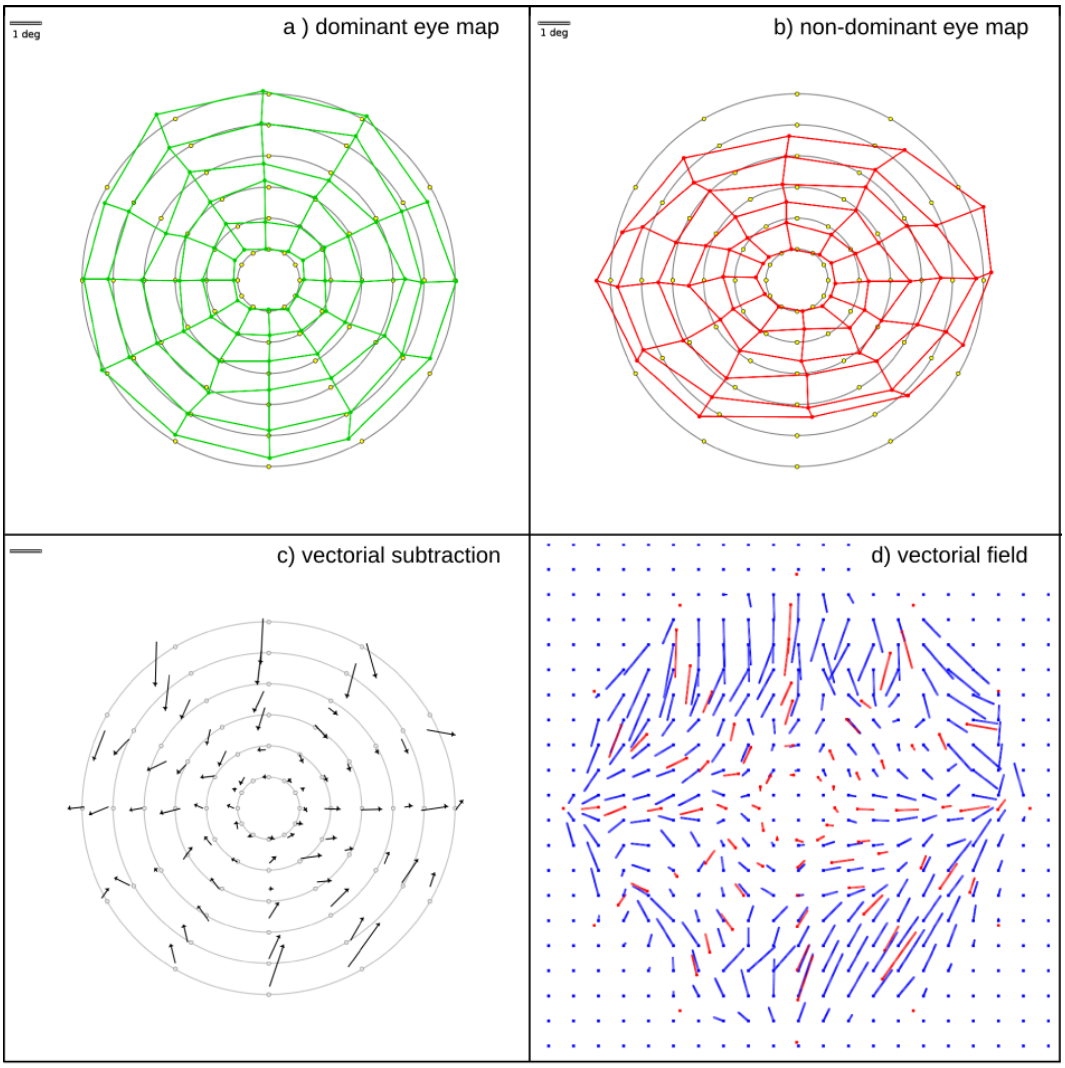


Figure 5.3: Algorithm implementation based on the data of the strabismic and anisometropic amblyope B.B. (for orthoptic data see Table 4.1 on page 32). *a*), *b*) monocular distortion maps; *yellow points* distributed on circles: mean position of the points to be memorized; *coloured points* distributed on spider-web like patterns: mean position of the settings of the subject. *c*) vectorial subtraction: *base of arrows*, dominant eye; *tip of arrows*, non-dominant eye; *d*) interpolated control grid;

The perspective transforms are used to distort a controlling rectangular grid, of an arbitrary granularity. The finer the grid, the smaller the artefacts like tearing or aliasing in the final image. Also, in order to avoid these artefacts, the calculation is done in reverse: The *destination (i.e. distorted)* image is constructed point by point ($x, y$ ), and the source color of this point is found in the *undistorted, original image* ($sx, sy$). This reverse mapping technique seems counterintuitive, but it ensures the consistency of all points in the destination image, even if there are huge distortions like enlargements or rotations.

All these steps are summed up in the Fig. 5.3 . The control grid is depicted in d) as the array of dots, and every displacement that should be followed by the pixels in the image, is represented as lines originating in these dots. For convenience and clarity, only parts of the grid are shown, and the original vectorial data is represented as red lines.

We generated artificially distorted images, for each patient (based on its own vectorial displacement data) and for each of the four stimuli, used as input pictures.

The comparison between the drawings based on the reports of the subjects and the computer-generated images was performed for each pattern and each subject.

Figure 5.4: Example of applied distortion algorithm: a) original image b) distorted image based on the vectorial map of subject B.B., presented in Fig.5.3.

## 5.3 Results

The computer-generated distorted images of the high and low spatial frequency gratings are shown in the Figs. 5.5-5.7 (upper panels), alongside with the subjective drawings of the same subjects (lower panels).

At a first glance, it appears that for strabismic and strabismic-anisometropic amblyopes, there is a better agreement between the subjective drawings and the computer-generated images in the low, rather than in the high spatial frequency domain (see subjects L.P. and S.B., Fig. 5.5 and C.L., Fig. 5.7). This might reflect a limitation of the experimental procedure: the interpolating method still allowed assessment of visual field regions in which no data could be collected, thus rendering the interpolation too smooth (see for instance subjects S.B., M.K. and D.S., Fig. 5.5).

On the other hand, the computer-reconstructed images of some anisometropic amblyopes in the high spatial frequency domain (see subjects T.S. and H.L., Fig.5.6) are rather bizarre, presumably as a reflection of their increased spatial uncertainty.

Also, we successfully tested the method for arbitrary images (see for instance Fig. 5.4 on the preceding page or Fig. 5.8 on page 56).

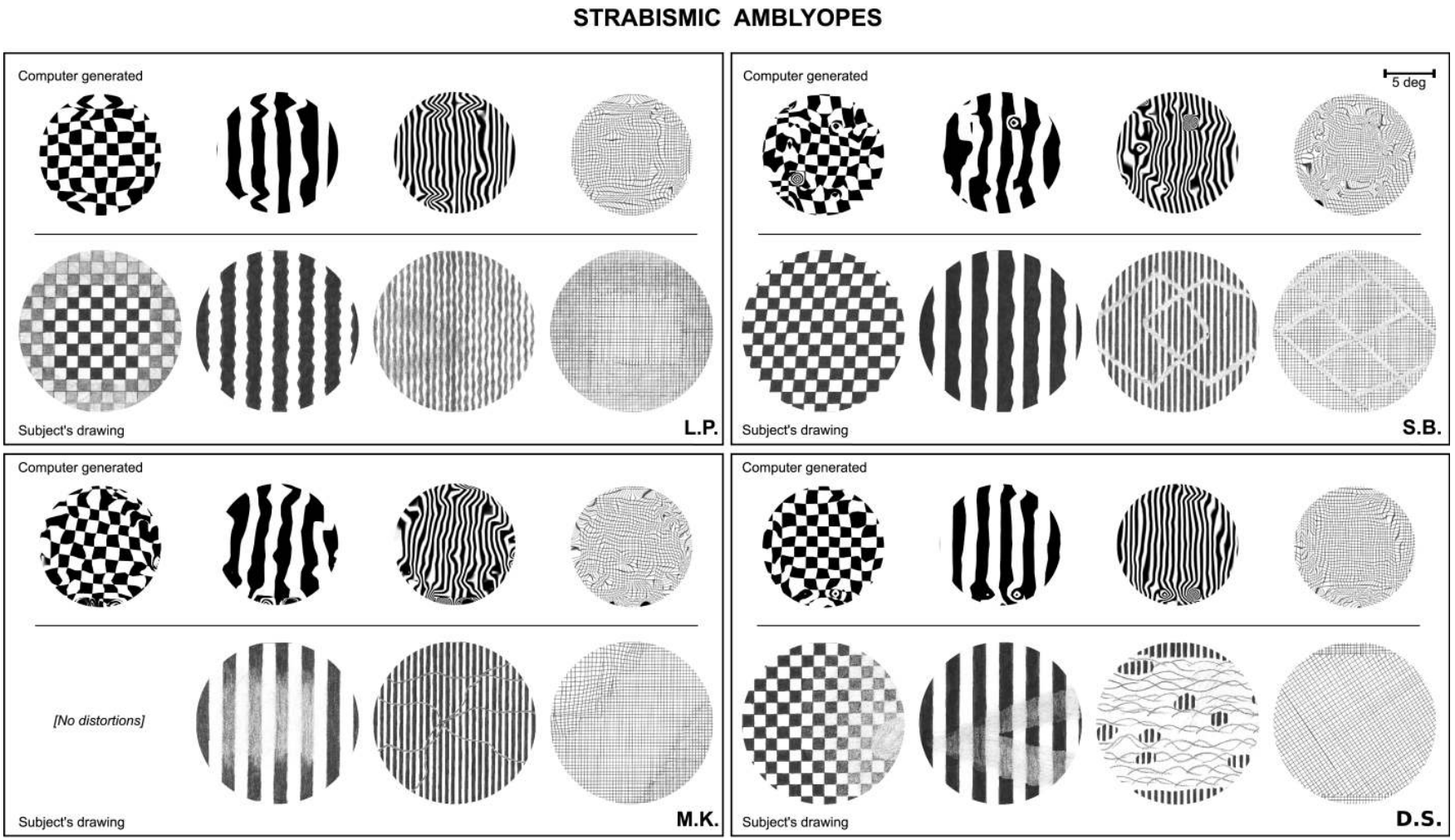


Figure 5.5: Computer reconstructions (upper panels) and visualizations of subjective perceptions (lower panels) of strabismic amblyopes (subjects L.P., M.K., S.B., D.S.).

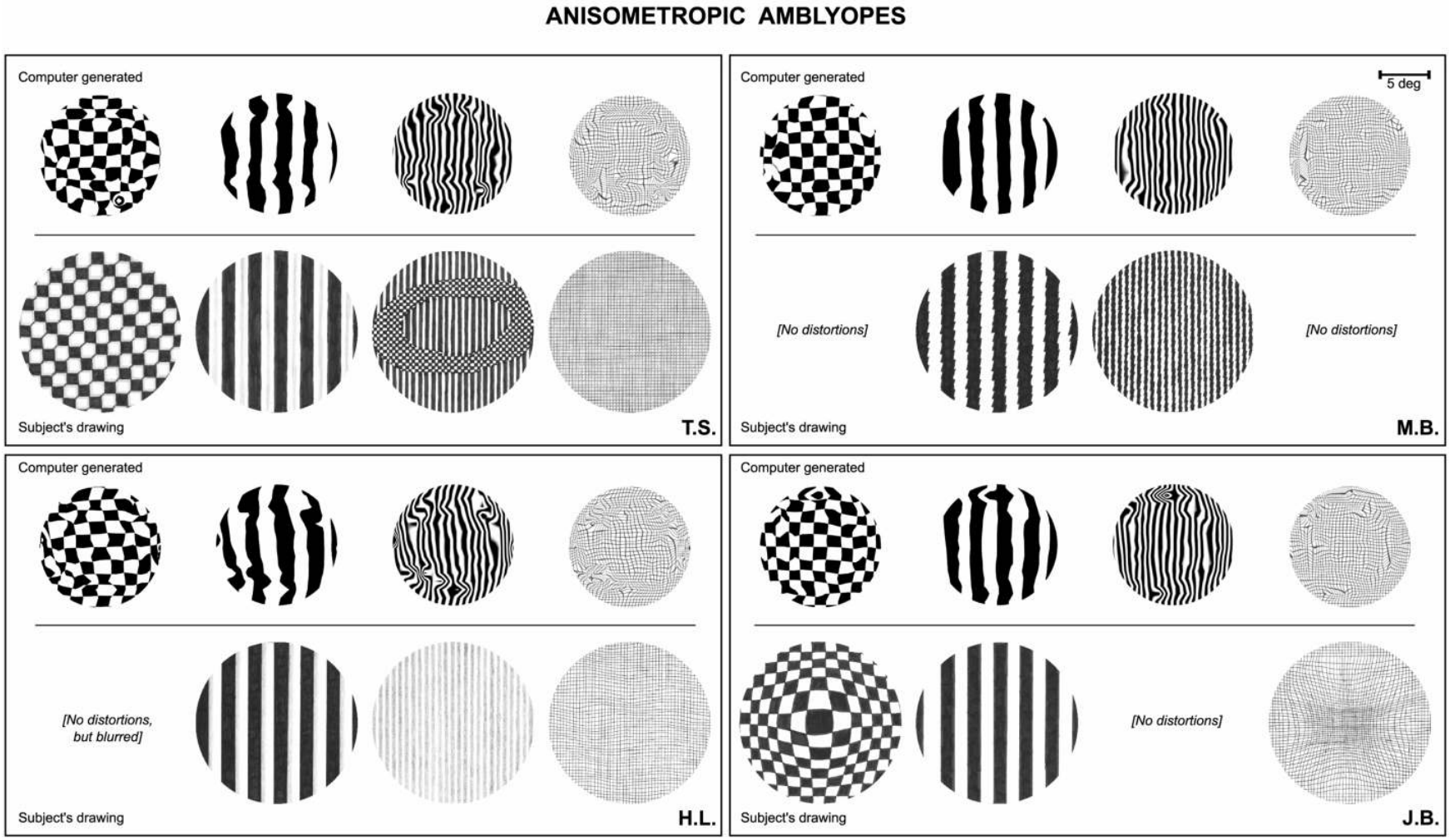


Figure 5.6: Computer reconstructions (upper panels) and visualizations of subjective perceptions (lower panels) of anisometropic amblyopes (subjects T.S., H.L., M.B., J.B.).

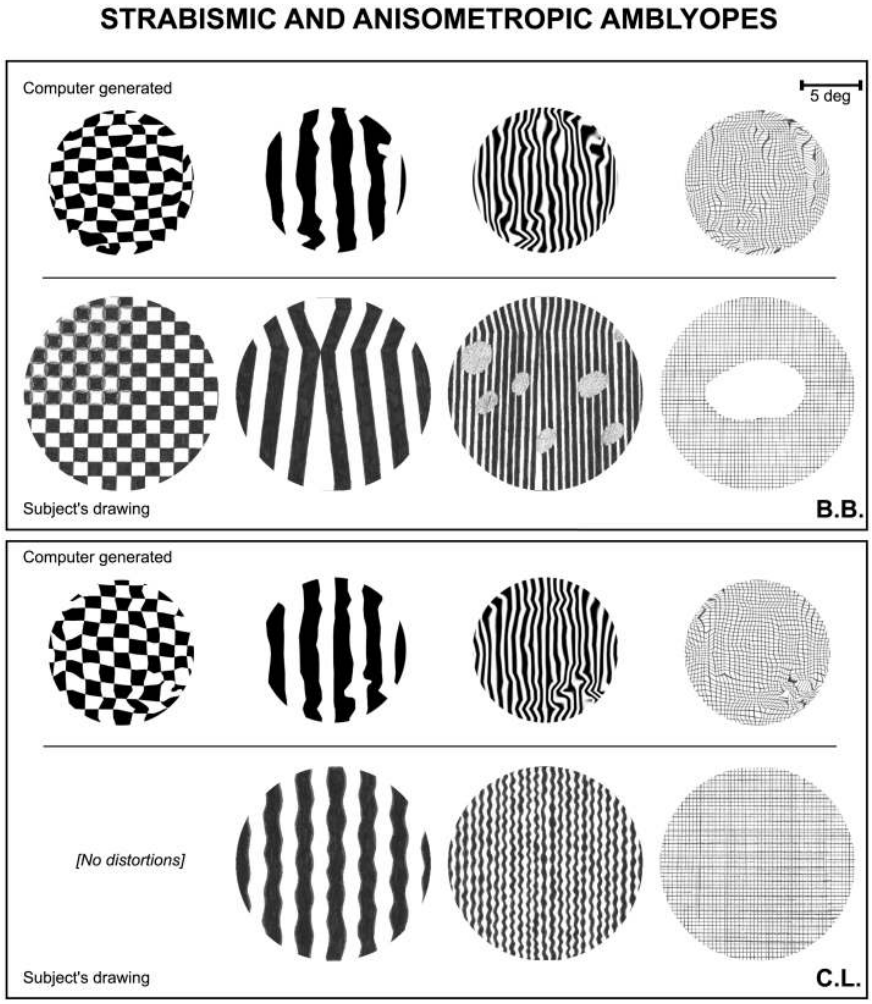


Figure 5.7: Computer reconstructions (upper panels) and visualizations of subjective perceptions (lower panels) of strabismic and anisometropic amblyopes (subjects B.B., C.L.).

## 5.4 Discussion and Conclusions

Our results provide an automated, fine-grain visualization of the amblyopic percept, based on psychophysical measurements. These methods might be generalized to the simulation of the amblyopic perception of natural, everyday images.

However, the accuracy of the simulation is directly dependent on the sampling frequency of the visual field. This might be the reason why in higher frequency domain there are noticeable differences between the simulated images and subject-described ones. We plan to further investigate the numerical relationships between the scale-invariant position inaccuracies and the scale of distortions.

*Complexity of the amblyopic percept cannot be reduced only to spatial distortions. One striking difference appears if we compare the* same *vectorial displacement data with different image inputs.*

For instance, if we look at a distorted image based on a highly regular, known objects (like letters), the resulted image will appear grossly distorted, and might be even unreadable (see Fig. 5.8.a, on page 56).

But if we look at a distorted image based on natural scenery (with fractal objects like trees), the distortions become less obvious to the observer, even if it is the same point-by-point displacement like in the previous figure (see Fig. 5.8.b).

*We speculate that this finding could explain why amblyopic patients do not complain often about the distortions in the real life. Also it strongly suggests that some categories of stimuli elicit higher subjective distortions. Therefore, the conclusion seems to be that: in order to observe spatial distortions and temporal instability in an amblyopic patient, the clinician ophthalmologist should not rely on patient description of casual images. The patient should be asked to describe his / her perceptions of special crafted images instead.* We believe that the best images are the high contrast regular patterns, with sharp edges (not sinewave variations). In the following chapters we will bring some more support to our finding.

As a side result, we were able to create movies of temporal instabilities based on this method: we incorporated a temporal jitter (of about 2 Hz in frequency) on the vectors, but maintaining them in the $SD_{areas}$. These movies cannot be reproduced on the printed media, but are presented on the accompanying CD and website. Thus, we could try to have an artificial glimpse in the confusing world of spatial and temporal distortions. While these movies are neither quantitative nor validated by the subjects they can give a general impression of how amblyopic percept might look like (this is of particular interest for the parents of children with amblyopia).

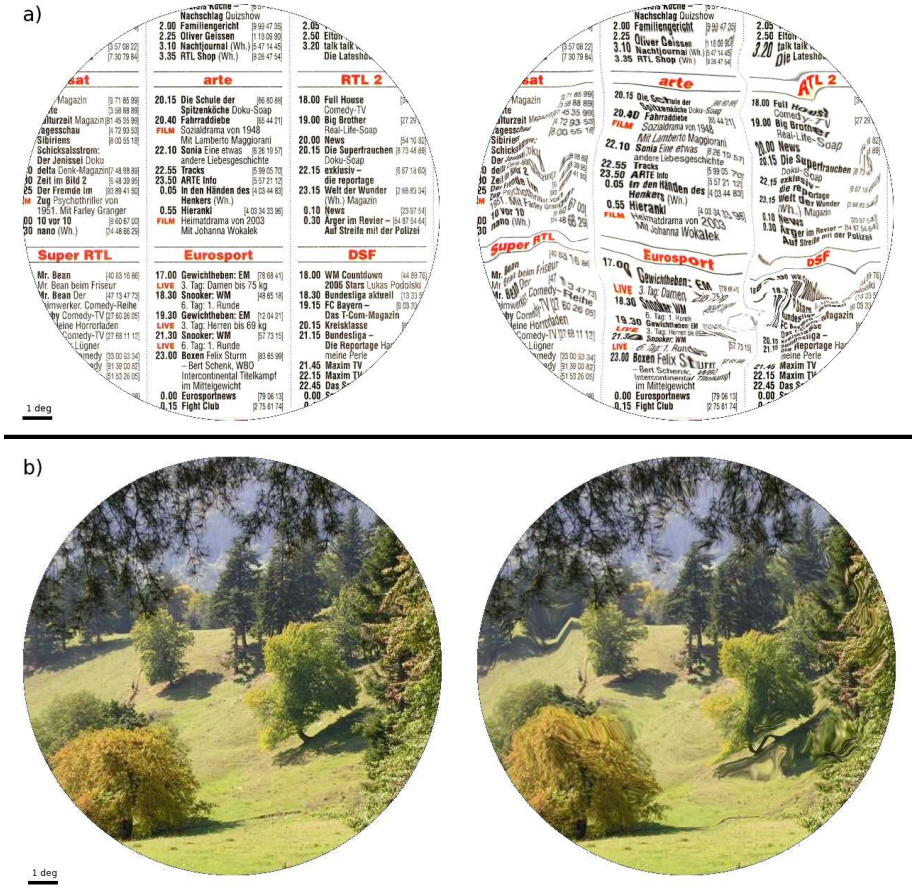


Figure 5.8: Comparison of different real-world images. *Right figures*: undistorted images; *Left figures*: distorted images, with the same vectorial data (from subject C.L.). a) highly ordered patterns (letters and numbers from a newspaper. b) natural landscape.

# Part III

# Analysis of subjective spatial distorted images and temporal instabilities

# Chapter 6

# Recording distortions (brief introduction)

This chapter contains a brief explanation on the methods we used to get the distorted images from the subjects. While not the focus of this thesis, we feel it is required to ease the understanding of the procedures described in the next chapters.

This new way of collecting-and-comparing the data is an improvement to the one introduced by C. Baeumer (BAEUMER, 2005), and is described in greater detail by A. Thiel (THIEL, 2009). The images and movies we analyzed here came from Psychophysics Lab of Prof. Ruxandra Sireteanu, and were recorded by Psych. Aylin Thiel.

Before entering the experiments the subjects were carefully assessed by licensed orthoptists, and they wore their best eye corrections if needed.

We started with a data collecting procedure also used in other experiments (SIRETEANU/LAGREZE/CONSTANTINESCU, 1993), described more detailed in (SIRETEANU/BAEUMER/IFTIME, 2008). Subjects were asked to observe a set of four static images using only the amblyopic eye. The stimuli images, were chosen in order to cover both low and higher spatial frequencies on the horizontal direction (horizontal gratings) and both vertical and horizontal directions (checkerboard and grid). We avoided the sine-wave patterns because it is very hard for the subjects to report some perceptual problems when they are used ( like blurring or edge jagging). The spatial frequencies were: - lower frequencies: grating of 0.4 cycles / degree (Fig. 6.1.a) and checkerboard of 0.4 cycles / degree (Fig. 6.1.b) - higher spatial frequencies: grating of 1.6 cycles / degree (Fig. 6.1.c) and rectangular grid of 3.2 cycles / degree (Fig. 6.1.d)

For each image, the subjects were asked to memorize what they are seeing with the amblyopic eye (their own perception) and to sketch it afterwards on paper, but using their sound eye. They were also allowed to freely describe the perception verbally; this was recorded and used afterwards. There was no time restriction in this task.

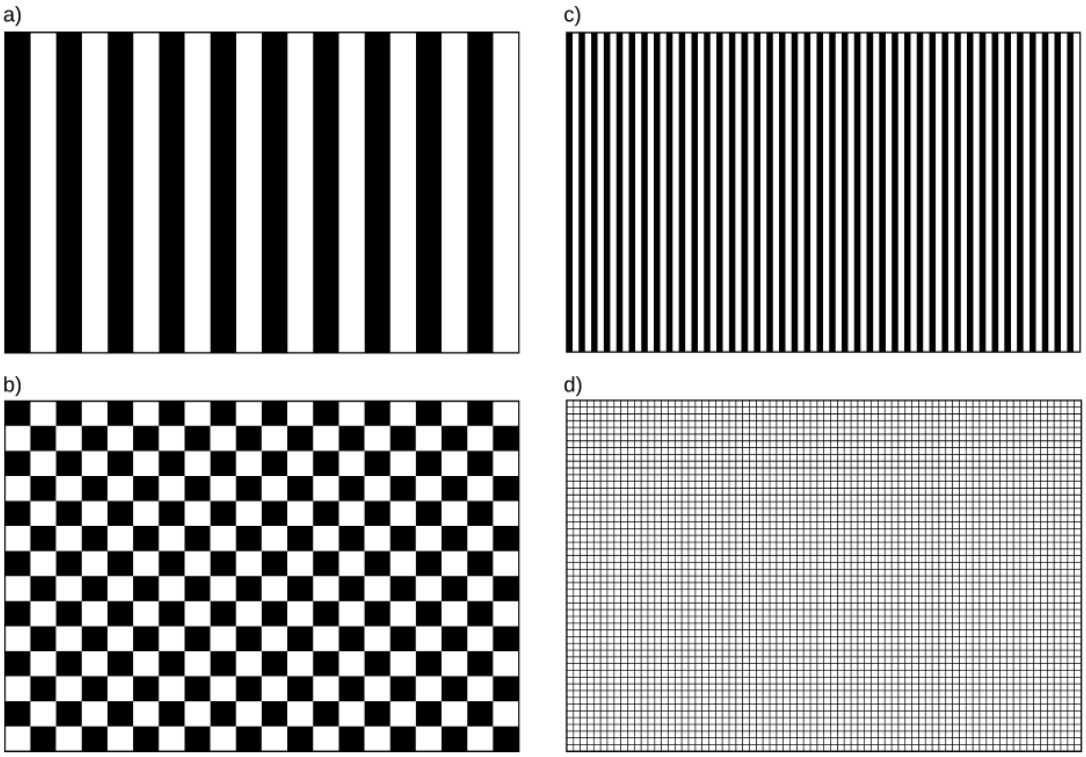


Figure 6.1: Static images used as stimuli. Each image was printed on an A4-sized paper. *a*) grating of 0.4 cycles/deg; *b*) checkerboard of 0.4 cycles/deg; *c*) grating of 1.6 cycles/deg; *d*) rectangular grid of 3.2 cycles/deg.

A trained psychologist (A. Thiel) redraw digitally their sketches (guided by verbally described perception) using standard graphic software packages (*Adobe Photoshop*, *Adobe Image Ready* and *Inkscape*). A standard multi-layer drawing approach was used to allow easy adjustments of tiny details. If the subjects reported movements in their perceptions, digital animation techniques were used to adjust the pictures accordingly (obtaining thus a movie).

The resulting still images or movies were shown to the subjects in following experimental sessions. They were allowed to observe alternately the initial static stimulus with the amblyopic eye and the corresponding digital movie with the sound eye. They could make comparisons between the two of them and tell the differences. If they were different, the digital version was changed accordingly by the psychologist. After the completion of the session, digital still image or animation was therefore improved to look more similar to what the subject was seeing with the amblyopic eye. For all the subjects at most four sessions like this were required to get to a level where they could not report any differences between the animation and their percept.

The stimuli were printed on white A4 paper, arranged in such way that the patterns were 25.4° x 15.8° degrees in the central visual field of the subjects. A chin-rest ensured the same distance to the stimuli through the measurements. Black-white contrast was

0.76 (at 43.7 cd/m$^2$). Ambient lighting was ensured with diffused light sources without shadowing in the experimental setup area. Photometric measurements were performed with a LiteMate 500 laboratory lightmeter.

The orthoptics of the investigated subjects are given in Table 6.1.

We have repeated the procedure for each subject and each stimulus image, obtaining thus a corresponding distorted still image or movie. Not all of the patients reported temporal instability of perception for each stimulus.

In the present thesis we propose four different methods for measuring the amount of distortions:

- for spatial distortions:
  - ENTPACK (in Chapter 7, starting on page 63)
  - ENTGRID (in Chapter 8, starting on page 69)
- for temporal instabilities:
  - ENTPACK-TEMP, an indirect method (in Chapter 9, starting on page 78)
  - TEDI, a direct method (in Chapter 10, starting on page 85)

| Subject | Gender, Age | Eye | Refraction | Visus c.c. (near) | Fixation | Strabismus (sim. cover test) | Stereo (TNO) | History |
|---|---|---|---|---|---|---|---|---|
| ***Strabismic Amblyopia*** | | | | | | | | |
| SG | female<br>36 yr | RE<br>LE* | +3.00 -0.75/124°<br>+3.50 -1.00/ 19° | 1.40<br>0.04 | central<br>nasal foveal rim, unsteady | far +13° +VD 3°<br>near +15° +VD 3° | ∅ | Squint detected at 3 yr, first RX at 4 yr, occlusion therapy from 3 to ~8-9 yr, left-handed (crossed dominance), LE crowding |
| LP | female,<br>36 yr | RE<br>LE* | +0.50<br>+0.75 | 1.00<br>0.25 | central<br>temporal | far -12 ½° +VD 1°<br>near ca. 0° | ∅ | Congenital strabismus, occlusion therapy at 4-5 yr, first RX at 5-6 yr; Turner syndrome, LE crowding |
| SS | female,<br>42 yr | RE*<br>LE | plano<br>plano | 0.32<br>1.25 | parafoveolar<br>central | far +3°<br>near +3° | ∅ | Congenital esotropia; surgery RE at ca. 2-3 yr (x2); occlusion therapy at 4-6 yr, glasses from 6 until 11 yr; crossed dominance, RE crowding |
| KK | female,<br>20 yr | RE*<br>LE | +3.75<br>+4.00 | 0.70<br>1.25 | central<br>central | far +1°<br>near +2° | Titmus fly | Microstrabismus; occlusion therapy between 5 and 7 yr, first RX with 7 yr |
| ***Strabismic & Anisometropic Amblyopia*** | | | | | | | | |
| BSB | female,<br>32 yr | RE*<br>LE | -0.75<br>-1.75 -2.00/175° | 0.063<br>0.90 | temporal, nyst.<br>central, nyst. | far - 3° + VD 2 ½°<br>near - 3° + VD 2 | ∅ | Squint since birth, surgery at 20 months, first RX with 3 yr, alternating occlusion therapy from 3 to 6 yr |
| KB | male,<br>45 yr | RE<br>LE* | +0.50<br>+2.50 -1.00/90° | 1.25<br>0.125 | central<br>parafoveolar | far -½° -VD 2½°<br>near -5° -VD 3° | Titmus fly | Family history, first RX ca. 10 yr, occlusion & pleoptic therapy between 9-11 yr; history of strabismus |
| KF | female,<br>42 yr | RE<br>LE* | -1.50 -0.25/ 60°<br>0.00 -0.50/ 0° | 1.00<br>0.40 | central<br>central | far - 19°<br>near - 17 ½° | ∅ | First RX with 3 yr, occlusion therapy from 3 yr to school entry |
| KHW | male,<br>61 yr | RE*<br>LE | + 5.50 -4.50/ 10°<br>- 0.75<br>RE/LE add. +2.5 | 0.63<br>1.00 | central<br>central | far ca. 0°<br>near - 1° +VD 1½ | Titmus fly | Family history of anisometropia; first RX with 18 yr |
| KL | female,<br>24 yr | RE*<br>LE | +1.00 -0.75/114°<br>- 3.00 -0.50/ 61° | 0.70<br>1.00 | unsteady<br>central | far +1° +VD 1½°<br>near +1° +VD 1½° | Titmus fly | Very premature birth, respirator; congenital strab. sursoadductorius; first RX with 3 yr; regular occlusion therapy from 3 to 7 yrs, surgery at 10 yr; microstrab. conv. et vert. od (with identity), RE crowding, anisometropia |

Table 6.1: Orthoptics data for 2nd group of subjects. The same color-coding of categories will be used in the following chapters. *LEGEND*: *RE* - right eye; *LE* - left eye; *visus c.c.* - corrected decimal visual acuity; *Ø* - no stereopsis; *VD* - vertical deviation; *plano* - no correction required; * - amblyopic eye.

| Subject | Gender, Age | Eye | Refraction | Visus c.c. (near) | Fixation | Strabismus (sim. cover test) | Stereo (TNO) | History |
|---|---|---|---|---|---|---|---|---|
| ***Anisometropic Amblyopia*** | | | | | | | | |
| MK | male, 51 yr | RE<br>LE* | plano<br>+ 2.50<br>RE/LE add. +2,0 | 0.90<br>0.16 | central<br>central | far 0°<br>near 0° | Titmus fly | Family history, first RX with 16 yr |
| HMK | female, 50 yr | RE*<br>LE | +4.00 -2.50/ 55°<br>+2.75 -1.25/100°<br>RE/LE add. +1.75 | 0.50<br>1.00 | central<br>central | far 0°<br>near 0° | 60" | Family history; first RX with 21 yr; crossed dominance |
| AR | female, 25 yr | RE*<br>LE | plano (LASIK)<br>plano | 0.50<br>1.00 | central, unsteady<br>central | far 0°<br>near 0° | 120" | First RX at 7 yr, occlusion therapy and pleoptics at 7-8 yr for 1 yr, LASIK in 2006 at 24 yr, RE (previous refraction error: +3.50-4.75/ 9°); crossed dominance (distortions consecutive to LASIK!?) |
| FA | male, 32 yr | RE*<br>LE | -4.75 -2.00/ 10°<br>-2.25 -2.25/170° | 0.80<br>1.00 | central<br>central | far 0°<br>near 0° | ∅ | First RX with 14 yr |
| ***Deprivation Amblyopia (Ptosis)*** | | | | | | | | |
| MJ | female, 28 yr | RE*<br>LE | -1.00 -0.25/ 90°<br>-1.25 -0.75/ 6° | 1.00<br>1.25 | central<br>central | far ca. 0° + VD<br>near ca. 0° + VD | 60" | Ptosis RE in early childhood; first RX at 6 yr, 6 surgeries (RE), latent nystagmus |
| ***Esotropes with (not Free) Alternating Fixation*** | | | | | | | | |
| AL | female, 20 yr | RE<br>LE* | +2.25 -1.75/175°<br>+4.50 -2.25/ 12° | 1.40<br>1.40 | central<br>nasal, unsteady | far + 3°<br>near + 3° | ∅ | Family history; microstrabismus and anisometropia; first RX and glasses at ca. 2 yr (eso; presumably accommodative strabismus); occlusion therapy from 2-3 yr until ca. 12 years of age (RE); RE dominant (can hold fixation LE), LE crowding |
| LJ | female, 22 yr | RE<br>LE* | +0.50 -1.50/167°<br>-2.00 -2.25/175° | 1.00<br>1.25 | central, nyst.<br>central, nyst. | far + 14° unsteady DVD<br>near + 16° DVD 1½° | ∅ | Family history; anisometropia; squint onset in infancy; first RX at 1 yr of age; occlusion therapy from 1 yr until school age; surgery at 18 months; alternating fixation (RE dominant) |
| RW | male, 26 yr | RE<br>LE* | +2.25 -0.75/155°<br>+2.25 -0.75/155° | 1.40<br>1.25 | central<br>central | far + 6° + VD<br>near + 6° + VD 2° | ∅ | Squint onset in infancy; first RX with 2 yr, 2-3 surgeries; occlusion therapy, alternating fixation (RE slightly dominant) |
| FS | female, 28 yr | RE<br>LE* | plano<br>plano | 1.25<br>1.00 | central<br>central | far + 2°<br>near + 3° | ∅ | First RX at 2 yr, surgery at 6 yr (RE?), occlusion therapy from 2 yr until school age; not free alternator (can hold fixation LE) |
| PG | male, 22 yr | RE<br>LE* | plano<br>plano | 1.40<br>1.40 | central<br>central | far + 5° slight ±VD<br>near + 6° | ∅ | Initially large-angle strabismus, first RX at 6 yr, worn for 1 yr; occlusion therapy at 5-7 yr, two surgeries for both eyes; not free alternator (can fixate LE) |
| ***Exotropes with Free Alternating Fixation*** | | | | | | | | |
| TGF | male, 28 yr | RE<br>LE* | +1.25<br>+0.75 -0.50/ 3° | 1.25<br>1.40 | central<br>central | far - 15°<br>near - 15° | ∅ | Squint from birth; first RX at 3 yr; occlusion therapy at 2-4 yr, surgery at 20 yr (LE); free alternating fixation (RE dominant) |
| GZ | female, 25 yr | RE*<br>LE | plano<br>plano | 1.00<br>1.40 | central<br>central | far - 8°<br>near - 9° | ∅ | Squint onset at 2 yr, first RX with 2-3 yr, occlusion therapy and pleoptics at 2-3 yr; free alternating fixation (LE dominant) |
| JM | female, 29 yr | RE*<br>LE | +1.75 -0.25 /100°<br>+1.75 | 1.25<br>1.40 | central<br>central | far - 2°<br>near - ½° | ∅ | First RX at 3 yr of age, occlusion and pleoptic therapy at 3 yr; free alternating fixation (LE dominant) |

*(continued from previous page)*

# Chapter 7

# ENTPACK - Analysis of static distortions

## 7.1 Introduction

This new method is used in order to digitally and quantitatively investigate the amount of static spatial visual misperceptions reported by human amblyopic subjects. Our intention is to find a way to measure the subjective distortions reported by the subjects. With an objective measurement, it would be possible to investigate the relationship between the amount of spatial distortion and the aetiology or other particular features. We suggest that computing the entropy in the reported images might be useful for this purpose. Information entropy in an image increases with the number of internal variations in that image. As an example, see Fig. 7.1. The entropy analysis is a useful tool for a quick evaluation of amount of change in a pattern (DOGARU et al., 2003).

The acronym ENTPACK comes from "*Ent*ropy *Pac*kage", the name of the program that we created to automate the calculations described below.

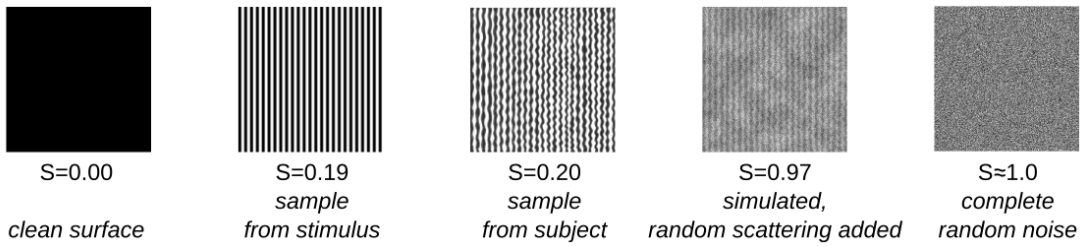


Figure 7.1: Different images, with increasing amount of variation (from none to complete random noise), and with corresponding entropy values (S).

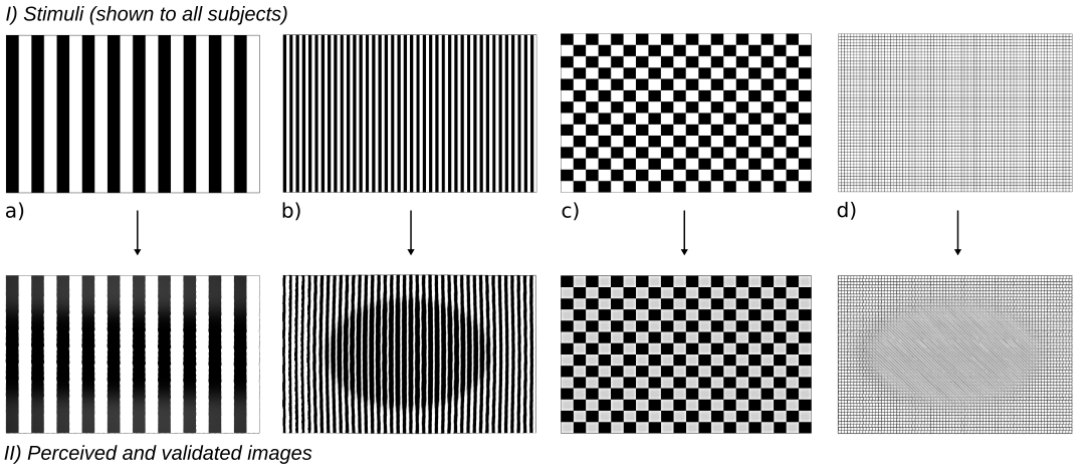


Figure 7.2: Example of validated spatial distortions reported. In this particular image, the distorted images were perceived by subject H.M.K. (see Table 6.1).

## 7.2 Materials and Method

Twenty-two subjects with strabismic, anisometropic, or mixed amblyopia (see 6.1 on page 61) were asked to describe and sketch their subjective percept of four different geometrical patterns as seen with the amblyopic eye. The stimuli we used were presented in Fig.6.1 (see page 59).

Based on their descriptions, digital images were generated until validated by the subjects (see Fig. 7.2).

It should be noted that the validation process brings up finer details than previously reported. It becomes obvious that the reported distortions (from the same subject) appear to be dependent on the stimulus used. For instance, subject H.M. reports (Fig. 7.2):

- image I.a) was perceived with a loss of contrast on top and bottom portions; margins were jagged.

- image I.b.) a central “blob” that appear to grow from the darker areas of the image; over all image, margins are jagged, irregular.

- image I.c) a general loss of contrast; darkening of white blocks, but with an apparent whiter margin.

- image i.d) a “blob” of irregular slanted lines, with low contrast, appears in the central visual field. Margins of the grid are perceived as irregular.

All subjects were asked to participate in these sessions, and we used in the following procedures only the subjects that reported spatially distorted images.

We analyzed images on different scales, applying the following steps for each one:

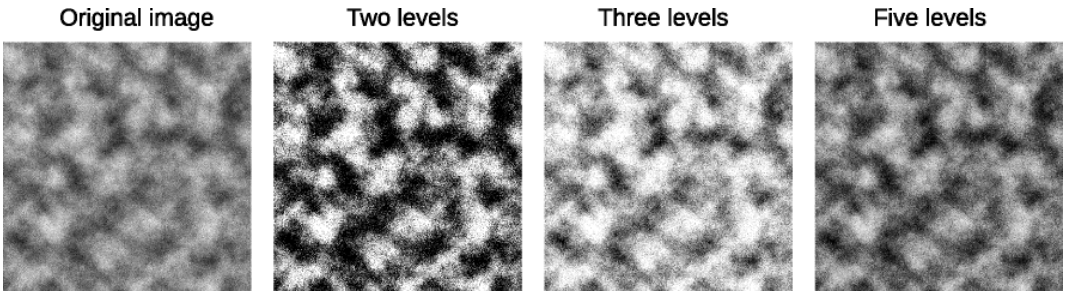


Figure 7.3: Different normalizations of an original, random image (left). Note the achieved similarity between the original image and five-levels image (right).

**a) Normalization**

In order to do a meaningful comparison, we made sure that the geometry of the images is the same. In order to insure that the stimulus image occupied the same area on the subject's retina, we used a chin-rest with a head-band, placed at a fixed distance of 57 cm from the stimulus image. The digitally created images were stored in the standard RGB colour space (8 bits per channel), and at the same dimensions.

The entropy calculation (see below) is computationally intensive, so in order to reduce the computation time to a manageable level, we normalized both the geometry and the colour-space of the images:

- *Geometry*: all images were reduced in size to 842 x 596 pixels. These operations were performed with standard image manipulation programs (*GIMP - GNU Image Manipulation Program* and we automated the process using scripts based on *ImageMagick Studio LLC*).

- *colour-space*: we reduced them to five levels of gray (matching perceptual luminance at pixel level). This step (and the entropy computation itself) was done by our program "entpack.jar", written in Java with *Java Advanced Imaging* extensions (from *Sun Microsystems*).

In entropy calculation, a black-and-white (two levels of colour) approach is often used because this reduction maintains the average geometry of the image. However, we believe that this approach might be insufficient in the present work, since many images contain blurring and shades of grey. In order to preserve also the grey areas, we chose to make a reduction to 5 levels of colour (white, black, and three shades of grey). An example of different colour reduction levels is given in Fig. 7.3.

**b) Small scale analysis**

We computed the Shannon entropy on the images produced by the subjects.

Briefly, the algorithm computes the apparition frequency ($p$) of any possible combinations of grey shades in an area of 3x3 pixels. Image as a whole (Fig.7.4) is scanned for all combinations ($i$) of gray shade configurations that appear. The Shannon entropy is as such:

$$S = \sum_{i=1}^{n} p(i) \cdot log \frac{1}{p(i)}$$

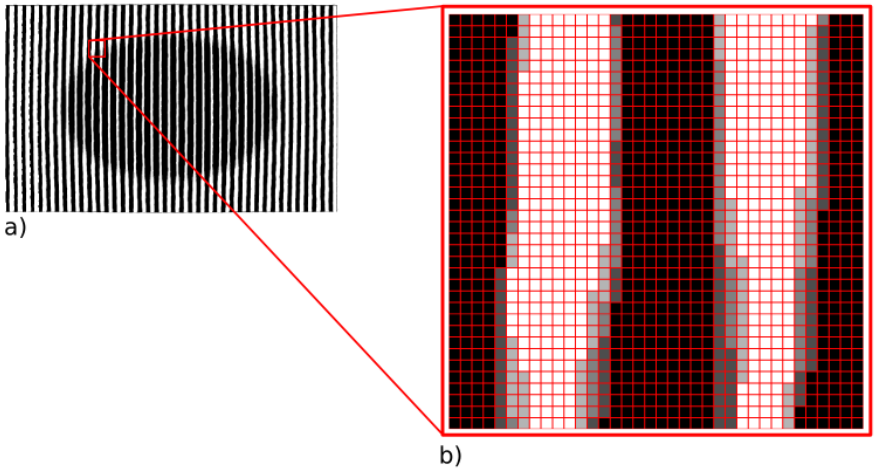


Figure 7.4: Small-scale analysis. Each small square represents one pixel from the original image (left).

We computed the occurrence frequency of unique patterns of 3x3 neighbouring pixels (the total number of possible patterns in these kind of images is $5^9$ = 1,953,125); some examples of pattern variation range:

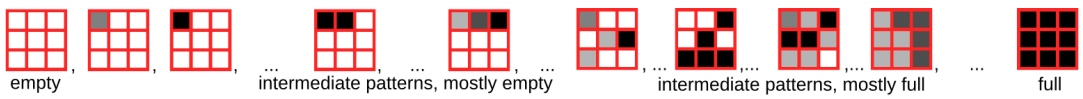


Based on these frequencies, Shannon entropy can be then obtained for overall image.

The entropy was computed for each image or movie reported by the subjects, and compared with the entropy of the original presented images.

## 7.3 Results

### Individual data

For the vast majority of the cases and for all the four stimuli, we have observed an increase in the overall entropy of the described images, as compared with the entropy level of the presented images (see Fig. 7.5, a, b, c, d). We interpret the observed increasing of entropy as a measure of loss of information structure in the subjects' visual processing flux.

### Group data

Comparing the group responses to stimuli, we found that for the first category (vertical gratings), there is a significant ($p < .0001$) higher entropy reported for the higher frequency grating than for the lower frequency one (mean S1= 1.244, StDev S1 = 0.202; mean S2= 1.535, StDev S2= 0.263). This is not the case for the second category of stimuli (crossed patterns). *These results seem to show that the exposure to simpler high frequency gratings is a better way to elicit the appearance of distorted perceptions in amblyopic subjects.*

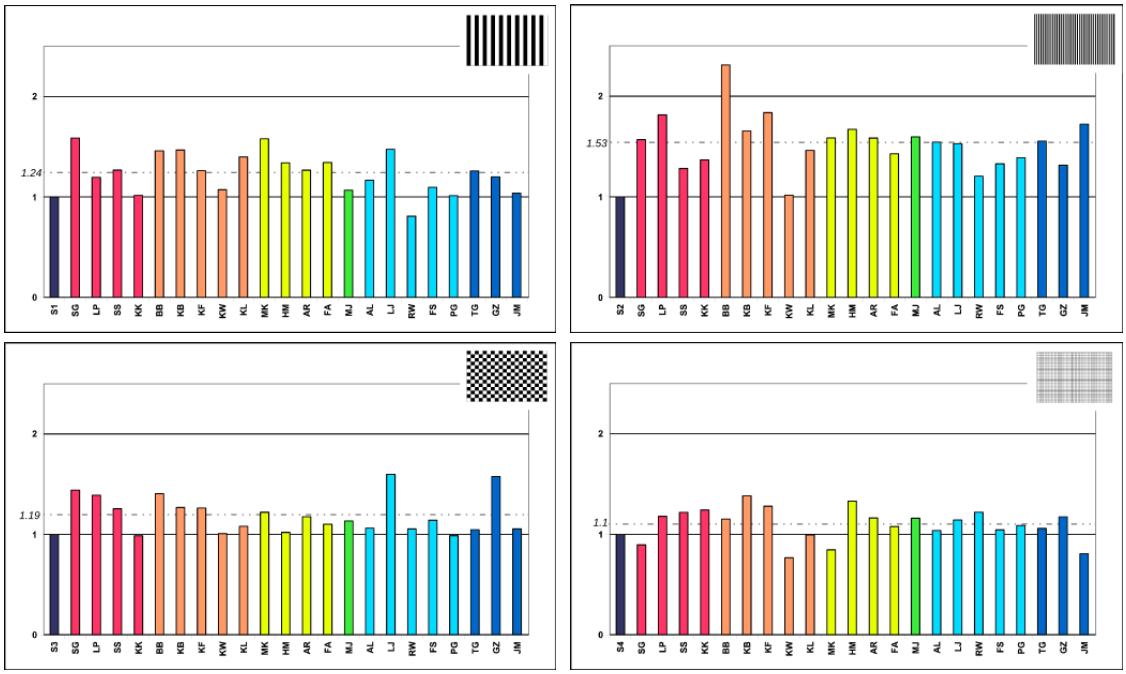


Figure 7.5: Individual entropy levels for each stimulus. Legend: *Ordinate*: the ratio of Shannon entropy values of each subject, to the entropy of the stimulus ($S_{subject}/S_{stimulus}$). *Dark-blue bar*: entropy level of the stimulus (normalized to 1.00); *Colored bars*: subjects' data; the aetiology of subjects is colour-coded like in the Table 6.1 on page 61; *Dotted line*: the averaged group response to the stimulus.

## 7.4 Discussion and Conclusions

*The finding that the distortion amount seems to be influenced by the content of the stimulus (presented image) is the main result of this method.* Our data suggest that stimuli like the one in Fig. 6.1.c (see page 59) are the best to use if one investigates the apparition of spatial distortions.

Using this method, it is also possible to compute the temporal frequency of the unstable perception, by computing entropy on frame-by-frame basis (see Chapter 9).

*ENTPACK Method* is independent from the data gathering procedure used (like the validation method discussed in Chapter 6). This feature makes us confident that the method can be used also in different circumstances, by other researchers.

Our results suggest one practical conclusion for clinical ophthalmologists who investigate an amblyopic patient: In addition to standard ophthalmological tests, the patient should be investigated for presence of spatial distortions. *However, the images used as stimuli for this investigation should be patterns with high spatial frequency, like we found in our study. These images are more likely to elicit spatial / temporal distortions than other images.*

# Chapter 8

# ENTGRID - Localization of distortions

## 8.1 Introduction

In the previous chapters we analyzed distortions in the whole images. We wonder if there are places in the visual field where the distortions are more likely to appear. For instance: do they appear at random positions? Is there a region that is more prone to appear distorted, and if yes, why?

We propose here a data analysis method based on the ENTPACK. Instead on computing the entropy on the whole image, we can analyze portions of it, and compare the variations between them. The acronym "ENTGRID" comes from "*Ent*ropy *Grid* Calculations".

## 8.2 Materials and Method

We analyzed the same image data as described in the previous chapter (from the twenty-two subjects described in the Table 6.1).

Instead of computing the entropy for the whole image, we computed it for small portions of the images, corresponding to an area of 1 $deg^2$ in the visual field. We divided images in a rectangular grid, spaced apart with 1 degree in both vertical and horizontal axis. Each cell of this grid is a portion of the image, and using the same algorithm described in the previous chapter, we computed the local entropy value in this cell.

Thus, for each image we obtained an array of values (a matrix) with entropy values in each corresponding 1 $deg^2$. In order to ease the data visualization, we display them as "entropy maps": areas with lower entropy are coloured in darker shades of grey, areas with higher entropy values are lighter. For an example of the entropy maps, see Fig. 8.1.

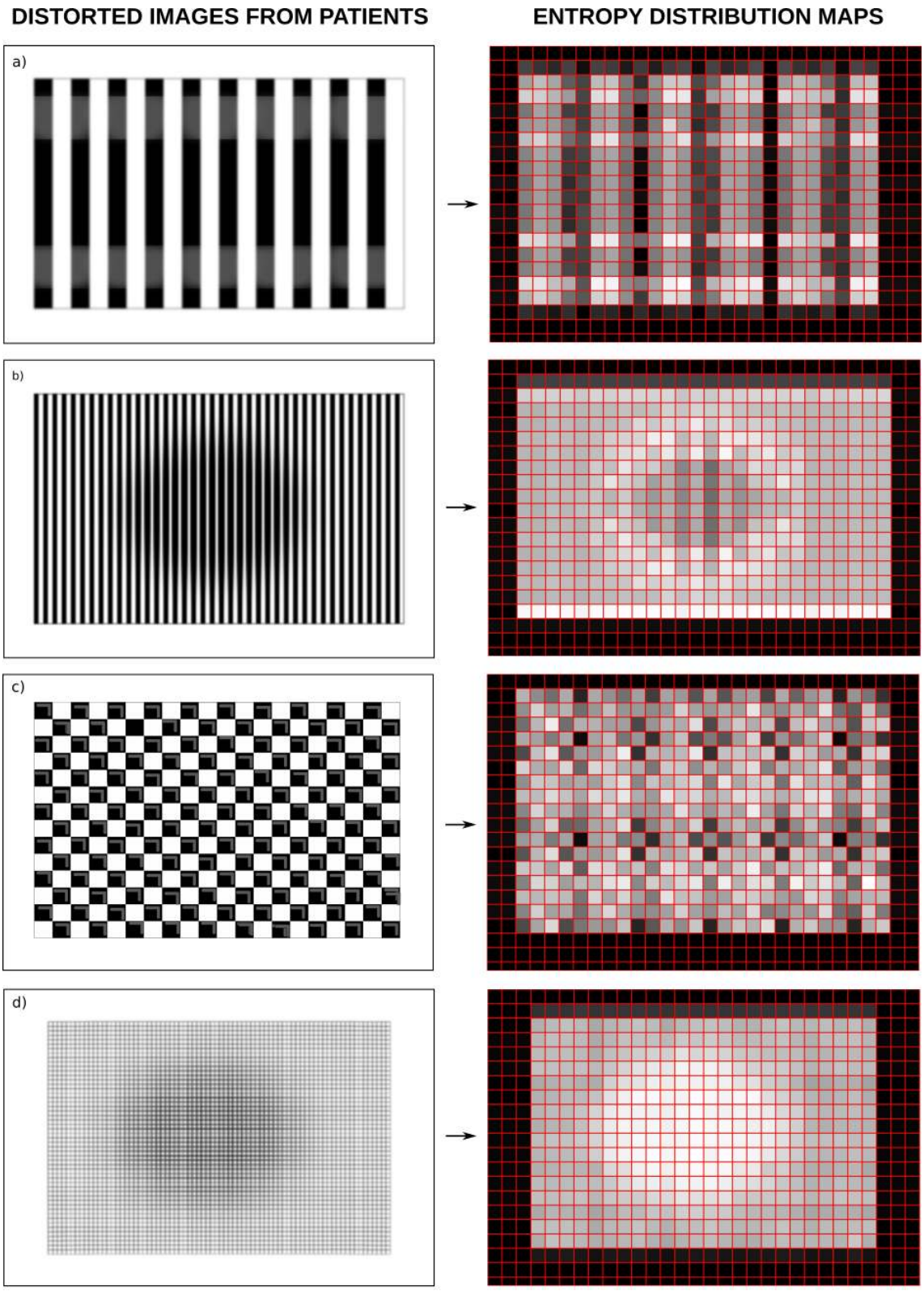


Figure 8.1: Entropy maps example (from subject K.B.). *Left column*: original distorted images, as perceived by the subject. *Right column*: the corresponding entropy distribution in the images. Black corresponds to a zero entropy value (S=0.0), and white corresponds to maximum entropy (S=1.0); *Red grid*: 1 degree in visual field.

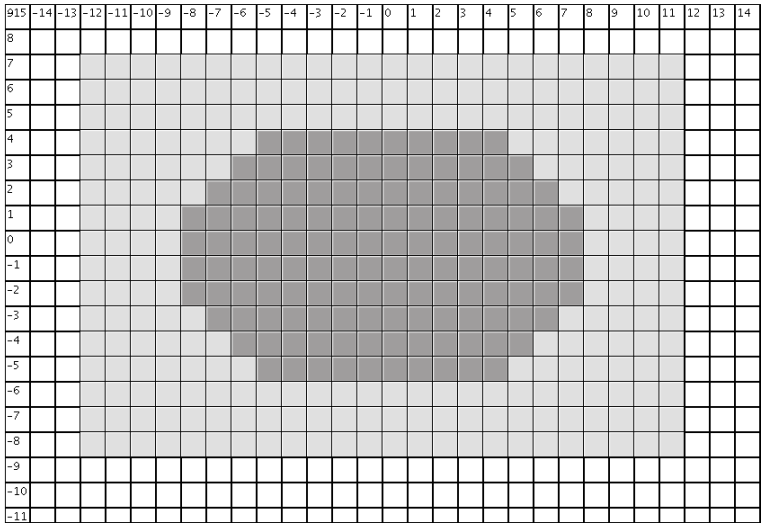


Figure 8.2: Image zones. *Dark grey*: inner part; *Light-grey*: outer part; *Numbers*: coordinates (in visual degrees) from the center of the image.

After computing entropy distribution in each image collected from subjects, we tested if there is a difference in distribution of entropy values between the central part of the images and the periphery.

We visually observed that in several cases the main distortions were described by the subjects as being confined in a central ellipsoidal area. We wondered if this subjective observation is true from a statistical point of view. Therefore we measured the average entropy in central part of image and in periphery and look if there is a significant difference; we repeated the procedure for all the images.

We define the “central part” as an ellipsoid (dark grey in the figure 8.2), spanning 12. deg horizontally and 10 deg. vertically and an outer part (light grey, the rest of the image). While defining the portions of the image, we take care not to include the empty border of the images (white), as depicted in Fig. 8.2.

## 8.3 Results

We found a highly significant ($p < 0.001$) difference between entropy values in the central and in the peripheral parts of the images described by the subjects, regardless of the stimulus. Thus, our subjective observation seems to be true: for the data coming out of our subjects, the entropy is higher in the central portions of the visual field. The areas with higher entropy values (bigger distortions) are more often confined in a roughly ellipsoidal area centred in the visual field.

## 8.4 Discussion and Conclusions

We interpret this disparity of entropy distribution as a consequence of completely non-overlapping receptive fields of both eyes.

We propose as an explanation a 3D overlapping model which shows that for a given strabismus angle, the degree of overlapping varies with eccentricity (less overlap in central areas, more in periphery). The resulting overall shape of area containing non-overlapping fields is also ellipsoidal, centred in the visual field; as far as we know, this was not previously reported in the literature. The phenomenon can be described by a comparison between normal and pathological states of visual receptive fields.

**Normal state of visual receptive fields**

In healthy individuals, the fusion of the two images generated by the eyes is accurate at the point of fixation (centre of visual field, which falls on fovea). Each eye sees a field of view of about ~ 140 degrees on horizontal plane, asymmetrically distributed (on the medial side, the nose blocks the view). This is depicted in figure 8.3, (top view), on page 74. In all the descriptions and images that follow in this section, the left eye is coloured in red, right eye, in green. The field monocular field of view of each eye is represented by simple textured area, matching in colour.

The binocular area is the region where stereo vision forms. It is represented by a cross textured area (red and green), spanning ~ 100 degrees. It is symmetrical, centred around the fixation point (marked with 0° on the protractor). The direction of the gaze is marked with red and green lines, toward the fixation point.

Ganglion cells (which are the output cells of the retina) have a *receptive field on the retina*, which is defined as the contiguous region of photoreceptors from which a ganglion cell receives input. The receptive field on the retina receives information from a limited portion of the space (the portion of the image that gets projected by the optical media on those particular photoreceptors) . Thus, a ganglion cell “sees” only a limited portion of the visual space; this portion is also called the *receptive field-of-view* of the ganglion cell(TESSIER-LAVIGNE, 2000).

The human eye gets two powerful features by varying the size of the receptor fields:

- the central zone gets a high-resolution image; this is accomplished by very small receptive fields (in fovea, one photoreceptor corresponds to one ganglion cell

- the periphery gets a large field-of-view but a low resolution, because a larger area of the visual field is analyzed by a single ganglion cell.

In the Figures 8.3 - 8.5 (pages 74-77), in TOP VIEW sections, these receptive fields-of-view are represented by coloured sectors (red and green) adjacent to protractor’s

edge. The size variation starting form the centre towards the periphery is anatomically accurate for adult human vision (SIRETEANU, 1990).

In order to get a clear, sharp image and stereo perception, the receptive fields of the right eye must match those on the left eye (they have to overlap the same portion of the visual field). This situation is depicted in Fig. 8.3 on the following page.

We constructed a 3D representation of the elements described above. The colour code is the same: green for elements related to the dominant eye, red for the elements related to non-dominant, amblyopic eye. The discs represent the area of the visual field deserved by a ganglion cell. Note that only the receptive fields from the left eye are visible (Fig. 8.3 on the next page, 3D-VIEW).

In the bottom panel, we represented the spread of the visual fields, in the same situation, but from frontal view. The image is a flattened projection from the 3D-view.

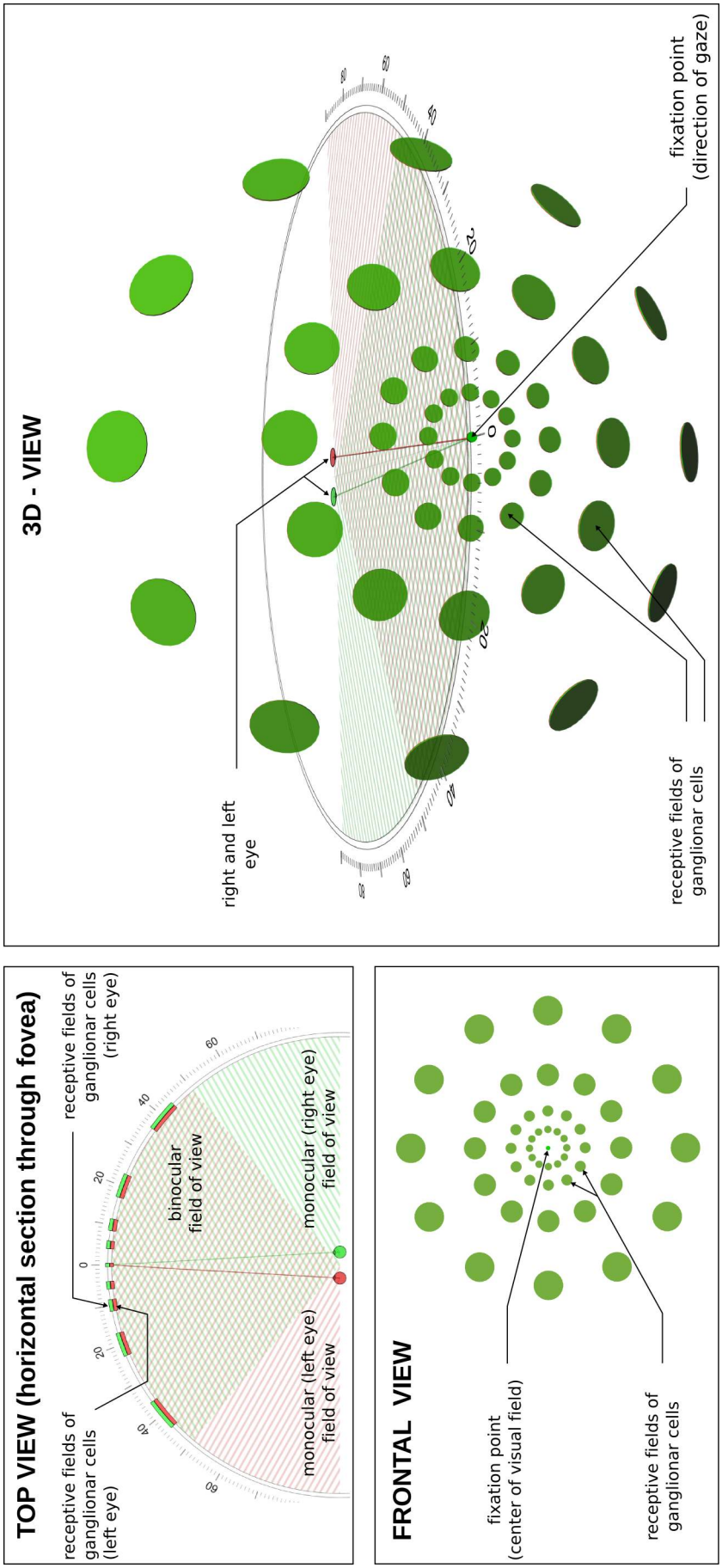


Figure 8.3: Model of *normal* overlapping receptive fields. Red: information related to the left eye, green - to the right eye. The regions of space that are processed by a single ganglion cell in the retina (the receptive fields) do overlap perfectly. The overlapping is a requirement to get a normal binocular vision. The receptive fields are represented as segments in top view, as disks in the frontal and 3D-view.

**Altered states of visual receptive fields**

This precise alignment is not preserved in pathological conditions that might lead to amblyopia. In strabismus, a squinting occurs, leading to a geometrical mis-alignment of the receptive fields. In figure 8.4 on the following page, a squinting of 2.1 degrees is shown (the right eye, green, cannot fixate on the target, but is deviated to the left).

Due to different receptive fields' sizes, there are two distinct situations:

- a) **in the central part there is a *complete misalignment* of the receptive fields**. The ganglion cell from an eye receives information that is from a different region of space than from the other eye. The binocular vision is therefore disrupted in this area. This area is represented with a dark-grey shade.

- b) **in the periphery there is a *partial overlap*.** Therefore correspondent ganglion cells have a chance to fuse the images; the binocular vision is therefore preserved. It should be noted that the relative overlapping area increases away from the centre (the relative size of the receptive fields is bigger than the squinting angle).

An interesting observation arises if we examine the 3D representation: the area of binocular loss is not symmetrical on horizontal and vertical axes. The surface of this area is an ellipsoid (marked with dark-grey shade in FRONTAL VIEWs). As the squinting angle increases, the size of the visual loss increases, but it retains its ellipsoidal shape; see Fig. 8.5 on page 77 for an example of the phenomena at the 6.1 degree squinting angle.

*We speculate that this area of total binocularity loss is the major source of distortions in the images. Its shape could explain the frequent reports of "ellipsoidal blobs" with different features in distorted images.* We believe that a similar model holds for anisometropia: even if the geometrical blurring of the retina is uniform, the central part suffers the most (due to smaller receptive fields).

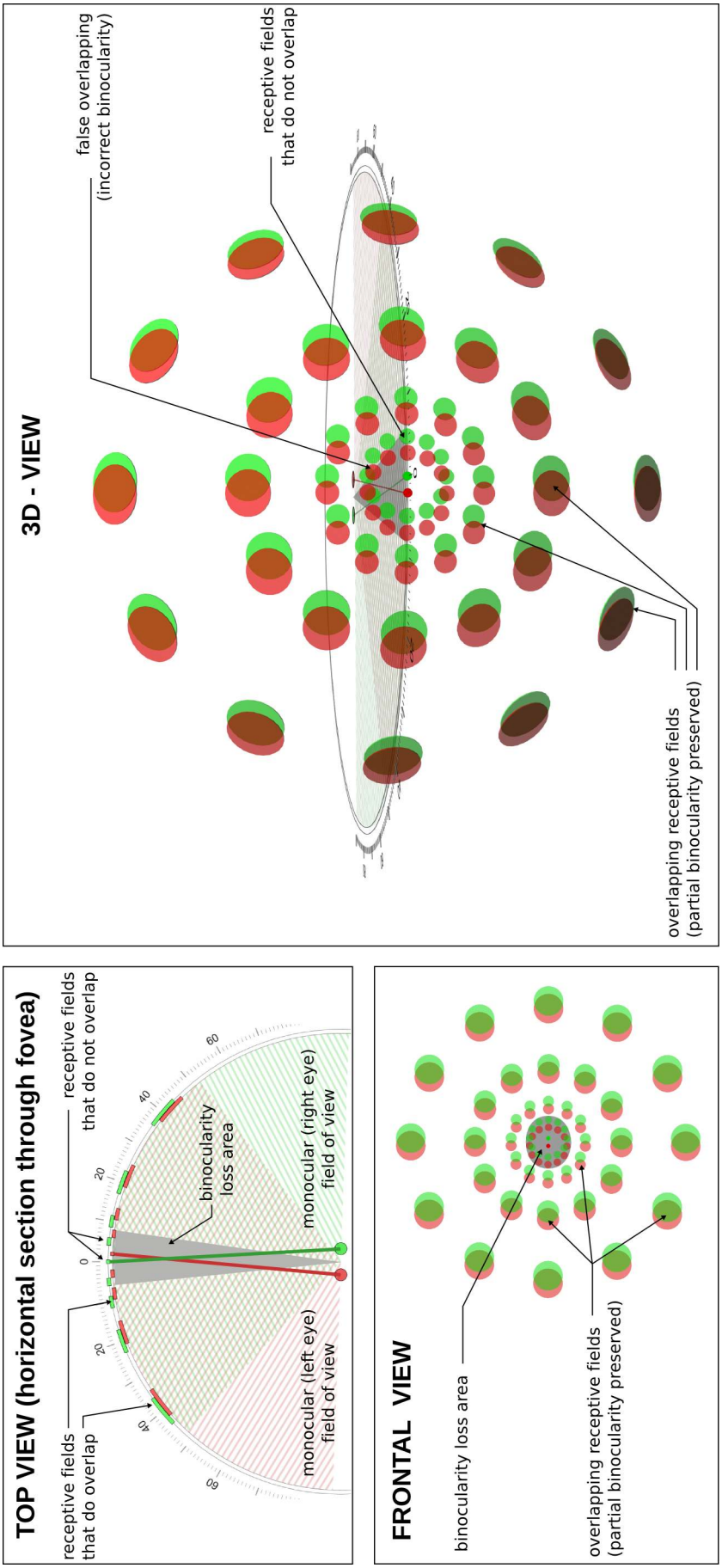


Figure 8.4: Partial overlapping at ~ 2.1 deg. squinting angle. *Red*: information related to the left eye, *green* - to the right eye. The left eye gaze is abnormally shifted, and therefore its receptive fields. Because the receptive fields are smaller in the central portion, they do not overlap (therefore there is binocularity loss). In the peripheral portions of the retina, receptive fields are bigger, and there is a degree of overlap, therefore the cortical neurons can have a chance to get binocular vision. In the frontal view can be seen that the area of binocularity loss is ellipsoidal in shape.

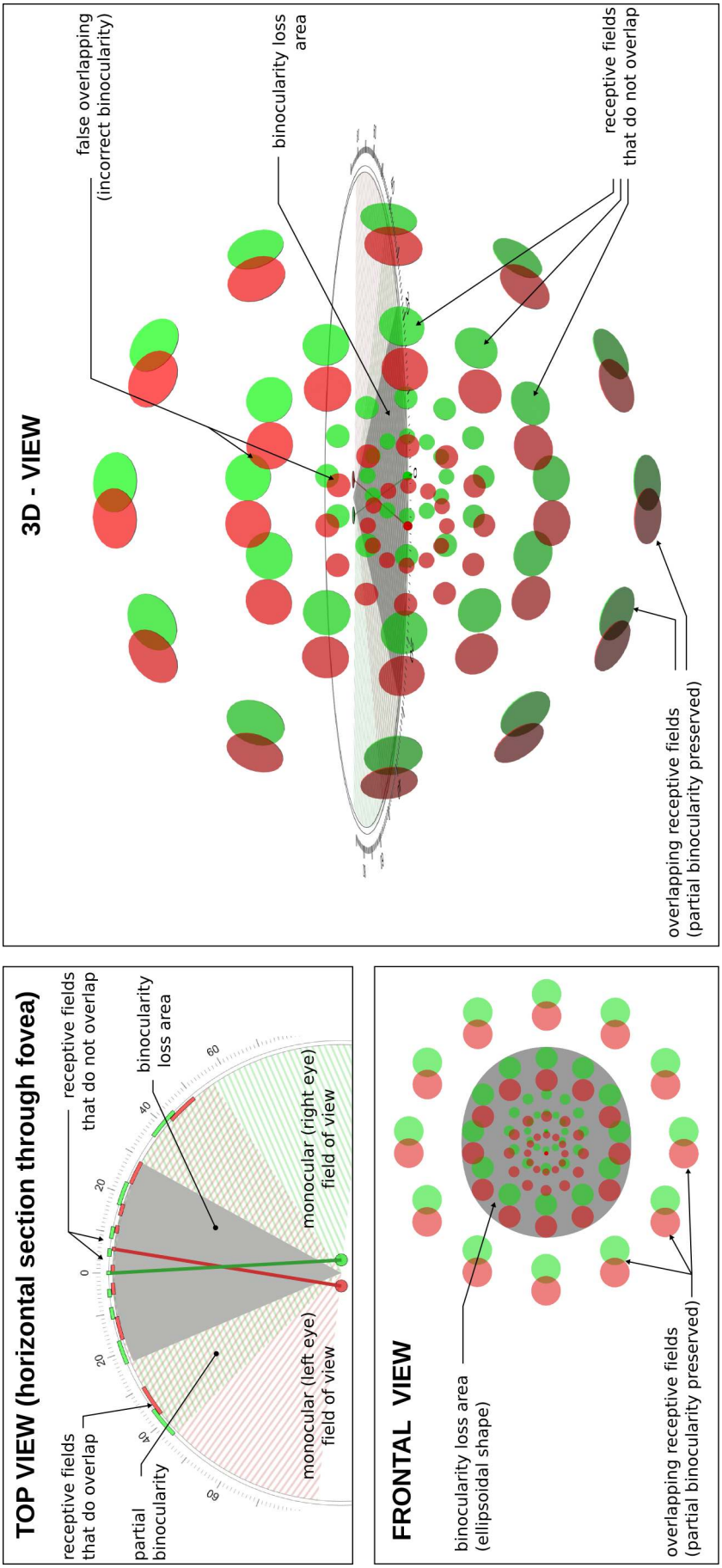


Figure 8.5: Partial overlapping at ~ 6 deg. squinting angle. *Red*: information related to the left eye, *green* - to the right eye. The left eye gaze is abnormally shifted, and therefore its receptive fields. The non-overlapping number of visual fields increased (as compared with the previous figure). In a frontal view, one can notice that the area of binocularity loss is ellipsoidal in shape, and its size increases as the squinting angle increases also.

# Chapter 9

# ENTPACK-TEMP Method

## 9.1 Introduction: Analysis of recorded temporal instabilities

In the previous chapters we have examined in detail the static perceptual distortions. Some of the subjects also reported that the distortions they saw were moving. The subjects were aware that what they were seeing (i.e. their percept) was unstable, not stimulus itself.

In this chapter and the next one we examine the data obtained from the same lot of subjects described in 6.1 on page 61. The data collecting procedure was devised and performed by Psych. Aylin Thiel, under direct supervision of Prof. R. Sireteanu; this data procedure is described on page 58.

The image below (Fig. 9.1) is an example of a recorded a movie (i.e. some of its frames) from the subject S.S., for the stimulus presented in Fig. 6.1.c (page 59). While looking at the static stimulus image using the amblyopic eye, she reports the appearance of a darker, ellipsoidal pulsating spot. The expansion and contraction of this spot are cyclical. Because of space constraints, we reproduce here only 9 frames from the animation.

## 9.2 Purpose of using the ENTPACK-TEMP method

We intend to create an indirect method able to measure the variation speed of reported amblyopic perceptions over a short time scale (minutes).

We refer to this method as an “indirect” one because we plan to use the subjective descriptions of the amblyopic percept (i.e. subjects’ sketches and descriptions, but recorded in a rigorous way, as described in Chapter 6).

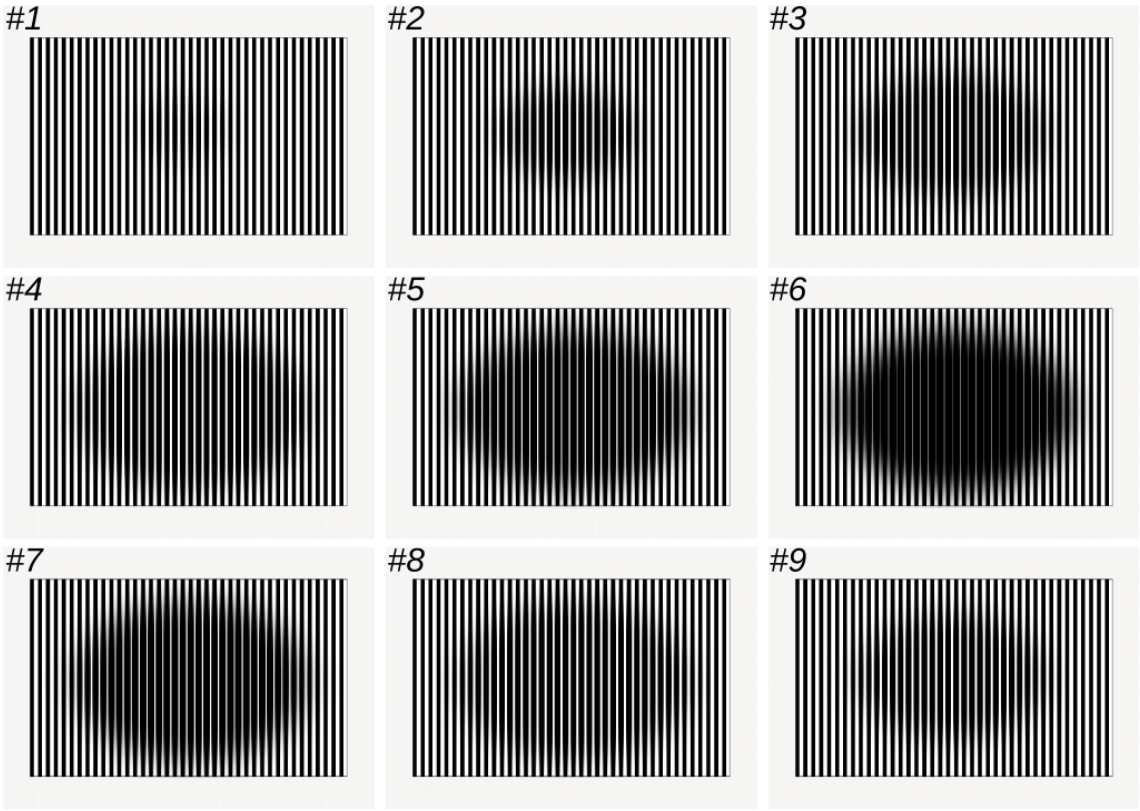


Figure 9.1: Videoframes from patient SS. Frame time is 200 ms.

The method should give as a result the variation speed expressed in Hertz (for cyclical movements) or degree/second (for drifting motions). „ENTPACK-TEMP" is an improved extension of „ENTPACK" method (see Chapter 7).

## 9.3 Materials and Method

We have investigated 22 human subjects with diagnosed amblyopia, having different aetiologies (strabismus, anisometropia, ptosis, combinations - see Table 6.1 on page 61).

First approach was to simply make a survey across all subjects to see which one reported temporal instabilities. For each stimulus, the subjects were asked to describe if they see the stimulus as stable or unstable over time. If it was unstable (i.e. the perceived image was moving or had elements in motion) the subjects were asked to verbally describe in detail what they saw; they were allowed to sketch it on paper if they wanted to, in order to aid their description.

The second approach was more elaborated: we tried to find a way to quantitatively estimate the severity of perceptual distortions over time. We used the same algorithm (see Chapter 7) to compute the Shannon informational entropy in each image (frame)

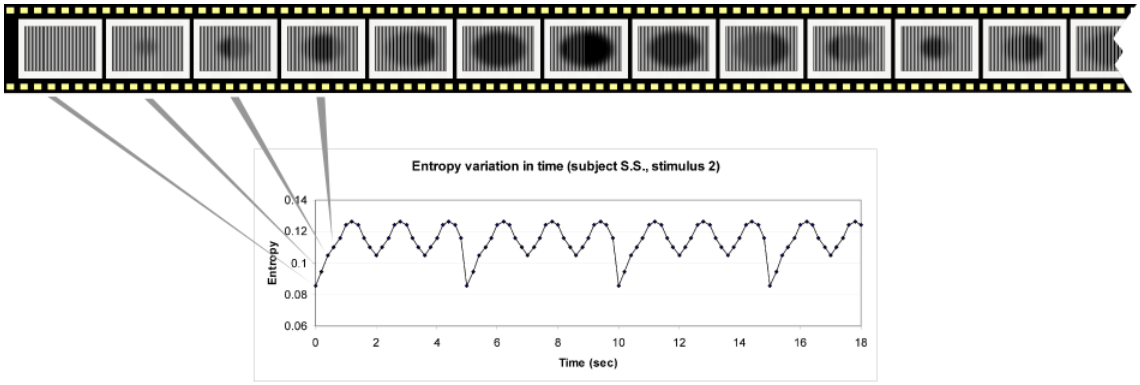


Figure 9.2: Entropy variation for a given movie (subject S.S.)

of the movie. The movies were split in individual image files, one for each frame, in order to ease the analysis.

Thus, for each movie we get an array of numbers representing the entropy variation in time, for that movie. We consider this as a possible approximation of perception variation over time (i.e. how fast the distortion is changing). Taking in account each frame duration, we can obtain a plot of entropy variation over time (9.2).

From the data set obtained it is thus possible compute the average cyclical frequency. (i.e. how fast the things are changing), for each subject and stimulus. In Fig. 9.3. is an example from the same subject SS, for all four stimulus images.

## 9.4 Results

**a) Occurrence of temporal instability in relationship with stimuli**

Nineteen of 22 subjects reported temporal instabilities in amblyopic perception when investigated with this method. *We could observe that the static stimuli with higher spatial frequencies (Fig. 6.1.c and d) tend to yield temporal instabilities more frequently than other stimuli (see Table 9.1 for detailed results per subject).*

**b) The speed of temporal instabilities**

*The temporal instabilities present themselves as cyclical phenomena, with frequencies < 2 Hz, for almost all the cases that we investigated.* Individual frequencies that we obtained through this method are displayed in Table 9.2. To the best of our knowledge, this is the first time when these kind of precise values were reported (IFTIME/THIEL/SIRETEANU, 2008). The temporal instabilities reported have different speeds for each stimus: stimulus a) was perceived with an average of 0.73 Hz, stimulus b) with an average of 0.65 Hz, stimulus d) with an average of 1.35 Hz, stimulus d) with and average

of 0.87 Hz.

All subjects could be investigated through this method, except J.M. who found difficult to verbally describe and validate its perception of stimulus 6.1.d. For this reasons we have excluded these results from the data set.

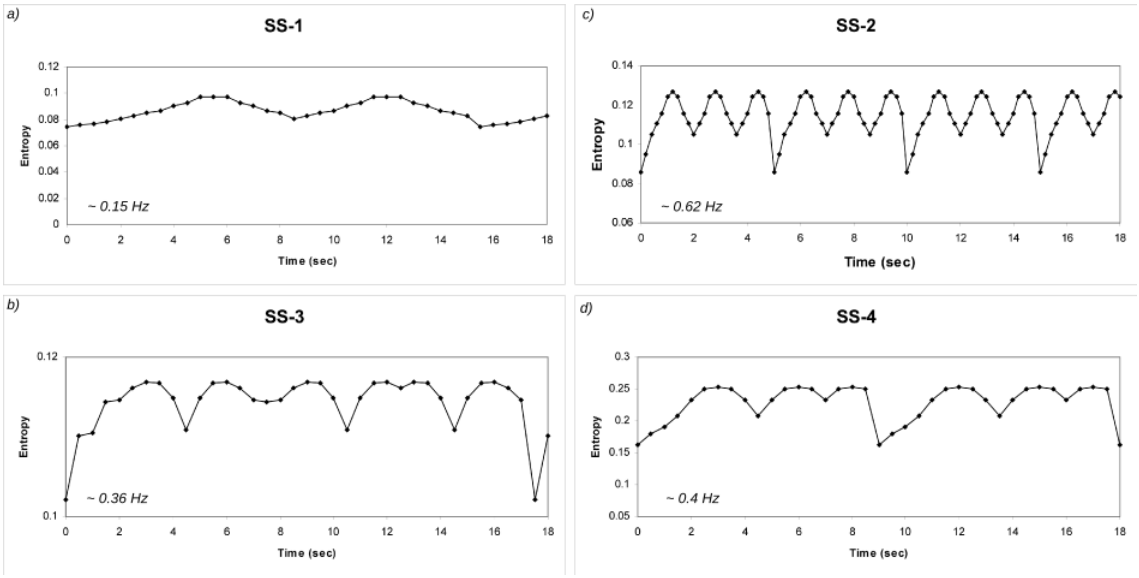


Figure 9.3: Entropy variation in time (example from subject S.S.). Each graph represents the entropy plot vs. time obtained for each stimulus image (SS-1 for $1^{st}$ stimulus image, etc); the stimuli images were presented page 59. This example shows that the entropy variation is roughly cyclical and has different frequencies for each stimulus. The second stimulus elicits a higher frequency variation than the other stimuli. *Insets*: average cyclical frequency.

| | | Temporal instabilities reported ? | | | |
|---|---|---|---|---|---|
| **Subject** | **Category** | ***Stimulus a)*** ***(grating low)*** | ***Stimulus b)*** ***(checkerboard)*** | ***Stimulus c)*** ***(grating high)*** | ***Stimulus d)*** ***(grid)*** |
| SG | SA | + | - | + | - |
| LP | | - | - | - | - |
| SS | | + | + | + | + |
| KK | | - | - | + | - |
| BSB | SAA | - | - | - | - |
| KB | | - | - | + | + |
| KF | | - | - | + | + |
| KHW | | - | - | - | + |
| KL | | + | + | + | - |
| MK | AA | - | + | + | + |
| HMK | | - | - | + | + |
| AR | | - | - | + | - |
| FA | | + | + | - | - |
| MJ | DA | + | + | + | + |
| AL | ENAF | + | - | + | + |
| LJ | | - | - | + | - |
| RW | | - | - | + | - |
| FS | | - | + | + | + |
| PG | | - | - | + | - |
| TGF | EAF | + | - | + | + |
| GZ | | - | - | - | - |
| JM | | - | - | + | + |
| This stimulus was perceived as temporally unstable by % subjects | | **32 %** | **27 %** | **77 %** | **50 %** |

Table 9.1: Subjects with temporal instabilities. The order and categories match the orthoptic table 6.1 on page 61.

| | | Frequency (Hz) | | | |
|---|---|---|---|---|---|
| **Subject** | **Category** | **Stim. a)** | **Stim. b)** | **Stim. c)** | **Stim. d)** |
| SG | SA | 1.000 | - | 2.500 | - |
| LP | | - | - | - | - |
| SS | | 0.154 | 0.364 | 0.625 | 0.364 |
| KK | | - | - | 0.278 | - |
| BSB | SAA | - | - | - | - |
| KB | | - | - | 1.176 | 0.222 |
| KF | | - | - | 0.500 | 1.000 |
| KHW | | - | - | - | 0.211 |
| KL | | 0.833 | 0.500 | 0.833 | - |
| MK | AA | - | 0.428 | 0.308 | - |
| HMK | | - | - | 0.833 | 0.667 |
| AR | | - | - | 0.750 | - |
| FA | | 0.294 | 0.500 | - | - |
| MJ | DA | 1.000 | 0.833 | 2.500 | 1.000 |
| AL | ENAF | 1.000 | - | 2.500 | 2.500 |
| LJ | | - | - | 1.667 | - |
| RW | | - | - | 2.500 | - |
| FS | | - | 1.250 | - | 1.000 |
| PG | | - | - | 1.000 | - |
| TGF | EAF | 0.800 | - | 1.111 | - |
| GZ | | - | - | - | - |
| JM | | - | - | 2.500 | non-computable** |
| Average frequency of cyclical temporal instabilities (Hz) | | **0.73** | **0.65** | **1.35** | **0.87** |

Table 9.2: Individual and average frequencies for each stimulus. The order and categories match the orthoptic table 6.1 on page 61.

## 9.5 Discussion and Conclusions

The present data sets suggest that both the apparition and the intensity of the temporal instabilities in amblyopic perception could be related to the characteristics of the stimuli (their spatial frequencies). This could explain why the same patient reports different distortions in different visual settings. This finding could be of particular interest for clinicians:

- our results suggest that the best stimuli that yield temporal distortions are those with higher spatial frequencies (in our study, 1.6 cycles / degree). This is a confirmation of our findings presented in previous chapters (where we used different methods). The checkerboard pattern was the least likely to yield temporal instabilities.

- the usage of other stimuli (like orthoptic charts, sinewave images, etc) may not yield these distortions which may lead to the conclusion that the amblyopia patient does not have anomalous temporal instabilities. We speculate that these temporal distortions are therefore under-diagnosed in most cases.

This method gives another insight in the understanding of the amblyopic perception: it is temporally instable over a short frame time with a rather low frequency (about 2 changes / second). For the equivalent category of stimuli there seems to be a correlation between the spatial frequency of the stimulus and the speed of temporal instability: the greater the spatial frequency, the greater the temporal instability, which agrees with our findings presented in the previous chapters.

# Chapter 10

# TEDI Experiment

## 10.1 Purpose

We wondered if it is possible to find a way to directly measure the variation speed of temporal instabilities. By "speed" we understand how fast the distortions are changing over a small time frame. We attempted to build an experimental setup that allows subjects to alter in real time the presentation speed of a movie until it matched their percept. The acronym "TEDI" comes from "*Te*mporal *D*istortion and *I*nstabilities".

## 10.2 Materials and Method

The setup consisted of a dual monitor system, presenting different images on each monitor. We built it in such a way that the subjects could observe only one monitor at a time, monocularly.

Subjects were seated and the head was fixed on a chin-rest 57 cm away from the monitors. The subjects could observe the right monitor with the right eye and the left monitor with the left eye, alternately, using a frontal eye-occluder. To ensure that the left and right eyes were receiving images only from the corresponding monitor, a vertical shield was placed along the mid-line. (See Fig. 10.1; in the figure, the amblyopic eye is the left one).

On the monitor corresponding to the amblyopic eye, a static stimulus (like previously described, see Fig. 6.1 on page 59) was presented continuously. The subjects were free to examine the stimulus without any time constraint and to memorize their percept. The image was calibrated to have the same dimensions in the visual field as in the previously described experiments.

After this step the amblyopic eye was covered. They were asked to look on the

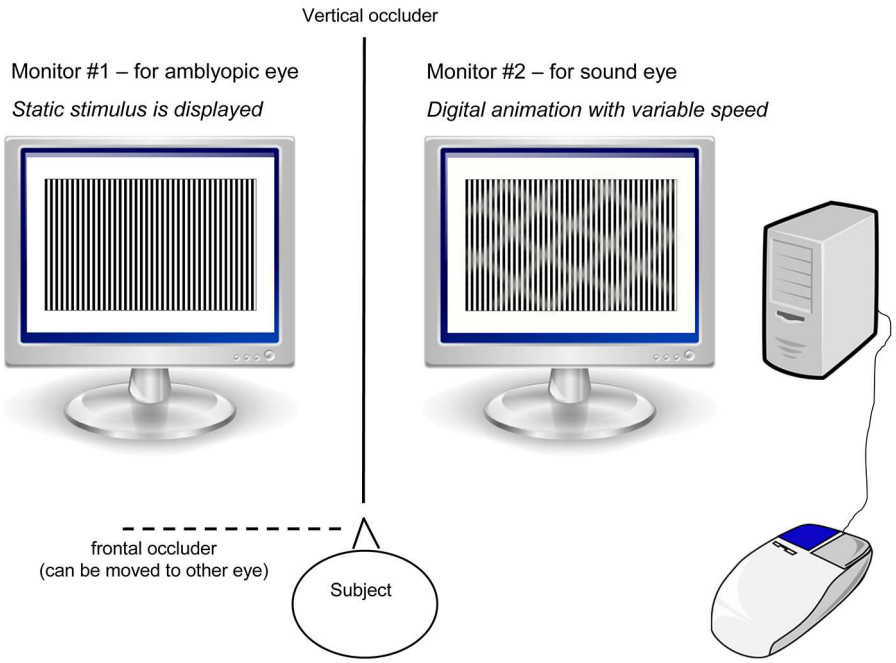


Figure 10.1: ”*TEDI*” experimental setup

second monitor, using the sound eye. On this monitor, the computer presents the digital movie of the corresponding distortion that they described in the previous experiment.

The initial speed of the animation was however modified (it was presented slower or faster than they previously validated). The task was to adjust the speed of the animation until they felt that was similar with the memorized perception. They could increase or decrease the speed of the presented animation using the scroll button of a mouse. If they felt necessary, they were allowed to look again at the static stimulus, using the amblyopic eye, while the sound eye was covered with the occluder.

We used an adaptive algorithm (TREUTWEIN, 1995) to find the perceived speed. The main constraint for us was that the results should be found quickly, in few minutes (patients were having difficulties in maintaining attention with the amblyopic eye for a longer period of time). The steps of our algorithm were:

- we chose at the beginning the *smallest fixed step of variation*. If needed to increase or decrease the speed at a higher rate, we used multiples of this step. In this way, we could increase the precision of our measuring very easy, but there was a penalty: the higher the desired precision (i.e. very small step), the longer the experiment. We have found empirically that the best smallest step is 0.1 Hz. This was comfortable for the patients (they found the tasks not very difficult) and one measurement time was maximum 5 minutes.

- an initial speed of animation for the dominant eye was chosen outside of possible

correct range, for instance very high (~20) Hz or very low (~0.1 Hz). For the simplicity in explanation, we will exemplify with a case starting at a very high speed.

- Patients had to compare the presented animation (to the sound eye) with what they saw with the amblyopic eye. They were using a single eye at a time, and could switch freely between the eyes using the occluder.
- At each negative answer from the patient (i.e. “the speed is too high”), the algorithm slowed the animation speed with three units (i.e. 3 x 0.1 Hz).
- When the patient had a positive response (“i.e. the speed is too low”), this is considered a turning point (called “1” in Fig 10.2); The algorithm increases the speed with 1 unit (i.e. 1 x 0.1 Hz).
- The algorithm will wait for further answers from the patient, and then increases (with 1 unit) or decreases (with 3 steps) the animation speed. This produces a noticeable difference in the animation speed variation according to the answers of the patient.
- These variations are thereafter reduced to 2 units (2 x 0.1 Hz) and finally to 1 step (0.1 Hz) see (in Fig. 10.2).
- After at least three oscillations (with the smallest step) around the same averaged value, the algorithm stops and reports this value. In Fig. 10.2, the last steps are „4”, „5” and „6” and the average value is 0.4 Hz.

## Control experiment

We wanted to see if the task presented above is not too difficult for the amblyopic subjects. Our main concern was that the subjects could not compare directly the amblyopic percept with the normal vision from the sound eye; they had to do it indirectly, through the short term memory.

We used four naïve, healthy volunteers. We wanted to find if it is easy for them to do a video matching task on our setup described above.

The subjects could observe monocularly with the non-dominant eye a cyclical animation movie presented on a monitor (e.g. monitor no. 1 in Fig. 10.1). This movie was presented continuously, and consisted of several black objects swinging at a fixed speed over a distance of ~ 1 deg., on a white background. They were allowed to observe it freely and try to remember the speed of the animation.

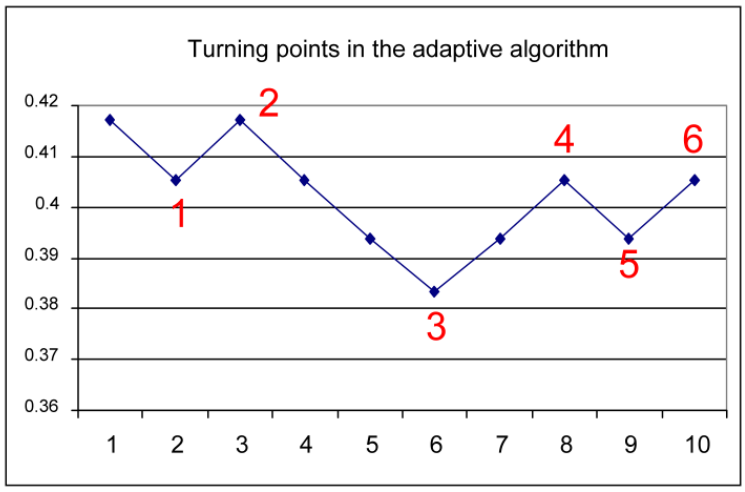


Figure 10.2: Adaptive algorithm with a response collected as an averaged value from the last four out of 6 turning points (labelled with grey numbers in graphic). On Y-axis the speed is expressed in Hz, on X-axis there are all the steps (dots) where the subject made a choice.

On the second monitor we presented the same animation, but played at a different speed. This monitor could be observed only with the dominant eye, while the non-dominant eye was occluded.

The subjects' task was to adjust the animation speed on the second monitor until it matched the speed on the first monitor, using the same algorithm as the amblyopic subjects, and in the same conditions.

Each subject had a period of learning the commands until they felt confident. The measurements in this control group were repeated three times for each subject. We obtained an average error of the matching process of ± 0.2 Hz. This small value of error in the control experiment confirmed us that the matching task can be done with this setup.

## Technical details of TEDI setup

A critical element was the timing control on the displays. We wanted to be confident that the timings we got were not affected by additional errors in software or in the hardware we used.

In the video presentation algorithm we introduced a control mechanism based on two different hardware clocks (CPU processor clock and the video processor clock). These clocks can have accuracies of about 1 nanosecond and precisions around tens of nanoseconds (depending on the hardware used). We used computers with AMD / Intel processors, dual-core, with frequencies in range 2.0 to 2.5 GHz, and dual-head

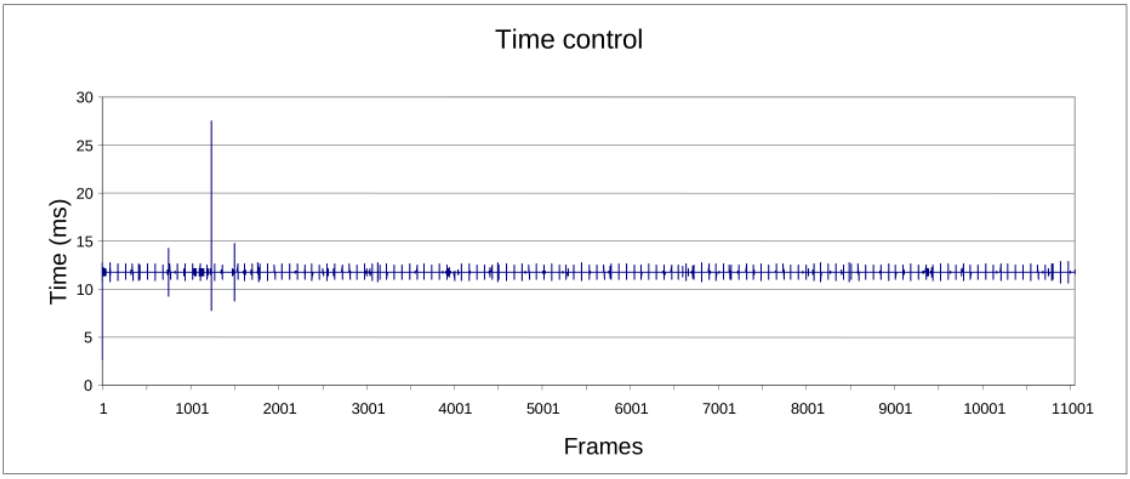


Figure 10.3: Controlled times for each video frame in an animation

video boards from Matrox and Nvidia. The usage of dual-core processors is encouraged because it allows true multithreading to be performed without speed penalties.

In the program we have implemented two separate threads:

1. one thread taking care of handling subjects' responses and changing the animation accordingly;

2. a separate thread checking if the display timing reported by the video board for each photogram was indeed that one, matching it with the timing reported by the CPU timer. If there were any differences, they were logged, so we can check the accuracy of our measurements. If a photogram was displayed for a longer time, the next one was skipped accordingly, in order to compensate the timings.

Using these criteria, the algorithm maintains a reliable throughput of video frames at precisely controlled intervals, with an almost zero error rate. For instance, in a 2.2 minute recording there were 11000 frames presented, each one with 12 ms duration. Only three frames had different timings (not greater than 25 ms), which is a negligible error (see Fig. 10.3).

## Particular conditions imposed by TEDI setup

Because of the novelty of our approach and the particular setup, we choose to experiment it with a small number of amblyopic participants. Our inclusion criteria were:

- to be a participant in the previous experiment (ENTPACK-TEMP), in order to be able to do a comparison of temporal instabilities measured by both methods.

- to be confident using a mouse and dynamic images on the monitor (like computer games experience)

- to feel comfortable while voluntarily switching between amblyopic and sound eye, using the occluder. *For an amblyopic patient, this switching between the eyes is not a trivial task.* Psychologist A.Thiel who personally conducted the drawing sessions of the subjects observed that some amblyopic subjects can report mild nausea or other neuro-vegetative symptoms while contemplating their own temporally unstable percept. Therefore, the measurements should take in account this fact and allow the subjects to easily stop it at any time.

Four subjects were selected for participating in this trial; we performed 24 measurements in total (six for each subject).

Illumination conditions: Stimuli were presented on two CRT monitors Samtron 98 PDF 19" diagonal, gamma calibrated so they have an identical light output. Their absolute maximum luminosity for a 100% white shade was set at $106 \pm 1$ cd/m$^2$. Black-white contrast was 2000:1 at a refresh rate of 85 Hz for a resolution of 800x600 pixels. The experimental room was illuminated with diffuse incandescent light (to eliminate flickering with monitor surfaces) and the light sources were arranged such that there were no direct shadows nor glare in the subjects' visual field. Light measurements were performed with a LiteMate 500 photometer.

## 10.3 Results

By analyzing the obtained data set, we obtained the following results using TEDI method:

- Numerical values for each stimulus and subjects are listed in the Table 10.1 on the next page, alongside with a comparison from the ENTPACK-TEMP method. It can be observed that TEDI method produces higher values (i.e. speedier).

- Stimulus c) (high frequency grating) produces the fastest variations in amblyopic percept. Using this kind of static stimuli, it seems that the higher the spatial frequency, the higher the chances for observing a temporal instability (the same behaviour was observed in ENTPACK-TEMP).

- We have found a big discrepancy for the subject A.L. between the value of 2.5 Hz (ENTPACK-TEMP) and ~9.6 Hz (Tedi). We believe that this might reflect a higher-order temporal instability (i.e. the instability rate might vary over a longer time frame). In order to test this speculation, perhaps several assessments should be done over a longer time span (days or weeks).

| Subject | Cat. | Measured temporal instability frequency (Hz) | | | | | | | |
|---|---|---|---|---|---|---|---|---|---|
| | | *Stimulus a)* | | *Stimulus b)* | | *Stimulus c)* | | *Stimulus d)* | |
| | | *ENTPACK-TEMP* | *TEDI* | *ENTPACK-TEMP* | *TEDI* | *ENTPACK-TEMP* | *TEDI* | *ENTPACK-TEMP* | *TEDI* |
| **SG** | SA | 1.000 | ***1.079*** | - | **-** | 2.500 | ***1.804*** | - | **-** |
| **KL** | SAA | 0.833 | **-** | 0.500 | **1.454** | 0.833 | **-** | - | **-** |
| **AL** | ENAF | 1.000 | ***2.325*** | - | **-** | 2.500 | ***9.574*** | 2.500 | ***2.874*** |
| **JM** | EAF | - | **-** | - | **-** | 2.500 | ***1.633*** | non-measurable | ***1.520*** |

Table 10.1: Measured temporal instability frequency - comparison between TEDI and ENTPACK-TEMP values.

- Using this method we could attempt a measurement of the instability reported by patient J.M, which could not be measured with ENTPACK-TEMP.

## 10.4 Discussion and Conclusions

TEDI experiment seems to be a good companion to ENTPACK-TEMP method. *Its main advantage is that it requires considerably shorter measurement time* (minutes vs. days, considering the time required for repeated validation procedures).

We believe ENTPACK TEMP method to be more precise, but it requires a huge volume of calculations, which can be a limiting factor in its usage.

Numerical values obtained have rather an individual importance; our subject's set was too small to draw conclusions related to aetiology influences. The intention of this study was to provide a quantitative insight in the temporally unstable amblyopic percept.

As a final word, these arguments suggest that TEDI method could be used as an initial screening method. It can rapidly find the approximate range of frequency values of temporal instabilities of an amblyopic patient. Thus the time required to validate the results obtained through ENTPACK-TEMP method can be reduced. For instance, for our subjects, we used up to four visits to the lab in order to fully validate their reproduced percept; if it is possible to spare even a single visit, this is a substantial gain for the subject's precious own time.

We suggest that these methods can be used to build tools for monitoring the patient's evolution in time. To the best of our knowledge, there is no method available today that can monitor systematically and objectively the evolution of temporal instabilities of amblyopia patients.

# Part IV

# Conclusions

# Chapter 11

# Summary of the original contributions

In this thesis we presented our novel approach to amblyopic percept; we tried to characterize it in an objective, measurable way. We have analyzed three broad categories of data:

1. spatial mis-localizations ("Circle Experiment" psychophysics method results),
2. reported spatial distortions (validated images of amblyopic percept),
3. reported temporal instabilities (validated movies of amblyopic percept).

For each of these categories of data we have proposed methods for measurements and have obtained the following categories of results:

## 1. Spatial mis-localizations

**$SD_{Area}Ratio$ and $AVL$ indices calculation and analysis**

We propose the calculation of the two different indices as synthetic expressions for the displacement maps obtained through psychophysical tests.

We suggest that $SD_{Area}Ratio$ index (*Standard Deviation Area Ratio*) can be used as a synthetic expression of how worse the amblyopic eye is (versus the sound eye) in the localization tasks. A typical healthy subject will score a value around 1.0 (both eyes perform similarly). The greater the value above 1.0, the worse the difference between the eyes is. This index can be also used as a tool for predicting if the amblyopic subject has temporal instabilities (subjects reporting temporal instabilities tended to cluster in the higher range of this index value).

In order to evaluate the total displacements that happen in an amblyopic field of view, we calculated a separate index. $AVL$ (*Average Vector Length* ) represents the average value of all the displacement vectors in the map. This index is expressed in

visual degrees. For an ideal healthy subject, *AVL* would be very close to 0° (in our control group it was 0.27°). For an amblyopic subject, the *AVL* value would be greater, and its value reflects the severity of displacement errors (the greater the displacement, the greater the value of this index).

*AVL*s were significantly larger in subjects with a history of strabismus than in normally sighted observers. The difference was not statistically significant in subjects with a refractive error aetiology. There was no significant difference between the *AVL*s of the subjects with a history of strabismus and those of subjects with a refractive error aetiology. Thus, according to our results, it seems that both a deep acuity loss and a history of strabismus are related to increased spatial displacements and higher spatial uncertainty.

Analyzing both indices we reached the conclusion that the subjects experiencing temporal instabilities show significantly more pronounced spatial uncertainty in the amblyopic eye than do subjects with stable perception. The indices calculation and results are described in Chapter 4 starting on page 30.

**Digital simulation of spatial distortions**

We have developed a method and an accurate algorithm to produce artificially distorted images, based on psychophysical displacement data obtained through "Circle Experiment" procedure. The procedures are described starting with page 46. We tried to compare the digital results with the validated images from the subjects; the two data sets agreed rarely. Therefore we can conclude that complexity of the amblyopic percept cannot be reduced only to spatial distortions, and more research is needed in this area.

One striking result of our simulation appears if we apply the same algorithm on different, natural images. If we use the same displacement data set, we would expect to obtain a degree of similarity in the distorted images. We observed instead very different visual results, which is quite remarkable if one image is a regular pattern (i.e. a checkerboard) and the other is a natural image (i.e. trees). The natural world image appear very little distorted, even if pixel displacement is identical in both pictures.

We speculate that this finding could explain why amblyopic patients do not complain often about the distortions in the real life. Also it strongly suggests that some categories of stimuli elicit higher subjective distortions. Therefore, the conclusion seems to be that: in order to observe spatial distortions and temporal instability in an amblyopic patient, the clinician ophthalmologist should not rely on patient description of casual images. The patient should be asked to describe his / her perceptions of special crafted images instead. We suggest the best images to be used are high contrast regular

geometrical patterns (like stripes or checkerboards).

## 2. Reported spatial distortions analysis.

Leaving aside the displacement maps, we focused on the images that patients do sketch or describe verbally when they are seeing the world using only the amblyopic eye. In order to standardize the data, we used four printed images that subjects were asked to look and describe. A trained psychologist carefully made digital replicas of their descriptions and refined the drawings until they were validated by the subjects. We analyzed these digital images looking at overall entropy in the images and local entropy distribution.

### Overall entropy analysis.

We compared the entropy in the collected distorted images with the entropy of the stimulus images. For the vast majority of the subjects and for all stimuli images, we have observed an increase in the overall entropy of the described images (as compared with the entropy level of the presented images). We interpret the observed increasing of entropy as a measure of loss of information structure in the subjects' visual processing flux.

We compared also the entropy values among the four categories of stimuli used. The high frequency grating image yielded the biggest increase in entropy (i.e. produced the most distorted images). This is not the case for the crossed patterns images. These results seem to show that the exposure to simpler high frequency gratings is a better way to elicit the appearance of distorted perceptions in amblyopic subjects; this confirm the psychophysical finding described at point 1 above.

The finding that the distortion amount seems to be influenced by the content of the stimulus (presented image) is the main result of this method (see Chapter 7, starting on page 63).

### Local entropy distribution

We tried to answer the following question: what is the distribution of amblyopic perceptual problems in the visual space? To answer that question we performed an entropy analysis in portions of the image: we segmented the images in square-shaped areas equivalent to 1x1 degree in the visual field. We have found that the entropy is significantly higher in the central portions of the visual field. This area has an ellipsoidal shape.

An interesting observation arises if we examine the 3D representation of the receptive fields of the ganglionar cells: the area of binocular loss is not symmetrical on horizontal and vertical axes. The surface of this area is also an ellipsoid that is similar in shape with the areas where there are higher entropy values. We speculate that this area of total binocularity loss might be the major area or source of distortions in the images. Its shape could explain the frequent reports of "ellipsoidal blobs" with different features in distorted images. These correlations can be further researched in relationship with aetiology (see Chapter 8, starting on page 69).

## 3. Reported temporal instabilities

Some subjects reported that their perception of the distorted images changes in time (over the few minutes of continuously looking at the static stimulus image). This phenomenon is known as "temporal instability", and previously described only in qualitative terms. We think that the variation speed of these instabilities can be measured and we propose two different methods:

- an indirect method, based on entropy analysis
- a direct method, based on an interactive matching experiment.

#### Entropy analysis over time

We performed an evaluation of entropy variation in each frame of the movies representing the temporal instabilities, as reported by the subjects. These movies were produced by a trained psychologist and adjusted until they were validated by the amblyopic subject (see Chapter 9, starting on page 78).

The amount of variation of the distortions, their speed of change, and their different shapes can seem perplexing at first. But analysing the variation of entropy in the movies, we observed that the temporal instabilities tend to present themselves often as cyclical phenomena, with frequencies < 2 Hz, for almost all the cases that we investigated. To put this result in other words: the amblyopic percept seem to be temporally unstable over a short frame time with a rather low frequency (about 2 changes / second).

A second observation that we made was that there is a significant difference between the temporal instabilities yielded by different static stimuli:

a) not all the subjects reported temporal instabilities for all the images. We found that the best stimuli that yield temporal distortions are those with higher spatial frequencies (in our study, 1.6 cycles / degree).

b) it seems that there is a relationship between the speed of temporal instability and the type of the static stimulus used: the higher the spatial frequency of the stimulus

image, the higher the temporal instability frequency. However, this finding was not consistent among all the four categories of stimuli used.

**Interactive matching experiment**

We propose an experimental setup that can be used to investigate in finer detail the temporal instabilities. It is based on an adaptive algorithm that allows the subject to adjust the speed of a movie until he / she feels it that matches his / her own amblyopic percept. The results seem to agree in a reasonable range with the findings described in the previous section. However we were unable to perform a statistical analysis of the data due to the small number of subjects that participated in this first pilot experiment. (see Chapter 10, starting on page 85).

...

Regardless of the content of the spatial distortions or the methods used, the temporal aspects of amblyopic percept can be divided in two categories:

1. *cyclical variations* (vast majority). These can be described as vibrating edges, oscillations like back-and-forth movements or increasing / decreasing of apparent size of features in the visual fields (blobs, foggy areas, contrast variation in time, etc).

2. *drifting motions.* These are hard to describe; the patients have the impression that the image is continuously moving ( appears to endlessly move in one direction)

The results seem to indicate that the temporally amblyopic percept has some patterns of its manifestation. As far as we know, our work is the first report of amblyopic temporal instability measurements and also of its relationship with the static stimulus used. By knowing the precise values of cyclical manifestation of temporally unstable percept, it is possible to investigate further the subjects (fMRI, EKG, and other functional methods) in order to start looking for the possible neural correlate for their percept.

# Chapter 12

# Publications related to this thesis

This thesis presents in greater detail our findings published in several articles or conferences as posters / abstracts. We list them here for clarity:

**Full text articles (peer-reviewed journals)**

1. Sireteanu R., Thiel A., Fikus S., **Iftime A**., (2008), 'Patterns of spatial distortions in human amblyopia are invariant to stimulus duration and instruction modality', **Vision Research**, 48, 1150-1163; ISSN:0042-6989; DOI: 10.1016/j.visres.2008.01.028 ***[ISI]***

2. Sireteanu R., Baeumer C., **Iftime A.** (2008) 'Temporal instability in amblyopic vision:Relationship to a displacement map of visual space', **Investigative Ophthalmology and Visual Science**, 49, 3940-3954; ISSN: 0146-0404; DOI: 10.1167/iovs.07-0351 ***[ISI]***

3. **Iftime, A.**; Baeumer, C.C. & Sireteanu, R. (2007), 'An Automated Method for Creating Simulated Distorted Images in Amblyopic Vision', **Strabismus**, Volume 15, Issue 1 January 2007 , pages 21 - 27; ISSN: 1744-5132 (electronic) 0927-3972 (paper) ; DOI: 10.1080/09273970601175016 ***[MEDLINE]***

4. Sireteanu, R.; Baeumer, C.C.; Sarbu, C. & **Iftime, A.** (2007), 'Spatial and temporal misperceptions in amblyopic vision', **Strabismus**. Volume 15, Issue 1 January 2007 , pages 45 - 54; ISSN: 1744-5132 (electronic) 0927-3972 (paper); DOI: 10.1080/09273970601180263 ***[MEDLINE]***

**Abstracts - International Scientific Conferences (peer-reviewed):**

1. **Iftime A,** Thiel A, Sireteanu R, (2008), 'An objective evaluation of temporal instabilities in amblyopic perception', **Perception**, 37, ECVP Abstract Supplement, p. 112

2. **Iftime A,** Thiel A, Sireteanu R, (2007), ‘An objective evaluation of information loss in amblyopic perception’, **Eur Biophys J**, 36, EBSA Abstract supplement 1

3. **Iftime A,** Thiel A, Sireteanu R, (2007), ‘A 3-D model of amblyopic visual field’, **Perception**, 36, ECVP Abstract Supplement, ISSN 0301-0066 ***[ISI]***

4. **Iftime, A,** Baeumer, C.C. & Sireteanu, R. (2006), ’Computer simulations of spatial misperceptions in amblyopic vision’, **Perception** 35, ECVP06 Abstracts Supplement. ***[ISI]***

# Bibliography

**Altmann, L./Singer, W.:** Temporal integration in amblyopic vision. Vision Research, 26 1986, 1959

**Arden, G. B.:** The importance of measuring contrast sensitivity in cases of visual disturbance. Br J Ophthalmol, 62 1978, 198

**Baeumer, C.:** Temporal and spatial distortions in adult amblyopia. Ph. D thesis, Johann Wolfgang Goethe-Universitaet, Frankfurt am Main, 2005

**Barbeito, R. et al.:** Effects of luminance on the visual acuity of strabismic and anisometropic amblyopes and optically blurred normals. Vision Res, 27 1987, Nr. 9, 1543

**Barbeito, R./Bedell, H.E./Flom, M.C.:** Does impaired contrast sensitivity explain the spatial uncertainty of amblyopes? Invest Ophthalmol Vis Sci, 29 1988, Nr. 2, 323

**Barrett, B T. et al.:** Nonveridical Visual Perception in Human Amblyopia. Invest Ophthalmol Vis Sci. 44 2003, 1555

**Bedell, H. D./Flom, M. C.:** Monocular spatial distortion in strabismic amblyopia. Invest Ophthalmol Vis Sci, 20 1981, Nr. 2, 263

**Bedell, H. E./Flom, M. C.:** Normal and abnormal space perception. Am J Optom Physiol Opt, 60 1983, Nr. 6, 426

**Bedell, H. E./Flom, M. C.:** Bilateral oculomotor abnormalities in strabismic amblyopes: evidence for a common central mechanism. Doc Ophthalmol, 59 1985, Nr. 4, 309

**Bedell, H. E./Flom, M. C./Barbeito, R.:** Spatial aberrations and acuity in strabismus and amblyopia. Invest Ophthalmol Vis Sci, 26 1985, Nr. 7, 909

**Blackmore, S. J.:** Consciousness - A very short introduction. Oxford University Press, 2005

**Bradley, A./Freemann, R.:** Temporal sensitivity in amblyopia: an explanation of conflicting reports. Vision Research, 25 1985, 39

**Dogaru, R. et al.:** An exhaustive analysis of emergent behaviors in recurrent cellular computing systems with outer-totalistic cells. In INTERNATIONAL SEMICONDUCTOR CONFERENCE, VOLS 1 AND 2, PROCEEDINGS. 2003

**Duke-Elder, S./Wybar, K.:** Ocular Motility and Strabismus. St. Louis, CV Mosby, 1973, 294

**Ellemberg, D. et al.:** Influence of monocular deprivation during infancy on the later development of spatial and temporal vision. Vision Research, 40 2000, 3283

**Flom, M.C./Bedell, H.E.:** Identifying amblyopia using associated conditions, acuity, and nonacuity features. Am J Optom Physiol Opt, 62 1985, Nr. 3, 153

**Flom, M.C./Kirschen, D. G./Bedell, H. E.:** Control of unsteady, eccentric fixation in amblyopic eyes by auditory feedback of eye position. Invest Ophthalmol Vis Sci, 19 1980, Nr. 11, 1371

**Flom, M.C./Weymouth, F. W./Kahneman, D.:** Visual resolution and contour interaction. J Opt Soc Am, 53 1961, 1026

**Fronius, M./Sireteanu, R.:** Monocular geometry is selectively distorted in the central visual field of strabismic amblyopes. Investigative Ophthalmology & Visual Science, 30 1989, 2034

**Fronius, M. et al.:** Preliminary report: monocular spatial localization in children with strabismic amblyopia. Strabismus, 8 2000, Nr. 4, 243

**Greenwald, M. J./Parks, M. M.:** Chap. 10, Vol.1 In Duane's Clinical Ophthalmology. Volume 1, C. Lippincott Williams and Wilkins, 2000

**Hess, R. F./Campbell, F. W./Greenhalgh, T.:** On the nature of the neural abnormality in human amblyopia: Neural aberrations and neural sensitivity loss. Pflugers Arch, 377 1978, 201

**Hess, R. F./Howell, E. R.:** The threshold contrast sensitivity function in strabismic amblyopia:Evidence for a two type classification. Vision Res, 17 1977, 1049

**Hess, R. F./Pointer, J. S.:** Differences in the neural basis of human amblyopia: The distribution of the anomaly across the visual field. Vision Res, 25 1985, 1577

**Hess, R. F./Woo, G.:** Vision through cataracts. Invest Ophthalmol Vis Sci, 17 1978, 428

**Iftime, A. M./Baeumer, C./Sireteanu, R.:** An Automated Method for Creating Simulated Distorted Images in Amblyopic Vision. Strabismus 2007

**Iftime, A. M./Baeumer, C. C./Sireteanu, R.:** Computer simulations of spatial misperceptions in amblyopic vision. Perception, 35 2006, ECVP06 Abstracts

**Iftime, A. M./Thiel, A./Sireteanu, R.:** A 3-D Model of Amblyopic Visual Field. Perception, 36 2007a, ECVP Abstract Supplement ISSN 0301–0066

**Iftime, A. M./Thiel, A./Sireteanu, R.:** An Objective Evaluation of Information Loss in Amblyopic Perception. Eur Biophys J, 36 2007b, EBSA Abstract supplement 1

**Iftime, A. M./Thiel, A./Sireteanu, R.:** An objective evaluation of temporal instabilities in amblyopic perception. Perception, 37, ECVP Abstract Supplement 2008, 112

**Jampolsky, A. et al.:** Unequal corrected visual acuity as related to anisometropia. Arch Ophthalmol, 54 1955, 893

**Jampolsky, A. J.:** Unequal visual inputs and strabismus man agement: A comparison of human and animal strabismus. Trans New Orleans Acad Ophthalmol 358 1978

**Lagreze, W. D./Sireteanu, R.:** Two-Dimensional Spatial Distortions in Human Strabismic Amblyopia. Vision Res. 31 1991, Nr. 7/8, 1271

**Levi, D./Carkeet, A.; Simons, Kurt, editor:** Chap. Amblyopia: a consequence of abnormal visual development. In Early Visual Development: Normal and Abnormal. Oxford University Press, USA, 1993

**Levi, D. M./Klein, S.:** Differences in vernier discrimination for gratings between strabismic and anisometropic amblyopes. Invest Ophthalmol Vis Sci, 23 1982, 398

**Mayer, D. L./Fulton, A. B./Rodier, D.:** Grating and recognition acuities of pediatric patients. Ophthalmology, 91 1984, 947

**Parks, M. M.:** Visual results in aphakic children. Am J Ophthalmol, 94 1982, 441

**Pugh, M.:** Visual distortion in amblyopia. Br J Ophthalmol, 42 1958, 449

**Sireteanu, R.:** Development and Plasticity of Visual Functions: Psychophysical, Electrophysiological and Clinical Studies. postdoctoral thesis (Habilitation) Johannes-Gutenberg University,Mainz, 1990

**Sireteanu, R.; Lennerstrand, G./Ygge, J., editors:** Chap. The binocular act in strabismus. In Advances in strabismus research: basic and clinical aspects. London: Portland Press, 2000, 63

**Sireteanu, R./Baeumer, C./Iftime, A.:** Temporal instability in amblyopic vision:Relationship to a displacement map of visual space. Investigative Ophthalmology and Visual Science, 49 2008, 3940

**Sireteanu, R. et al.:** Spatial and temporal misperceptions in amblyopic vision. Strabismus 2007

**Sireteanu, R./Lagreze, W. D./Constantinescu, D. H.:** Distortions in Two-Dimensional Visual Space Perception in Strabismic Observers. Vision Res, 33 1993, Nr. 5/6, 677

**Sireteanu, R./Singer, W.:** The "vertical effect" in human squint amblyopia. Exp Brain Res, 40 1980, 354

**Sireteanu, R. et al.:** Patterns of spatial distortions in human amblyopia are invariant to stimulus duration and instruction modality. Vision Research, 48 2008, 1150

**Sun Microsystems, Inc., editor:** Chap. 8 In Programming in Java Advanced Imaging. Release 1.0.1 edition. Sun Microsystems, Inc, 1999

**Tessier-Lavigne, M.; Kandel, E.R./Schwartz, J.H./Jessel, T.M., editors:** Chap. 26, Visual Processing by the Retina In Principles of Neural Science. 4th edition. McGraw-Hill, 2000

**Thiel, A.:** Reizspezifische Fehlwarhenhmungen von erwachsenen Personen mit Amblyopie. Ph. D thesis, Johann Wolfgang Goethe-Universitaet, Frankfurt am Main, 2009

**Treutwein, B.:** Adaptive psychophysical procedures. Vision Research, 35 (17) 1995, 2503

**Vaegan, T.D.:** Critical period for deprivation amblyopia in children. Trans Ophthalmol Soc UK, 99 1979, 432

**Walker, H. K./Hall, W. D./Hurst, J. W.; (MA), Stoneham, editor:** Chap. 116. Visual Fields In Clinical methods: The history, physical, and laboratory examinations. Butterworths Publishers, 1990 ⟨URL: `http://www.ncbi.nlm.nih.gov/bookshelf/br.fcgi?book=cm`⟩

# List of Figures

1.1 Clinical conditions that can lead to amblyopia. a) different types of *Strabismus* b) *Anisometropia* c) *Blefaroptosis* d) *Cataract* (in all examples, the right eye is the affected one) . . . . . 13

2.1 Different grating types. a) sine-wave vs. square-wave b) low frequency vs. high frequency c) different orientations d) low contrast (35%) vs. higher contrast (75%) 17
2.2 Different contrasts for the same stimulus. The left image has 100% contrast, the subsequent images have half of the previous (50%, 25%, 12.5% and 6.2%). The lower the contrast, the more difficult it is for us to perceive it. . . . . 19
2.3 Maps of normal and pathological visual fields (WALKER/HALL/HURST, 1990:) 20
2.4 A distortion map example. Correspondence pattern of subject S.M. Solid symbols indicate loci in the amblyopic eye corresponding to the 36 positions in the dominant eye (connected by lines). Figure from Lagreze and Sireteanu, 1991. . 22
2.5 Examples of spatial distortions, as recorded by Psych. C. Baeumer, Max Planck Institute for Brain Research. *Left*: patient S.B; *Right*: patient B.B. The images are their descriptions of amblyopic percept, while observing black-and-white regular stripes printed on paper. . . . . 23

3.1 "Circle Experiment" mapping data sample from subject C.L. *Top-left*: dominant (sound) eye map. *Top-right*: non-dominant (amblyopic) eye map. *Yellow dots*: presented target positions; *Coloured dots (red/green)*: recorded positions. *Centr*e: vectorial subtraction between left and right. . . . . 28

4.1 Example of $SD_{areas}$ (*a*) and (*b*) and the improved vectorial map (*c*). Data set from subject C.L. . . . . 35
4.2 Individual spatial displacement maps of the experimental subjects. The average displacements are indicated by *arrows* (bases of the arrows: average settings through the dominant eyes; tips of the arrows: average settings through the nondominant eyes). *Green areas*: $SD_{areas}$ of the dominant eyes; *Red areas*: $SD_{areas}$ of the nondominant eyes. Each point is based on five measurements. . . 39

4.3 Individual spatial displacement maps of the experimental subjects. The average displacements are indicated by *arrows* (bases of the arrows: average settings through the dominant eyes; tips of the arrows: average settings through the nondominant eyes). *Green areas*: $SD_{areas}$ of the dominant eyes; *Red areas*: $SD_{areas}$ of the nondominant eyes. Each point is based on five measurements. . . 40
4.4 Average vector lengths (a) and ratios of $SD_{areas}$ (b) for individual subjects, as a function of visual acuity. The different aetiology groups are indicated by different symbols. *Filled symbols*: subjects experiencing temporal instabilities; *open symbols*: subjects with stable perception. Not all categories are represented. 42
4.5 (a) Mean vector lengths and (b) ratios of $SD_{areas}$ for all subjects, grouped according to the depth of amblyopia (left clusters), their aetiology (middle clusters), and the presence of temporal stability (right clusters). Subjects in *group A* have either deeper amblyopia (left clusters), an aetiology of strabismus (middle clusters), or an unstable perception (right clusters). *Group B*: subjects with mild amblyopia (left clusters), with a refractive aetiology (middle clusters), or with stable perception (right clusters). Each cluster contains the data of all 15 experimental and 10 control subjects. . . . . 43

5.1 Sample stimuli (masked) used for the "DISIM" method . . . . . 47
5.2 Perspective transform. The points from one quadrilateral can be uniquely mapped into the space of the other. . . . . 48
5.3 Algorithm implementation based on the data of the strabismic and anisometropic amblyope B.B. (for orthoptic data see Table 4.1 on page 32). *a*), *b*) monocular distortion maps; *yellow points* distributed on circles: mean position of the points to be memorized; *coloured points* distributed on spider-web like patterns: mean position of the settings of the subject. *c*) vectorial subtraction: *base of arrows*, dominant eye; *tip of arrows*, non-dominant eye; *d*) interpolated control grid; . . 49
5.4 Example of applied distortion algorithm: a) original image b) distorted image based on the vectorial map of subject B.B., presented in Fig.5.3. . . . . 50
5.5 Computer reconstructions (upper panels) and visualizations of subjective perceptions (lower panels) of strabismic amblyopes (subjects L.P., M.K., S.B., D.S.). 52
5.6 Computer reconstructions (upper panels) and visualizations of subjective perceptions (lower panels) of anisometropic amblyopes (subjects T.S., H.L., M.B., J.B.). . . . . 53
5.7 Computer reconstructions (upper panels) and visualizations of subjective perceptions (lower panels) of strabismic and anisometropic amblyopes (subjects B.B., C.L.). . . . . 54

5.8 Comparison of different real-world images. *Right figures*: undistorted images; *Left figures*: distorted images, with the same vectorial data (from subject C.L.). a) highly ordered patterns (letters and numbers from a newspaper. b) natural landscape. . . . . 56

6.1 Static images used as stimuli. Each image was printed on an A4-sized paper. *a*) grating of 0.4 cycles/deg; *b*) checkerboard of 0.4 cycles/deg; *c*) grating of 1.6 cycles/deg; *d*) rectangular grid of 3.2 cycles/deg. . . . . 59

7.1 Different images, with increasing amount of variation (from none to complete random noise), and with corresponding entropy values (S). . . . . 63
7.2 Example of validated spatial distortions reported. In this particular image, the distorted images were perceived by subject H.M.K. (see Table 6.1). . . . . 64
7.3 Different normalizations of an original, random image (left). Note the achieved similarity between the original image and five-levels image (right). . . . . 65
7.4 Small-scale analysis. Each small square represents one pixel from the original image (left). . . . . 66
7.5 Individual entropy levels for each stimulus. Legend: *Ordinate*: the ratio of Shannon entropy values of each subject, to the entropy of the stimulus ($S_{subject}/S_{stimulus}$). *Dark-blue bar*: entropy level of the stimulus (normalized to 1.00); *Colored bars*: subjects' data; the aetiology of subjects is colour-coded like in the Table 6.1 on page 61; *Dotted line*: the averaged group response to the stimulus. . 67

8.1 Entropy maps example (from subject K.B.). *Left column*: original distorted images, as perceived by the subject. *Right column*: the corresponding entropy distribution in the images. Black corresponds to a zero entropy value (S=0.0), and white corresponds to maximum entropy (S=1.0); *Red grid*: 1 degree in visual field. . . . . 70
8.2 Image zones. *Dark grey*: inner part; *Light-grey*: outer part; *Numbers*: coordinates (in visual degrees) from the center of the image. . . . . 71
8.3 Model of *normal* overlapping receptive fields. Red: information related to the left eye, green - to the right eye. The regions of space that are processed by a single ganglion cell in the retina (the receptive fields) do overlap perfectly. The overlapping is a requirement to get a normal binocular vision. The receptive fields are represented as segments in top view, as disks in the frontal and 3D-view. . . . . 74

8.4 Partial overlapping at ~ 2.1 deg. squinting angle. *Red*: information related to the left eye, *green* - to the right eye. The left eye gaze is abnormally shifted, and therefore its receptive fields. Because the receptive fields are smaller in the central portion, they do not overlap (therefore there is binocularity loss). In the peripheral portions of the retina, receptive fields are bigger, and there is a degree of overlap, therefore the cortical neurons can have a chance to get binocular vision. In the frontal view can be seen that the area of binocularity loss is ellipsoidal in shape. . . . . 76

8.5 Partial overlapping at ~ 6 deg. squinting angle. *Red*: information related to the left eye, *green* - to the right eye. The left eye gaze is abnormally shifted, and therefore its receptive fields. The non-overlapping number of visual fields increased (as compared with the previous figure). In a frontal view, one can notice that the area of binocularity loss is ellipsoidal in shape, and its size increases as the squinting angle increases also. . . . . 77

9.1 Videoframes from patient SS. Frame time is 200 ms. . . . . 79

9.2 Entropy variation for a given movie (subject S.S.) . . . . . 80

9.3 Entropy variation in time (example from subject S.S.). Each graph represents the entropy plot vs. time obtained for each stimulus image (SS-1 for $1^{st}$ stimulus image, etc); the stimuli images were presented page 59. This example shows that the entropy variation is roughly cyclical and has different frequencies for each stimulus. The second stimulus elicits a higher frequency variation than the other stimuli. *Insets*: average cyclical frequency. . . . . 81

10.1 "*TEDI*" experimental setup . . . . . 86

10.2 Adaptive algorithm with a response collected as an averaged value from the last four out of 6 turning points (labelled with grey numbers in graphic). On Y-axis the speed is expressed in Hz, on X-axis there are all the steps (dots) where the subject made a choice. . . . . 88

10.3 Controlled times for each video frame in an animation . . . . . 89

# List of Tables


4.1 Orthoptic data of the 1st group of tested subjects. *LEGEND*: *RE* - right eye; *LE* - left eye; *visus c.c.* - corrected decimal visual acuity; *VD* - vertical deviation; *plano* - no correction required; *nrc* - normal retinal correspondence; *nh arc* - nonharmonious anomalous retinal correspondence; *h arc* - harmonious anomalous retinal correspondence; * - amblyopic eye. . . . . 32

4.2 *Average Vector Lengths* (*AVL*) and *Standard Deviation Areas (SD)* for all examined subjects . . . . . 37

6.1 Orthoptics data for 2nd group of subjects. The same color-coding of categories will be used in the following chapters. *LEGEND*: *RE* - right eye; *LE* - left eye; *visus c.c.* - corrected decimal visual acuity; *Ø* - no stereopsis; *VD* - vertical deviation; *plano* - no correction required; * - amblyopic eye. . . . . 61

9.1 Subjects with temporal instabilities. The order and categories match the orthoptic table 6.1 on page 61. . . . . 82

9.2 Individual and average frequencies for each stimulus. The order and categories match the orthoptic table 6.1 on page 61. . . . . 83

10.1 Measured temporal instability frequency - comparison between TEDI and ENTPACK-TEMP values. . . . . 91